THE GEOLOGY OF CEDAR VALLEY, IRON COUNTY, UTAH, AND ITS RELATION TO GROUND-WATER CONDITIONS

by
Hugh A. Hurlow

UTAH GEOLOGICAL SURVEY

The **UTAH GEOLOGICAL SURVEY** is organized into five geologic programs with Administration and Editorial providing necessary support to the programs. The **ENERGY & MINERAL RESOURCES PROGRAM** undertakes studies to identify coal, geothermal, uranium, hydrocarbon, and industrial and metallic resources; initiates detailed studies of these resources including mining district and field studies; develops computerized resource data bases, to answer state, federal, and industry requests for information; and encourages the prudent development of Utah's geologic resources. The **GEOLOGIC HAZARDS PROGRAM** responds to requests from local and state government entities for engineering-geologic investigations; and identifies, documents, and interprets Utah's geologic hazards. The **GEOLOGIC MAPPING PROGRAM** maps the bedrock and surficial geology of the state at a regional scale by county and at a more detailed scale by quadrangle. The **GEOLOGIC INFORMATION & OUTREACH PROGRAM** answers inquiries from the public and provides information about Utah's geology in a non-technical format. The **ENVIRONMENTAL SCIENCES PROGRAM** maintains and publishes records of Utah's fossil resources, provides paleontological and archeological recovery services to state and local governments, conducts studies of environmental change to aid resource management, and evaluates the quantity and quality of Utah's ground-water resources.

The UGS Library is open to the public and contains many reference works on Utah geology and many unpublished documents on aspects of Utah geology by UGS staff and others. The UGS has several computer databases with information on mineral and energy resources, geologic hazards, stratigraphic sections, and bibliographic references. Most files may be viewed by using the UGS Library. The UGS also manages the Utah Core Research Center which contains core, cuttings, and soil samples from mineral and petroleum drill holes and engineering geology investigations. Samples may be viewed at the Utah Core Research Center or requested as a loan for outside study.

The UGS publishes the results of its investigations in the form of maps, reports, and compilations of data that are accessible to the public. For information on UGS publications, contact the Natural Resources Map/Bookstore, 1594 W. North Temple, Salt Lake City, Utah 84116, (801) 537-3320 or 1-888-UTAH MAP. E-mail: geostore@utah .gov and visit our web site at mapstore.utah.gov.

TABLE OF CONTENTS

TABLES

ILLUSTRATIONS

PLATES

APPENDICES

THE GEOLOGY OF CEDAR VALLEY, IRON COUNTY, UTAH, AND ITS RELATION TO GROUND-WATER CONDITIONS

by
Hugh A. Hurlow

ABSTRACT

Cedar Valley is a north-northeast-trending topographic depression on the southeastern margin of the Basin and Range Province in Iron County, southwestern Utah. The towns of Cedar City and Enoch, and adjacent parts of the valley, experienced a 105 percent population increase and a 110 percent increase in public-supply water use between 1980 and 2000, creating potential water-supply and water-quality problems. This report addresses the geology of the Cedar Valley drainage basin and its influence on the storage and transport of ground water; it represents part of a cooperative, multidisciplinary study of the hydrogeology of Cedar Valley by the Utah Geological Survey and the U.S. Geological Survey, designed to help local officials address future water-supply issues.

The principal aquifer in the Cedar Valley drainage basin consists of Tertiary sedimentary basin-fill deposits, chiefly interbedded sand, gravel, silt, and clay. Most recharge is derived from infiltration of Coal Creek into alluvial-fan deposits near Cedar City. Coal Creek drains much of the Markagunt Plateau east of Cedar Valley; this highland receives the majority of the precipitation that falls in the drainage basin. The drainage basin is closed to surface outflow except during extreme precipitation events, but minor underflow of ground water occurs in places along its northwestern and southern margins.

Miocene- to Holocene-age normal faults bound the eastern and western margins of the Cedar Valley depositional basin. The eastern basin-bounding fault system (EBBFS) is physically more continuous and accommodated significantly greater displacement than faults along the western basin margin. Subsidence of the EBBFS hanging wall created the Cedar Valley depositional basin, which accumulated up to 3,800 feet (1,160 m) of basin-fill sediment. This sediment was derived chiefly from the uplifting footwall, and was deposited in alluvial-fan environments along the basin margins and in fluvial and lacustrine environments in the basin interior. Interpretation of seismic-reflection data collected by Mobil Exploration and Production Services U.S., Inc. reveals that the Tertiary basin fill contains three unconformity-bounded units and has a complicated subsurface structure that is not entirely reflected by present-day topography. These relations indicate a complex evolution of coupled faulting and basin subsidence during Tertiary time.

The transmissivity of the basin-fill aquifer, estimated from aquifer-test and specific-capacity test data, is greatest in coarse-grained alluvial-fan deposits along the eastern and southwestern basin margins, and gradually decreases toward the basin center as sedimentary deposits become progressively finer grained. Bedrock units are presently of secondary importance for water supply, but they are hydrologically connected to the basin-fill aquifer and include several high-transmissivity units that are important aquifers in other parts of southwestern Utah.

INTRODUCTION

This report describes aspects of the geology of Cedar Valley and adjacent areas, located in Iron County, southwestern Utah (figures 1 and 2), that most directly influence the occurrence and flow of ground water. The report focuses primarily on unconsolidated to semi-consolidated basin-fill sediments of Quaternary-Tertiary age beneath Cedar Valley because they are presently the most important aquifer for the valley, and secondarily on bedrock units because they are hydrologically connected to the basin fill and are the target of increasing ground-water development. A digitally compiled geologic map (plate 1) and accompanying cross sections (plate 2) illustrate the geology of the region. The cross sections and related isopach maps show the large-scale geometry and stratigraphy of the basin fill, and are based primarily on interpretations of 11 seismic-reflection lines obtained from Mobil Exploration and Production Services U.S., Inc. (now part of ExxonMobil).

The work summarized herein is part of a cooperative, multidisciplinary project by the Utah Geological Survey and the Water Resources Division of the U.S. Geological Survey to characterize the budget, flow, and chemistry of ground water in the Cedar Valley drainage basin. The goal of the project is to provide tools to help local and state officials manage ground-water development to sustain reserves and maintain high chemical quality. Such tools are necessary because the population of the study area increased by about 105 percent and water use from public suppliers increased by about 110 percent between 1980 and 2000, and ground-water levels have gradually declined in most of the valley since 1945 (Utah Division of Water Rights, 1982, 2000; Burden, 2000; Utah Governor's Office of Planning and Budget, 2001a).

The principal conclusions of this project are as follows. Unconsolidated Quaternary-Tertiary-age sediment in the Cedar Valley depositional basin forms two distinct sub-basins in the northeastern and southwestern parts of the valley. Both sub-basins comprise asymmetric, east-thickening
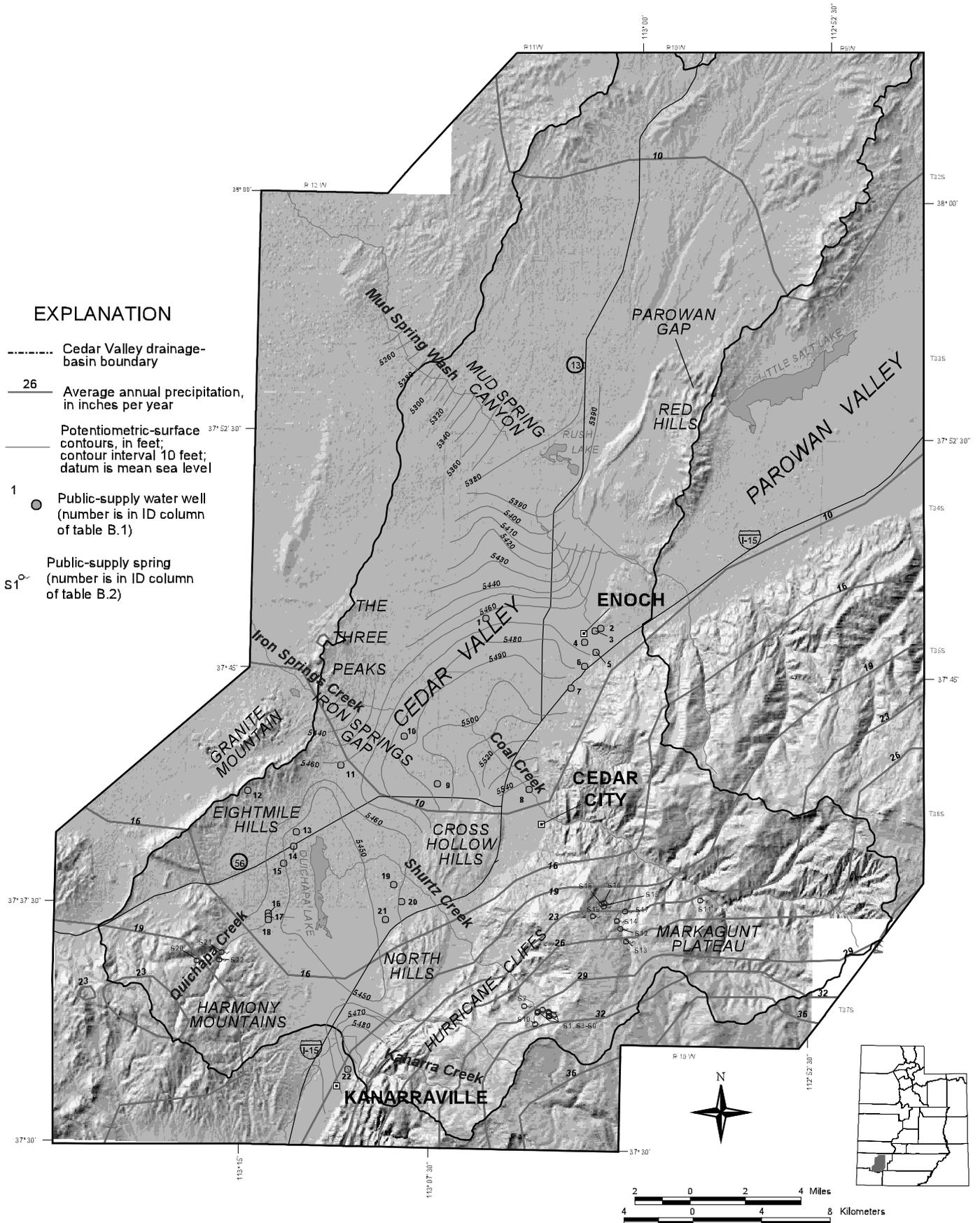
Figure 1. *Shaded-relief digital elevation model showing geographic and hydrologic features of Cedar Valley, Iron County, southwestern Utah. Potentiometric-surface contours from Bjorklund and others (1978); precipitation data from Daly and Weisburg (1997).*

Figure 2. *Photomosaic showing panoramic view across the southern and central parts of Cedar Valley taken from the northeastern part of Eightmile Hills (see figure 1 for location). The lower part of the figure is a view to the south; the upper part of the figure is a view to the east-northeast.*

wedges that terminate against the eastern basin-bounding fault system (EBBFS), a Quaternary-Tertiary-age normal-fault zone responsible for basin formation. The basin-fill sediment grades from coarse alluvial-fan deposits near the basin margins to finer grained alluvial and playa deposits in the basin center. This facies variation largely controls the distribution of transmissivity within the basin-fill aquifer, with values ranging from over 20,000 square feet per day (>1,860 m²/d) along the basin margins to less than 5,000 square feet per day (<465 m²/d) in the basin center. The best prospective bedrock aquifers in the area include fractured volcanic rocks below and adjacent to the southwestern basin margin, and fractured sedimentary rocks southeast of the basin.

To assist non-geologists in reading this report, many technical or specialized geologic terms are defined in a glossary located after the references. Geologic ages are reported with the abbreviations ka for thousands of years before present and Ma for millions of years before present. For example, the phrase "the Pleistocene epoch lasted from 1.6 Ma to 10 ka" means that the Pleistocene epoch began 1.6 million years before present and ended 10,000 years before present. Figure 3 shows the geologic time scale.

GEOLOGIC SETTING

The Cedar Valley drainage basin is in the transition zone between the Basin and Range and Colorado Plateau physiographic provinces (figure 4) (Threet, 1963; Scott and Swadley, 1995; Maldonado and others, 1997). The Basin and Range Province consists of north- to northeast-trending, normal-fault-bounded mountain ranges, composed of Cenozoic volcanic rocks and normal faults superposed on Mesozoic to early Cenozoic thrust faults and folds, and adjacent valleys filled with alluvial, lacustrine, and volcaniclastic sediment (Stewart, 1978; Eaton, 1982; Wernicke, 1992). The Mesozoic to early Cenozoic structures are part of the Cordilleran fold and thrust belt, which deformed much of western North America during Late Jurassic to Paleocene time (Armstrong, 1968; Royse and others, 1975; Allmendinger, 1992; Willis, 1999). The Colorado Plateau is typically structurally simpler than the Basin and Range Province, having experienced much less intense Mesozoic and Cenozoic deformation. Figure 5 illustrates the stratigraphy of rocks and unconsolidated sediment, and figure 6 is a simplified geologic map of the study area; appendix A and

Era	Period	Epoch		Age	Age estimates in Ma[1]
Cenozoic	Quaternary	Holocene			
		Pleistocene			0.01
					1.6
	Tertiary	Neogene	Pliocene		
					5.3
			Miocene		
					23.7
		Paleogene	Oligocene		
					36.6
			Eocene		
					57.8
			Paleocene		
					66.4
Mesozoic	Cretaceous	Late		Maastrichtian	
					74.5 (4)
				Campanian	
					84.0 (4.5)
				Santonian	
					87.5 (4.5)
				Coniacian	
					88.5 (2.5)
				Turonian	
					91.0 (2.5)
				Cenomanian	
					97.5 (2.5)
		Early		Aptian	
					113 (4)
				Albian	
					119 (9)
				Neocomian	
					144 (5)
	Jurassic	Late			
					163 (15)
		Middle			
					187 (34)
		Early			
					208 (18)
	Triassic	Late			
					230 (22)
		Middle			
					240 (22)
		Early			
					245 (20)

1. *Age estimates are from Palmer (1983), with uncertainties in parentheses, except where none are reported.*

Era	Period	Epoch		Age	Age estimates in Ma[1]
Paleozoic	Permian	Late			245 (20)
					258
		Early			
					286 (12)
	Pennsylvanian	Late			
					296 (10)
		Middle			
					315 (20)
		Early			
					320
	Mississippian	Late			
					352 (8)
		Early			
					360 (10)
	Devonian	Late			
					374 (18)
		Middle			
					387 (28)
		Early			
					408 (12)
	Silurian	Late			
					421 (12)
		Early			
					438 (12)
	Ordovician	Late			
					458 (16)
		Middle			
					478 (16)
		Early			
					505 (32)
	Cambrian	Late			
					523 (36)
		Middle			
					540 (28)
		Early			
					570
Proterozoic	Late Proterozoic				
					900
	Middle Proterozoic				
					1600
	Early Proterozoic				
					2500
Archean	Late Archean				
					3000
	Middle Archean				
					3400
	Early Archean				
					3800?

***Figure 3.** Geologic time scale after Palmer (1983) and Hansen (1991).*
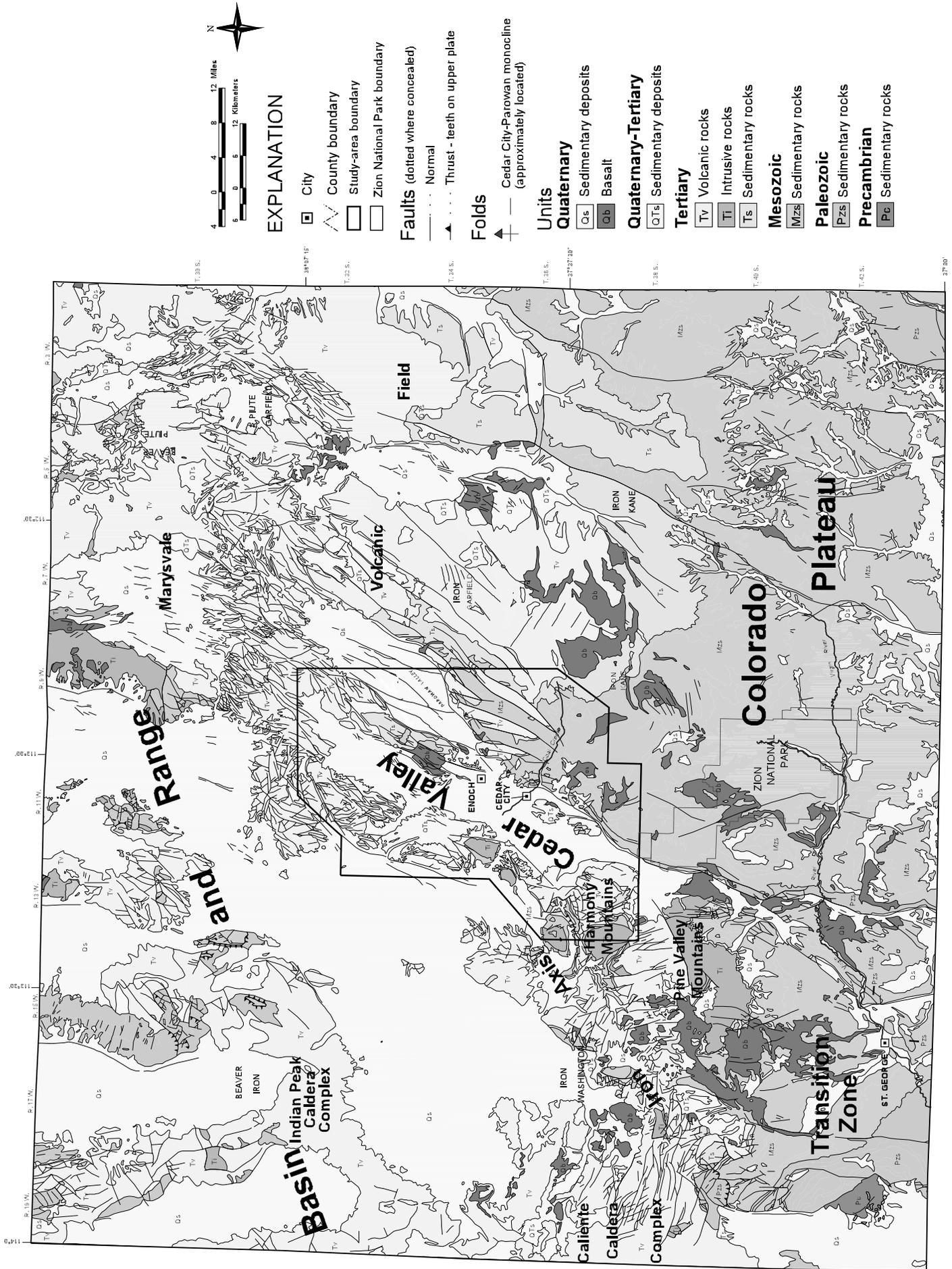
Figure 4. *Tectonic map of southwestern Utah, modified from Hintze and others (2000).*

plate 1 provide more detailed versions of figures 5 and 6, respectively.

Mesozoic sedimentary rocks and Cenozoic sedimentary, volcanic, and plutonic rocks crop out in the hills and mountains bounding Cedar Valley (figures 5 and 6). Triassic to Jurassic sedimentary rocks, consisting of interbedded sandstone, shale, and limestone deposited in shallow-marine and fluvial environments, crop out along the Hurricane Cliffs and in parts of the Red Hills and Three Peaks-Granite Mountain area where they are tilted and folded due to deformation associated with the Cordilleran fold and thrust belt. Creta-

ceous fluvial sandstone, conglomerate, and mudstone exposed adjacent to Cedar Valley accumulated during Cordilleran fold and thrust belt activity to the west, and then were deformed when the fold and thrust belt moved eastward into the study area (van Kooten, 1988; Fillmore, 1991; Goldstrand, 1994). Latest Mesozoic to early Cenozoic conglomerate, sandstone, and lacustrine limestone, exposed in the Hurricane Cliffs, Red Hills, and southern Three Peaks-Granite Mountain area postdate most activity in the Cordilleran fold and thrust belt (Taylor, 1993; Goldstrand, 1994; Goldstrand and Mullett, 1997).

Age (Ma)	Period	Map Symbol and Unit Name		Description	Approximate Thickness in feet (m)
1.6	QUATERNARY	Qs Sedimentary		Interbedded gravel, sand, silt and clay.	0 - 150+ (0 - 45)
		QTb Basalt		Flows and small cinder cones.	0 - 330+ (0 - 100)
	QUATERNARY-TERTIARY	QTs Sedimentary		Interbedded gravel, sand, silt and clay.	0 - 1,330 (0 - 405)
		Seismically defined basin-fill units	A	Interbedded gravel, sand, silt, clay and sedimentary breccia.	0 - 1,330 (0 - 405)
			B		0 - 1,825 (0 - 555)
			C		0 - 980 (0 - 300)
	TERTIARY	Ti Intrusive rocks		Quartz monzonite intrusions of the "Iron Axis."	
		Tv Volcanic rocks		Interbedded ash-flow tuff, volcanic breccia, flows, and related sedimentary deposits.	0 - 4,000 (0 - 1,200)
66		TKs Sedimentary rocks		Interbedded mudstone, siltstone, sandstone, conglomerate, and limestone.	2,190 - 2,320 (665 - 705)
	CRETACEOUS	Ks Sedimentary rocks		Interbedded sandstone, mudstone, conglomerate, and coal.	2,700 - 3,600 (825 - 1,100)
144	JURASSIC	Js Sedimentary rocks		Interbedded sandstone, siltstone, mudstone, and limestone.	3,900 - 5,150 (1,200 - 1,575)
205	TRIASSIC	Ƚs Sedimentary rocks		Interbedded sandstone, siltstone, mudstone, gypsiferous mudstone, and minor conglomerate.	2,100 - 2,400 (640 - 730)

Figure 5. Generalized stratigraphic column for Cedar Valley drainage basin. Units correspond to those on figure 6. See appendix A for relation of these map units to those on plates 1 and 2.
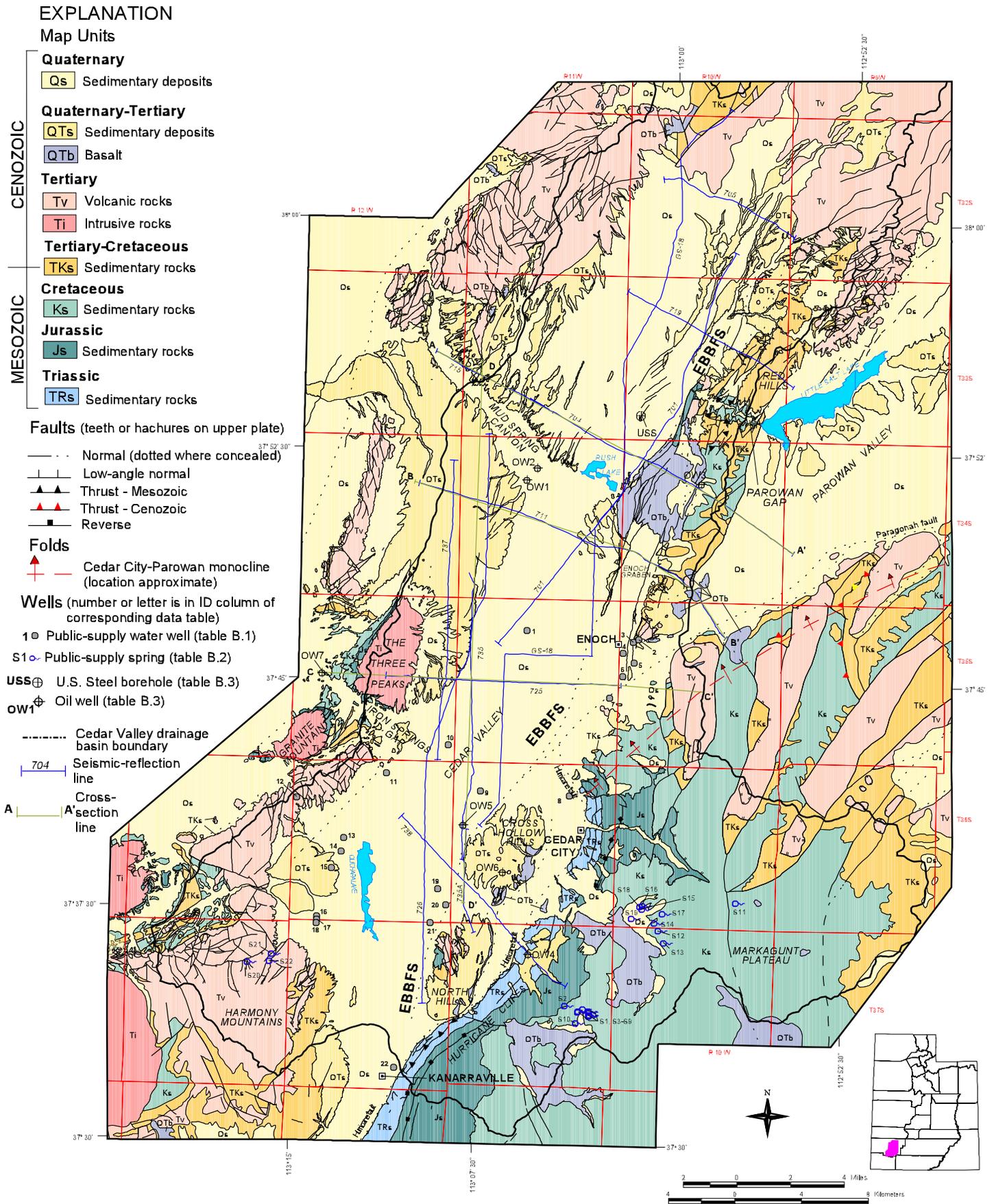
Figure 6. *Simplified geologic map of Cedar Valley drainage basin and adjacent areas. EBBFS is eastern basin-bounding fault system. See figure 5 for stratigraphic column, and appendix A for correlation of map units with those on plates 1 and 2.*

During mid-Tertiary time, the tectonic setting of southwestern Utah changed from fluvial and lacustrine sedimentation with little active faulting to calc-alkalic volcanism accompanied by relatively low-magnitude normal faulting (Rowley and others, 1979; Best and Christiansen, 1991). Voluminous Oligocene- to Miocene-age ash-flow tuffs, breccias, lava flows, and related deposits erupted from the Indian Peak, Caliente, and Marysvale caldera complexes during this time, covering much of southwestern Utah and eastern Nevada (figure 4; Mackin, 1960; Anderson and others, 1975; Rowley and others, 1979, 1994, 1995). Remnants of these volcanic deposits crop out in the hills and mountains bounding Cedar Valley (figure 6; plate 1). A northeast-trending belt of Miocene-age quartz monzonite intrusive masses, termed the Iron Axis for the associated iron-rich vein deposits in the plutonic rocks and adjacent sedimentary rocks, intruded the Jurassic Carmel Formation, producing topographic highs (Blank, 1959; Cook, 1960; Blank and Mackin, 1967; Rowley and Barker, 1978; Blank and others, 1992).

The Cedar Valley depositional basin formed as a graben during Miocene to Quaternary time, due to displacement on normal faults along its eastern and western margins. Evidence presented below indicates that the eastern faults, referred to herein as the eastern basin-bounding fault system (EBBFS), have greater displacement than the western faults, resulting in an asymmetric graben. Subsidence of the EBBFS hanging wall accommodated deposition and accumulation of basin-fill sediment, principally derived from the surrounding mountains in the footwall of the normal-fault system. The basin-fill deposits are chiefly alluvial and lacustrine sediments that thicken eastward toward the EBBFS. Fault displacement and sediment deposition occurred mainly during late Miocene through Pleistocene time (Anderson and Mehnert, 1979; Williams and Maldonado, 1995; Maldonado and others, 1997; Pearthree and others, 1998). Low sedimentation rates likely characterized the valley during Holocene time, except adjacent to active faults along the base of the Hurricane Cliffs and on both sides of the Red Mountains.

A relatively wet and cold climate characterized mid- to late Pleistocene time, when Quichapa Lake and Rush Lake formed in Cedar Valley and Little Salt Lake occupied the northwestern part of Parowan Valley (Williams and Maldonado, 1995). These lakes did not coalesce, but drained individually northwestward (Williams and Maldonado, 1995). Little Salt Lake drained through Parowan Gap to Rush Lake, which in turn drained to the Escalante arm through Mud Spring Canyon, and Quichapa Lake drained through Iron Springs Gap (see figure 1 for locations).

HYDROLOGIC SETTING

Cedar Valley, like most surface-drainage basins in the Basin and Range, is topographically closed and undrained to partly drained with respect to surface water (Eakin and others, 1976; Bjorklund and others, 1978). The Cedar Valley drainage basin covers about 580 square miles (1,500 km^2) including Cedar Valley, which ranges in elevation from about 5,300 to 5,900 feet (1,620-1,800 m), and adjacent hills and mountains (figure 1). The hills bounding the western, northern, and northeastern parts of the valley have relatively subdued relief. The precipitous Hurricane Cliffs form the southeastern boundary of the valley and the northwestern boundary of the Markagunt Plateau, locally over 10,000 feet (3,050 m) in elevation. The Harmony Mountains, which bound the southwestern part of the valley, are locally over 8,000 feet (2,440 m) in elevation. The drainage basin is open only at its south end, and at Iron Springs Gap and Mud Spring Canyon (figure 1). Surface flow through these openings occurs only following extreme precipitation events (the most recent instance of surface outflow was about 50 years ago), and outflow of ground water is relatively minor (Bjorklund and others, 1978). Annual precipitation is 10 to 12 inches per year (25-38 cm/yr) in the valley and adjacent low hills, and increases with elevation to over 40 inches per year (102 cm/yr) on the Markagunt Plateau and 15 to 20 inches per year (38-51 cm/yr) in the Harmony Mountains (figure 1) (Daly and Weisburg, 1997).

The potentiometric surface of ground water in Cedar Valley slopes radially away from Cedar City (figure 1; Bjorklund and others, 1978), reflecting infiltration of stream flow from Coal Creek, the main perennial stream entering the basin and the principal source of recharge to the basin-fill aquifer (Thomas and Taylor, 1946; Bjorklund and others, 1978). The potentiometric surface forms a closed low encircling Quichapa Lake, and is flat in the vicinity of Rush Lake (figure 1). Discharge occurs by well pumping, evapotranspiration, flow from springs, and minor outflow through Iron Springs Gap, Mud Spring Canyon, and the southern end of the valley.

Basin-fill sediments are the principal producing aquifer for the towns of Cedar City and Enoch, and adjacent residential and industrial developments. At least seven public-supply entities, including Cedar City and the towns of Enoch and Kanarraville, withdraw over 2.3x10^9 gallons (8.7x10^9 L) of ground water annually from the basin-fill aquifer (Utah Division of Water Rights, 2000). Private and small public-supply wells draw additional water from the basin-fill aquifer, though some is reintroduced by irrigation return-flow.

Cedar City is the only major public water-supply entity in Cedar Valley that currently collects water from springs for municipal use (Utah Division of Water Rights records). Most of these springs are in the Coal Creek drainage basin and issue from Cretaceous sedimentary rocks (figures 1 and 6; table B.2). Cedar City also draws water from three springs in the Quichapa Creek drainage in the northeastern Harmony Mountains; these springs issue from faults in volcanic rocks of the Quichapa Group (figures 1 and 6; table B.2).

Ground water in Cedar Valley is primarily calcium or magnesium-sulfate type, and the concentration of total dissolved solids ranges from greater than 1,500 parts per million near the mouth of Coal Creek to less than 300 parts per million in the southwestern part of the valley (Bjorklund and others, 1978). The high concentration of total dissolved solids in ground water at the mouth of Coal Creek results from infiltration of water from the creek. The primary source of the dissolved solids in Coal Creek is gypsiferous sedimentary rocks of the Triassic Moenkopi and Jurassic Carmel Formations, which crop out along the lower reaches of the creek and its tributary drainages (Bjorklund and others, 1978). Nitrate concentrations in Cedar Valley ground water are generally low, except in a limited area southwest of Enoch (Thomas and Taylor, 1946; Bjorklund and others,

1978; Lowe and Wallace, 2001). Naturally occurring nitrate in organic-rich sedimentary rocks of the Cretaceous Straight Cliffs Formation exposed along the Hurricane Cliffs to the east may be a source for some of this nitrate (Lowe and Wallace, 2001).

GEOLOGY OF BASIN-FILL DEPOSITS

Introduction

Geologic properties of basin-fill deposits considered here to most directly influence the movement and storage of ground water include:

1. large-scale basin geometry, including thickness, shape, and contact relations between basin fill and bedrock,
2. stratigraphy,
3. lithology, especially grain size, sorting, and lateral facies variations, and
4. composition, especially clay content.

The large-scale basin geometry and stratigraphic correlations are constrained by interpretation of seismic-reflection lines obtained from Mobil Exploration and Production Services U.S., Inc. (now part of ExxonMobil). Data on composition and facies variations are relatively sparse, and the conclusions presented here are based on drillers' logs of water wells, detailed logs of water-well cuttings (Wallace, 2001), and observations of exposed sediments.

Large-Scale Geometry and Stratigraphy

Methods

The geometry and stratigraphic correlations of the Cedar Valley basin-fill deposits were delineated in this study using 11 seismic-reflection lines, collected by Mobil Exploration and Production Services U.S., Inc. from 1979 to 1981 (figure 6), and geologic and geophysical logs from oil-test wells (table B.3) in and adjacent to the valley. Subsurface contacts on the seismic-reflection profiles were picked where the profiles intersect test wells having reliable geologic logs. The contacts were then extrapolated through the profiles by following individual reflectors interpreted as corresponding to the contacts.

The Odessa Cedar City #1 (OW5, table B.3; plate 1; figure 6) is critical for picking contacts on the seismic-reflection profiles because it is the only well in the hanging wall of the EBBFS having a reliable, detailed geologic log, and because an interpretation of a seismic-reflection profile (recorded by Arco Company [van Kooten, 1988]) that crosses this well is available. The interpretations are also based on the surface traces and dips of faults and contacts (plate 1), regional stratigraphy and geologic history, and previously published geologic cross sections (Williams and Maldonado, 1995; Maldonado and others, 1997). The Mobil seismic-reflection data forms a grid of intersecting profiles (figure 6), which permits cross-checking at intersection points, resulting in an internally consistent set of geologic interpretations. Figures 7 through 9 show three of the seismic-reflection profiles and

their geologic interpretations. The contacts drawn on the seismic-reflection profiles (figures 7b, 8b, and 9b) do not directly represent the subsurface geometry of the geologic units, because the vertical axes of the profiles are in units of time denoted as two-way travel time. The velocity of seismic waves in rock and sediment depends on composition and degree of consolidation, and is significantly lower in unconsolidated to semi-consolidated deposits such as the Cedar Valley basin fill than in bedrock (Telford and others, 1976, p. 257-261). The result of this variation in velocity is that the apparent thickness of the basin-fill deposits depicted on figures 7b, 8b, and 9b is disproportionately large compared to that of bedrock, and the apparent dips of faults bounding the basin-fill deposits are steeper than their true values. To remove this distortion and estimate the true geometry of the Cedar Valley depositional basin, four of the seismic-reflection profiles were converted to depth sections using the software program Geosec (access to the software provided by J. C. Coogan, independent consultant, Denver, Colorado, in October, 1999). Sonic logs of the oil-test wells in and adjacent to Cedar Valley provided velocity estimates for the bedrock units. The depth-converted seismic-reflection profiles were combined with surficial and well data to construct the geologic cross sections (plate 2).

For the purposes of this study, the most important factor in converting from time profiles to depth sections is estimating the velocity of seismic waves in the basin-fill deposits. Sonic logs for the basin-fill deposits encountered in the oil-test wells in Cedar Valley are unavailable. The procedure for estimating seismic-wave velocities of the basin-fill units included (1) making reasonable estimates of the velocity, derived from sonic logs of test wells in other Quaternary-Tertiary extensional basins in Utah, and (2) refining these estimates so that the calculated depth of the base of the basin-fill deposits on profile 735 at the Odessa Cedar City well matched the true depth of this contact of 1,290 feet (393 m), interpreted from the gamma-ray log of the well. The resulting velocities are 5,000 feet per second (1,524 m/sec) for basin-fill units A (youngest) and B, and 6,500 feet per second (1,981 m/sec) for unit C. Seismic-wave velocity in basin-fill sediments typically increases with depth due to compaction (Telford and others, 1976, p. 257-261), but the depth-conversion process did not account for this effect. The seismic velocities and resultant thicknesses of the basin-fill units should, therefore, be regarded as minimum values.

The reflection corresponding to the base of the Cedar Valley basin fill was first identified on seismic-reflection profile 735 where it intersects the Odessa Cedar City #1 well. This contact was identified on the other profiles using (1) ties with profile 735, (2) wells OW1, OW2, and USS (table B.3), which provide minimum thickness values for the basin fill, and (3) by comparison with published interpretations of seismic-reflection lines from other Tertiary extensional basins in the Basin and Range Province (Anderson and others, 1983; Smith and Bruhn, 1984; Effimoff and Pinezich, 1986; Liberty and others, 1994; Evans and Oaks, 1996).

The interpretations presented here proceeded with sparse supporting data compared to most industry-sponsored studies, most notably the lack of sonic logs and detailed geologic logs of exploration wells in the basin center. Such lack of data makes picking contacts on the reflection profiles a highly subjective process. The interpretations presented below

A

B

A,B,C - Subdivisions of Quaternary-Tertiary basin-fill sediment; Tqm - Quartz monzonite; Tv - Tertiary volcanic rocks; Ts - Tertiary sedimentary rocks; Kis - Iron Springs Formation; Jc - Carmel Formation; Ju - Navajo Sandstone, Kayenta, and Moenave Formations, undifferentiated; Ts - Triassic sedimentary rocks; Pzs - Paleozoic sedimentary rocks.

C
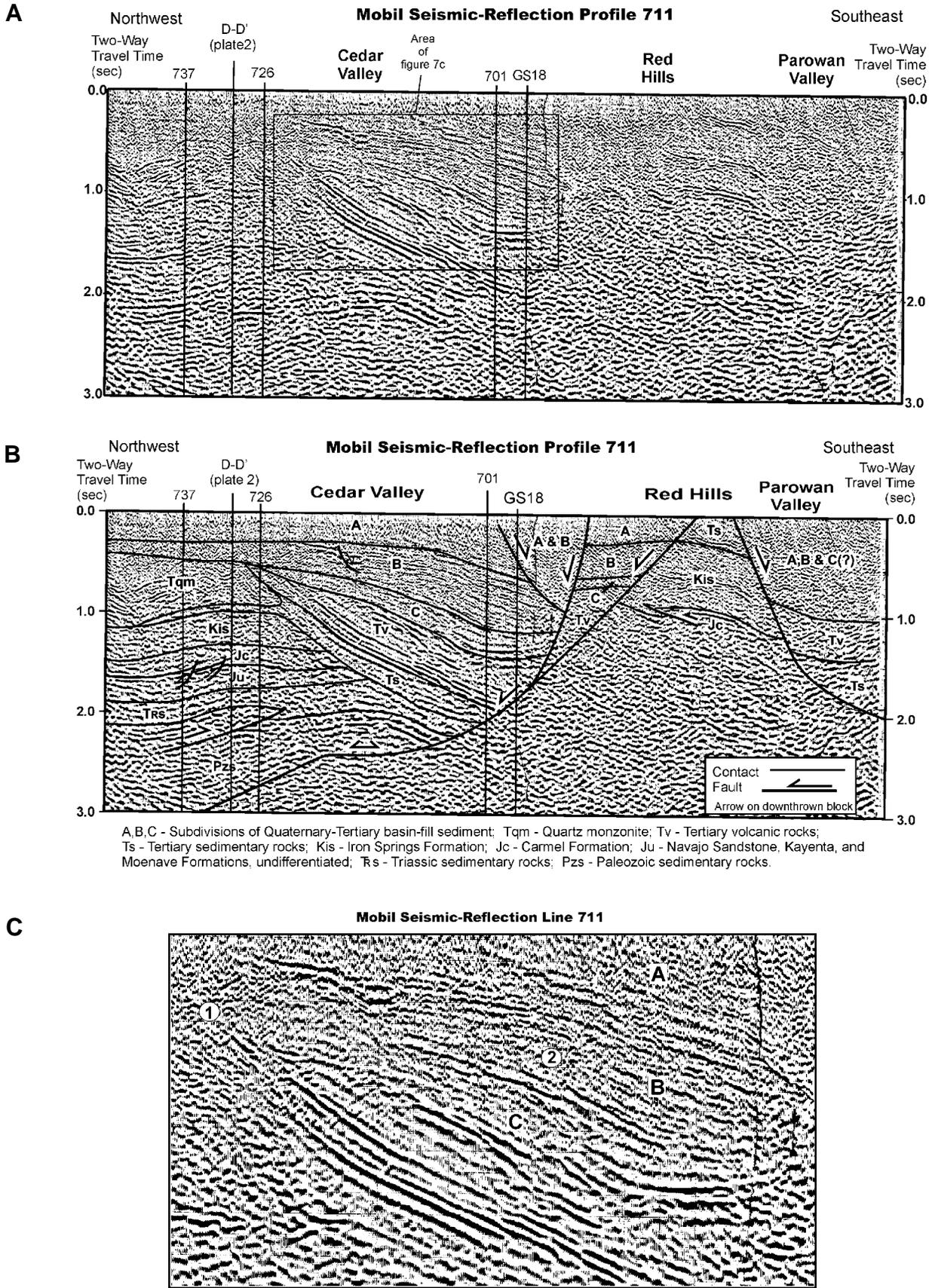
Figure 7. **A.** *Wave-migrated time section and geologic interpretation of Mobil seismic-reflection profile 711, showing intersecting profiles. See figure 6 or plate 1 for location.* **B.** *Geologic interpretation. Cross section B-B' (plate 2) is derived from a depth conversion of this interpretation.* **C.** *Detail of wave-migrated time section. Circled number 1 is just above angular unconformity between basin-fill deposits above and volcanic rocks below, and circled number 2 is just below contact between units A and B.*
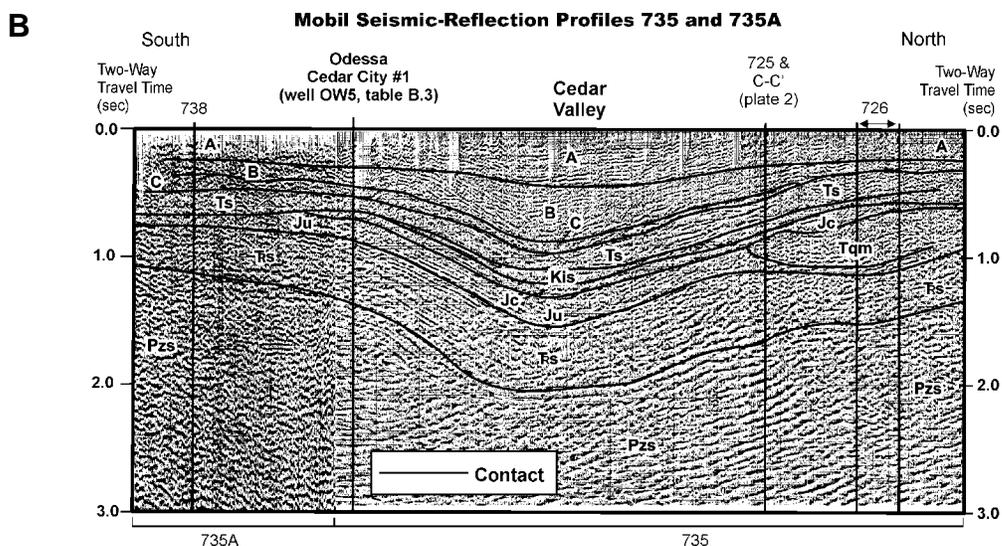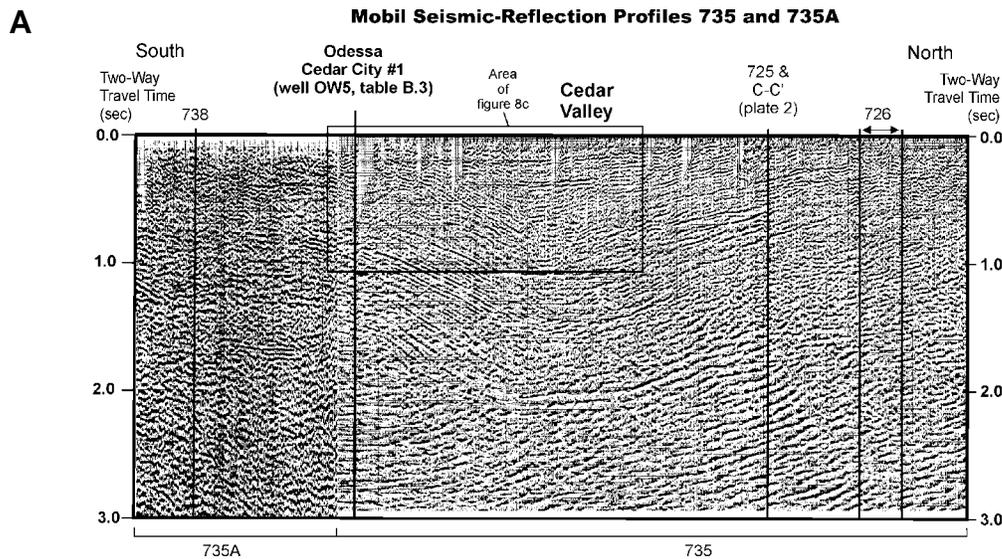
A

Mobil Seismic-Reflection Profiles 735 and 735A

B

Mobil Seismic-Reflection Profiles 735 and 735A

A,B,C - Subdivisions of Quaternary-Tertiary basin-fill sediment; Tqm - Quartz monzonite; Tv - Tertiary volcanic rocks; Ts - Tertiary sedimentary rocks; Kis - Iron Springs Formation; Jc - Carmel Formation; Ju - Navajo Sandstone, Kayenta, and Moenave Formations, undifferentiated; Ts - Triassic sedimentary rocks; Pzs - Paleozoic sedimentary rocks.

C

Mobil Seismic-Reflection Line 735 - Detail
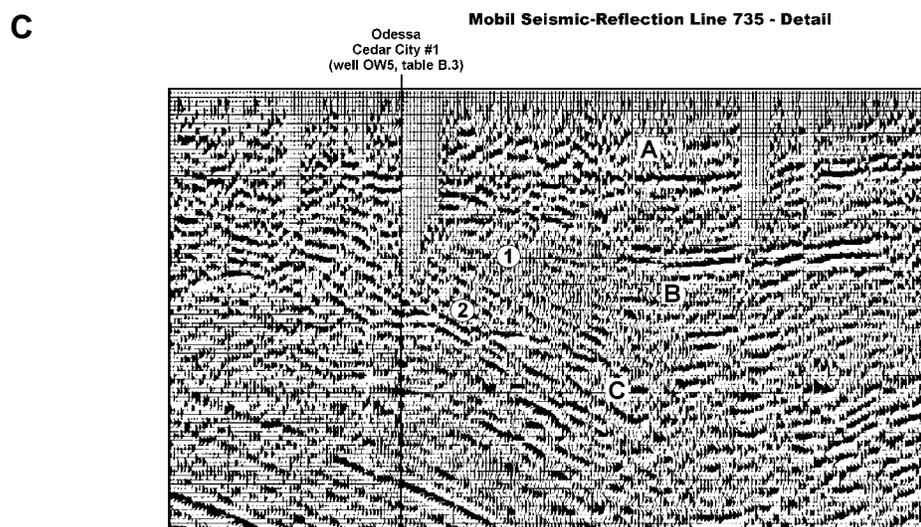
Figure 8. A. Wave-migrated time section and geologic interpretation of Mobil seismic-reflection profiles 735 and 735A, showing intersecting profiles. See figure 6 or plate 1 for location. B. Geologic interpretation. Cross section D-D' (plate 2) is derived from a depth conversion of this interpretation. C. Detail of wave-migrated time section. Circled number 1 is just below the angular unconformity that marks the contact between units A and B, and circled number 2 is just above the contact between units B and C.

A
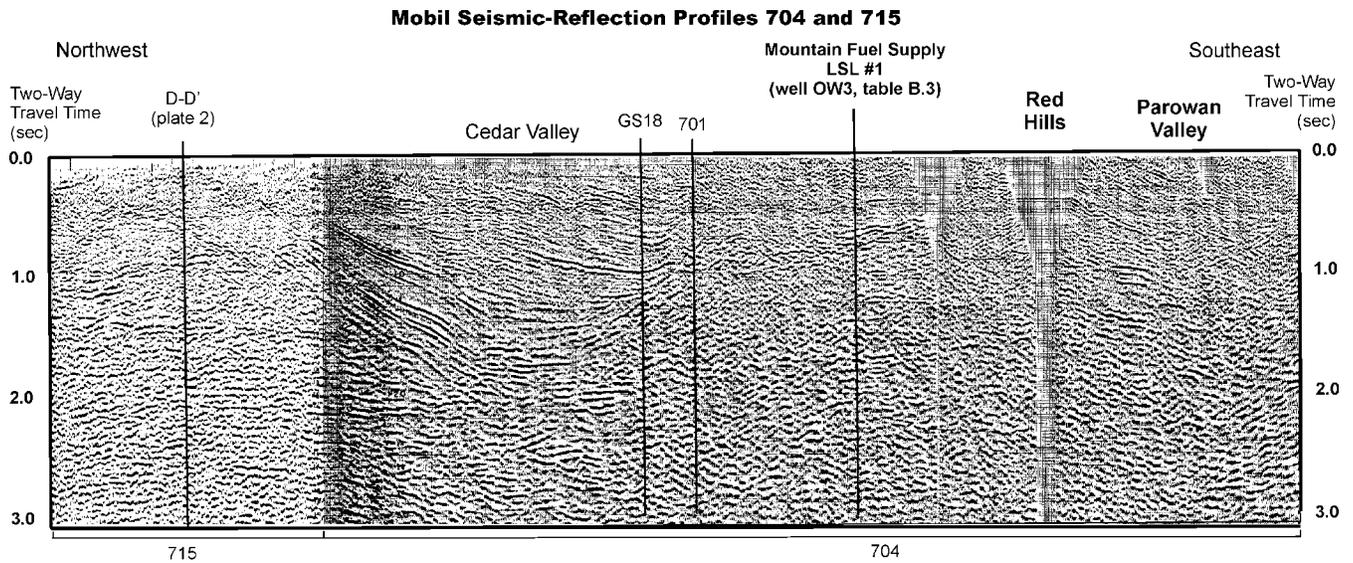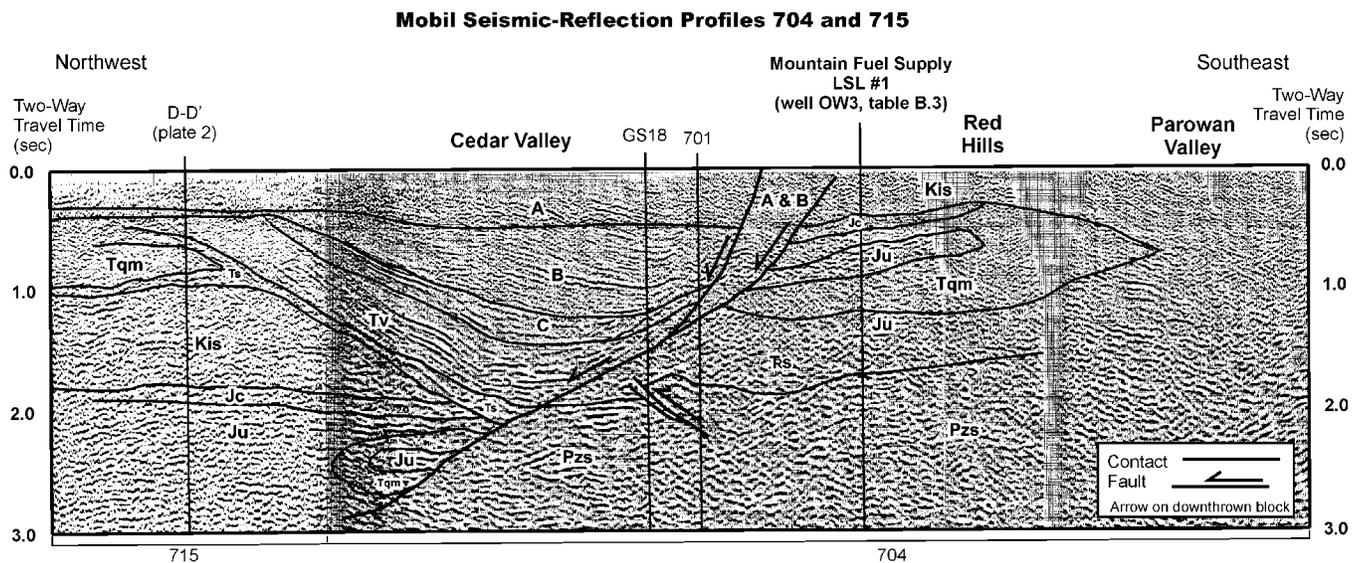
Mobil Seismic-Reflection Profiles 704 and 715

B

Mobil Seismic-Reflection Profiles 704 and 715

A,B,C - Subdivisions of Quaternary-Tertiary basin-fill sediment; Tqm - Quartz monzonite; Tv - Tertiary volcanic rocks;
Ts - Tertiary sedimentary rocks; Kis - Iron Springs Formation; Jc - Carmel Formation; Ju - Navajo Sandstone, Kayenta, and
Moenave Formations, undifferentiated; Ts - Triassic sedimentary rocks; Pzs - Paleozoic sedimentary rocks.

Figure 9. *A. Wave-migrated time section and geologic interpretation of Mobil seismic-reflection profiles 704 and 715, showing intersecting profiles. See figure 6 or plate 1 for location.* *B. Geologic interpretation. Cross section A-A' (plate 2) is derived from a depth conversion of a simplified version of this interpretation.*

and on plate 2 must, therefore, be regarded as preliminary, despite the detailed analysis and care invested in them.

Results

Stratigraphy: The basin fill contains two laterally persistent angular unconformities (figures 7b, 8b, and 9b), as interpreted from the seismic-reflection profiles. These two angular unconformities divide the basin fill into three informal units, in descending order A, B, and C. These units differ in reflectivity characteristics, geometry, and relations to the basin margins.

Unit A has the greatest areal extent of the three seismically defined basin-fill units, and relatively low reflectivity. The lower part of unit A thickens toward, and is offset by, the EBBFS (figures 7b, 8b, and 9b), but the upper part of unit A onlaps these faults. Unit A thins toward the western basin margin, where it onlaps unit B. Unit B is the thickest of the three basin-fill units, and is characterized by numerous strong reflections of limited lateral extent, pronounced thickening toward and moderate to large displacement by the EBBFS, and depositional thinning toward the western basin margin (figures 7b, 8b, and 9b). Units A and B both exhibit decreased reflectivity near the EBBFS, likely the result of a greater proportion of poorly layered alluvial-fan sediment within the basin fill (Anderson and others, 1983). Unit C, the thinnest seismically defined basin-fill unit, is characterized by large-amplitude, laterally persistent reflections, and by only minor thickening toward, and large offset by, the EBBFS. Unit C exhibits depositional thinning toward the western basin margin.

The near-surface geometry and surface projections of the contacts between the seismically defined basin-fill units cannot be determined from the seismic-reflection profiles, because the upper 0.2 to 0.3 seconds of these records, corresponding to approximately the upper 500 to 600 feet (152-183 m) of the basin-fill units, are of poor quality. Thus, the units cannot be traced to the surface. This fact, combined with the lack of wells with reliable, detailed geologic logs within the basin fill near any of the seismic-reflection profiles, makes characterization of the composition and age of units A, B, and C speculative. The following statements summarize interpreted timing relations between faulting and deposition of the basin-fill units.

1. Unit A overlies units B and C in all of the seismic-reflection profiles, and accumulated during displacement on the EBBFS, continuing to present time.
2. Unit B accumulated entirely during displacement on the EBBFS, and unit C formed during the earliest stages of fault motion.
3. Units B and C exhibit depositional pinchout against the western subsurface basin margin, and are onlapped by unit A.

Interpretation of the seismic-reflection profiles suggests, therefore, that unit A corresponds to all of the exposed Quaternary basin-fill units in Cedar Valley and adjacent hills (units QTa, Qa, Qaf, and Qp on plate 1, and units QTs and Qs on figure 6). Units B and C may correspond to older basin-fill units of map unit Tamf, plate 1 (see Description of Map Units, appendix A), exposed in the Cross Hollow Hills, North Hills, and the eastern Harmony Mountains. These sediments are composed of weakly to well-consolidated, volcaniclastic sedimentary breccia, gravel, sand, and silt derived from the Harmony Mountains and the Pine Valley Mountains (see figure 4 for location) (Averitt, 1967; Anderson and Mehnert, 1979). Unit Tamf is younger than 19 Ma, and its upper age limit is poorly constrained but likely older than about 1 Ma (Anderson and Mehnert, 1979). Possible lithologic changes in these older basin-fill deposits toward the center of the Cedar Valley depositional basin include (1) increased thickness, (2) variation in clast composition to reflect bedrock in adjacent mountains, and (3) addition of interbedded lacustrine deposits, as documented in other extensional basins in arid climates (Leeder and Gawthorpe, 1987).

Basin geometry and structure: Isopach maps depicting the total basin-fill thickness and the thicknesses of seismically defined basin-fill units A, B, and C (figure 10) illustrate the large-scale geometry of the Cedar Valley depositional basin. These isopach maps were derived by calculating the thickness of each basin-fill unit at regularly spaced intervals along each seismic-reflection profile, using the velocities estimated from the depth-conversion process described above. Calculated basin-fill thicknesses are consistent with the logs of water and oil-test wells in the valley.

The total basin-fill isopach map (figure 10a), representing the sum of the thicknesses of units A, B, and C, illustrates the following characteristics of the Cedar Valley depositional basin.

1. North and northeast of Cross Hollow Hills, the basin-fill deposits thicken eastward toward the EBBFS. The area of maximum basin-fill thickness is west of the surface trace of the fault system.
2. The Cedar Valley depositional basin is structurally complex, containing two major longitudinal sub-basins, designated the Rush Lake and Quichapa Lake sub-basins, separated by a low-relief, transverse intrabasin high, and several smaller sub-basins and structural highs.
3. The Cross Hollow Hills and North Hills southwest of Cedar City, and the area northwest of the Three Peaks intrusion near the buried western basin margin, represent structural highs with topographic expression. The isopach map (figure 10a) also reveals buried structural highs not reflected by surface topography within the basin-bounding fault system, located north and south of Enoch. Small-scale structural lows not reflected by surface topography exist: (1) below Cedar City between the Hurricane Cliffs and Cross Hollow Hills, (2) below basalt deposits within the Enoch graben north of Enoch, (3) along the western margin of the Red Hills north of the Rush Lake sub-basin, and (4) north-northwest of Cedar City, designated the Mid- Valley sub-basin.

The Bouguer gravity-anomaly map for Cedar Valley and adjacent areas (figure 11a) closely reflects the large-scale structure of the Cedar Valley depositional basin predicted here from interpretation of the Mobil seismic-reflection profiles. The two large gravity lows are centered roughly on the Rush Lake and Quichapa Lake sub-basins, but are offset from these features to the northwest and southwest, respectively.

EXPLANATION

Map Units

Quaternary

| Qs | Sedimentary deposits

Quaternary-Tertiary

| QTs | Sedimentary deposits

| QTb | Basalt

Tertiary to Triassic

Bedrock

Faults

Normal fault (dotted where concealed)

Folds

Cedar City-Parowan monocline (location approximate)

Contour of basin-fill thickness in feet; contour interval 500 ft. Tick marks point in direction of increasing thickness.

Cedar Valley drainage-basin boundary

704 Seismic-reflection line

A |‾‾‾‾‾‾| A' Cross section line

Wells (table B.3; letter is in ID column of table B.3)

USS ⊕ U.S. Steel borehole

OW1 ⊕ Oil Well
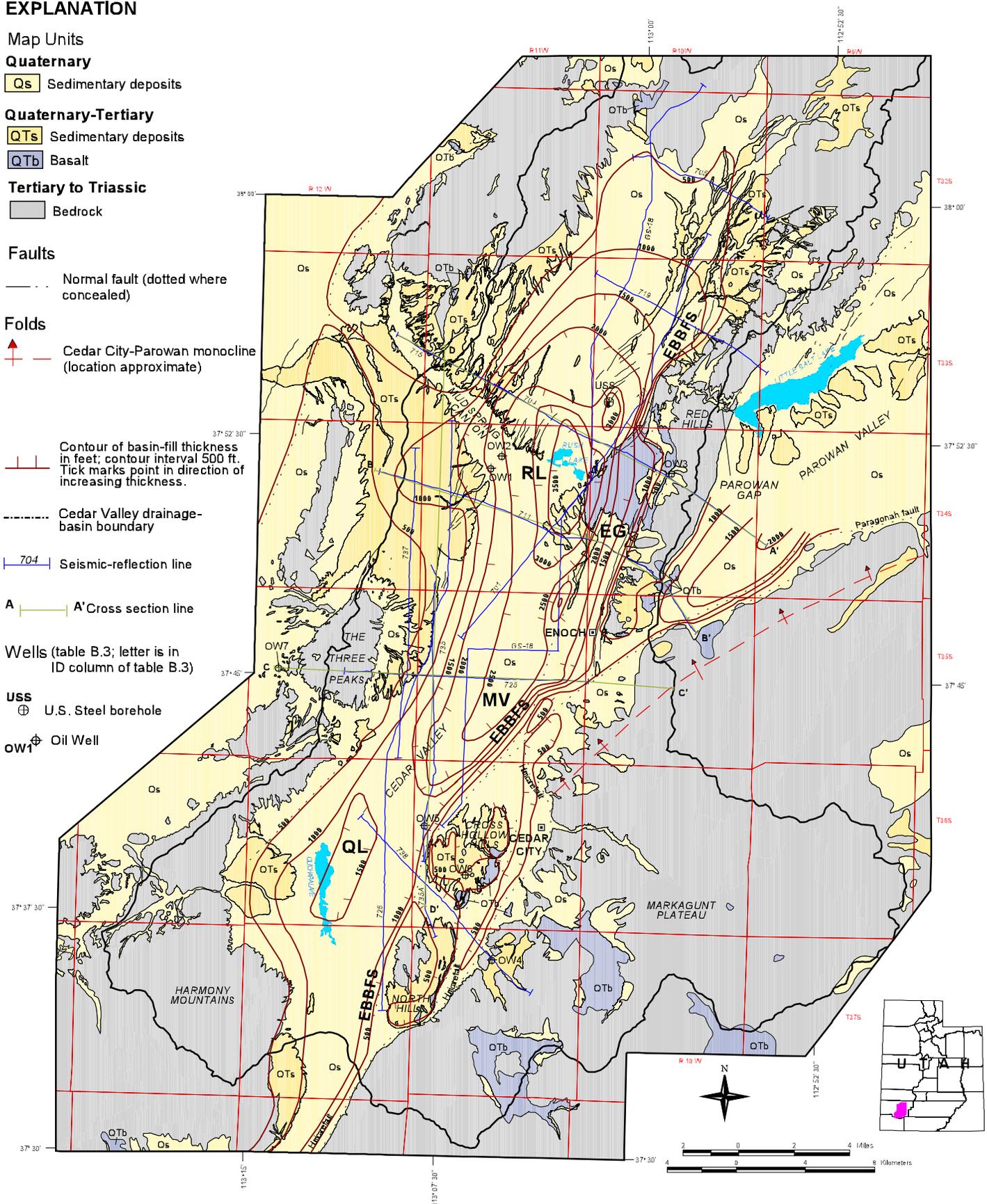
Figure 10A. *Isopach maps of Quaternary-Tertiary basin fill in Cedar Valley: RL - Rush Lake sub-basin; MV - Mid-Valley sub-basin; QL - Quicha-pa Lake sub-basin; EG - Enoch graben. EBBFS is eastern basin-bounding fault system. Entire basin fill, representing the sum of the thicknesses of seismically defined units A, B, and C.*

EXPLANATION

Map Units

Quaternary

Qs Sedimentary deposits

Quaternary-Tertiary

QTs Sedimentary deposits

QTb Basalt

Tertiary to Triassic

Bedrock

Faults

Normal fault (dotted where concealed)

Folds

Cedar City-Parowan monocline (location approximate)

Contour of basin-fill thickness in feet; contour interval 250 ft. Tick marks point in direction of increasing thickness.

Cedar Valley drainage-basin boundary

704 Seismic-reflection line

A ├─────┤ A' Cross section line

Wells (table B.3; letter is in ID column of table B.3)

USS ⊕ U.S. Steel borehole

OW1 ⊕ Oil Well

Figure 10B. *Seismically defined unit A.*

EXPLANATION

Map Units

Quaternary

| Qs | Sedimentary deposits

Quaternary-Tertiary

| QTs | Sedimentary deposits

| QTb | Basalt

Tertiary to Triassic

| | Bedrock

Faults

_____ . . Normal fault (dotted where concealed)

Folds

Cedar City-Parowan monocline (location approximate)

Contour of basin-fill thickness in feet; contour interval 250 ft. Tick marks point in direction of increasing thickness.

Cedar Valley drainage-basin boundary

_704_ Seismic-reflection line

A |_____| A' Cross section line

Wells (table B.3; letter is in ID column of table B.3)

USS U.S. Steel borehole

OW1 Oil Well
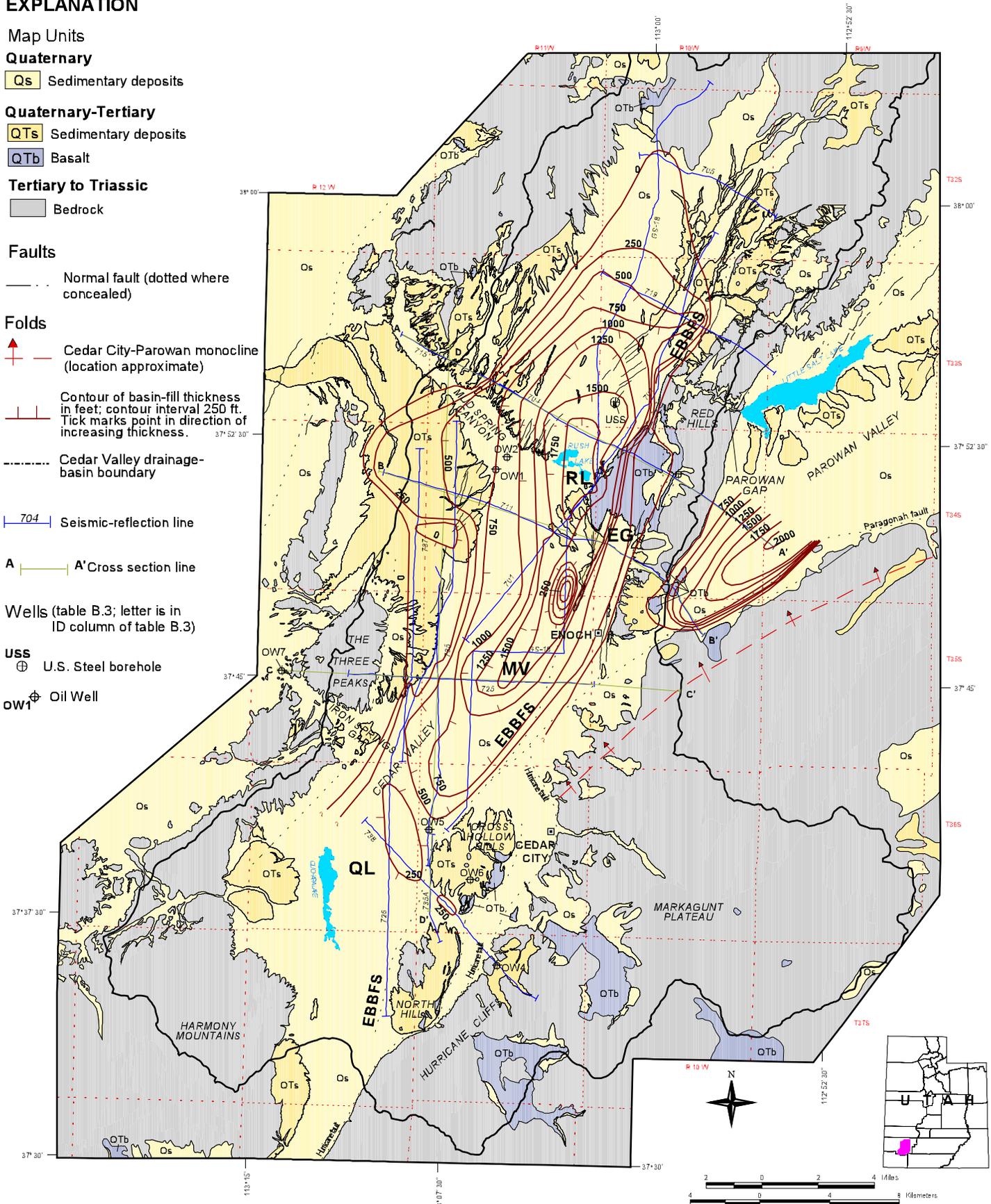
Figure 10C. *Seismically defined unit B.*

EXPLANATION

Map Units

Quaternary

Qs Sedimentary deposits

Quaternary-Tertiary

QTs Sedimentary deposits

QTb Basalt

Tertiary to Triassic

Bedrock

Faults

Normal fault (dotted where concealed)

Folds

Cedar City-Parowan monocline (location approximate)

Contour of basin-fill thickness in feet; contour interval 250 ft. Tick marks point in direction of increasing thickness.

Cedar Valley drainage-basin boundary

704 Seismic-reflection line

A ⊢⊣ A' Cross section line

Wells (table B.3; letter is in ID column of table B.3)

USS
⊕ U.S. Steel borehole

OW1 ⊕ Oil Well
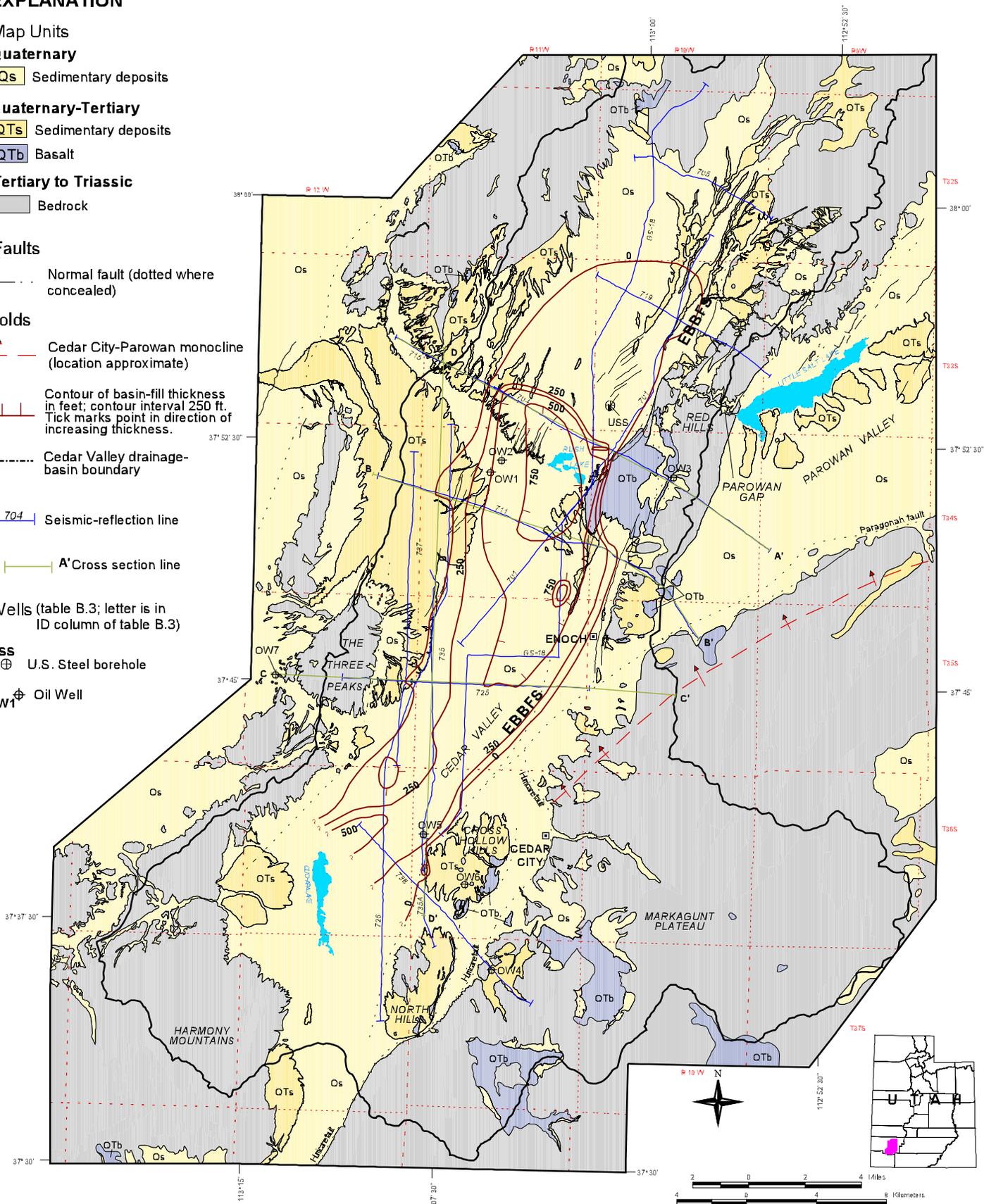
Figure 10D. *Seismically defined unit C.*

Interpretation of the seismic-reflection profiles and previous gravity modeling (Cook and Hardman, 1967) yield nearly identical estimates of the maximum basin-fill thickness below Rush Lake – 3,800 feet (1,160 m) from the seismic-reflection profiles (figure 10a), and 3,900 feet (1,190 m) from modeling of the gravity data by Cook and Hardman (1967). As discussed above, the thickness estimate from the seismic-reflection profiles depends strongly on the velocities chosen for the basin-fill units, which were derived to fit the Odessa Cedar City #1 well (well OW5, table B.3) located in a shallower part of the basin far from the Rush Lake sub-basin. Velocity estimation proceeded without knowledge of the resultant maximum basin thickness.

Based on their modeling of the Bouguer gravity-anomaly values, Cook and Hardman (1967, their figure 2) interpreted Cedar Valley as a graben bounded on the east and west by steeply dipping, planar normal faults of significant displacement (figure 12a). In their interpretation, the eastward thickening of the basin results from the presence of a relatively flat-floored sub-graben in the eastern part of the basin. Interpretation of the Mobil seismic-reflection profiles (cross sections A-A′ through C-C′, plate 2) suggests a different structure and evolution of the Cedar Valley basin.

The Mobil seismic-reflection profiles indicate that Cedar Valley basin is an asymmetric sag (Anderson and others, 1983) in the hanging wall of the EBBFS. The maximum displacement on the EBBFS is about 6,000 to 7,500 feet (1,830-2,285 m), greatly exceeding that on the western faults (cross sections A-A′ through C-C′, plate 2). This interpretation is consistent with a generalized cross section by Williams and Maldonado (1995, p. 259) (figure 12b), although the EBBFS is interpreted here to have a more complex listric geometry with both concave-upward and convex-upward shapes at different locations.

The complicated geometry of the basin-bounding faults at depth may result from (1) use of basin-fill velocities that are too slow, causing an apparent rise in fault surfaces and contacts underlying the basin, (2) soling of listric normal faults into gently dipping, relatively planar parts of pre-existing thrust faults above deeper, more steeply dipping ramps, or (3) incorrect interpretation of the geometry of the basin-bounding faults at depth. Basin-fill velocities were not adjusted after the initial depth conversions to produce geometrically simple fault surfaces, due to the coincidence between basin depths calculated from seismic and gravity (Cook and Hardman, 1967) methods, as described above. Although great care was taken in locating the EBBFS and other faults on the seismic-reflection profiles, this process was subjective, as described above, and other workers may interpret the same profiles differently.

Multiple generations of faults having opposite sense of displacement would likely result in complicated fault-plane geometries, and is considered here the most likely explanation for the fault geometries displayed on plate 2. This interpretation is best supported by seismic-reflection profiles 704 and 715 (figure 9), with corresponding cross section A-A′ (plate 2). Based on regional relations, the angular unconformity visible on the eastern part of the profile must be the base of Tertiary-age deposits, so formations below this unconformity must be Mesozoic age. Restoration of normal displacement on the EBBFS (not shown) places the depositional contacts between Mesozoic units in the hanging wall higher than those in the footwall, and results in a moderately west-dipping structural panel of Mesozoic rocks in the hanging wall, contrasting with the gently dipping footwall. The interpreted pre-extensional structure is a gently to moderately west-dipping thrust juxtaposing a hanging wall of moderately west-dipping Mesozoic rocks against a subjacent, gently dipping footwall composed of the same formations. The EBBFS initiated as steeply dipping normal faults near the surface that curved to shallower dips to meet the pre-existing thrust faults at depth. Such relations are common elsewhere along the eastern margin of the Basin and Range Province (Smith and Bruhn, 1984). Subsidence of the EBBFS hanging wall created the Cedar Valley depositional basin. Tertiary volcanic rocks that covered the region prior to normal faulting were buried below basin-fill sediment in Cedar Valley, and were largely eroded from adjacent, uplifting areas in the footwall of the EBBFS.

The seismic-reflection profiles do not confirm the presence of major east-side-down normal faults along the western basin margin or in the basin interior. Cross section A-A′ (plate 2) depicts the only normal fault cutting the western basin margin revealed by the seismic-reflection data. Steep Bouguer-gravity and aeromagnetic gradients are present in western Cedar Valley above the buried southeastern margin of the Three Peaks laccolith (figure 11) (Cook and Hardman, 1967; Blank and Mackin, 1967). These gravity and magnetic gradients, which result from strong density and magnetic contrasts, respectively, between the laccolith and adjacent basin-fill sediment, indicate that the southeastern laccolith margin is relatively abrupt but do not require a major east-side-down normal-fault system.

The isopach maps constructed for each of the seismically defined basin-fill units (figures 10b, 10c, and 10d) reveal important details not shown by the cumulative thickness map (figure 10a). Thickness variations in unit A define four sub-basins (figure 10b): (1) southeast of Rush Lake, directly west of the EBBFS, (2) in the Enoch graben, (3) northeast of Quichapa Lake, and (4) between the Cross Hollow Hills and the Hurricane Cliffs. Structural highs within unit A include the Cross Hollow and North Hills, a small subsurface uplift northwest of Cedar City, and the northern part of Cedar Valley (figure 10b).

The isopach pattern for unit B defines sub-basins below Rush Lake, in the geographic center of the valley (denoted as Mid-Valley sub-basin), and in the Enoch graben (figure 10c). The Mid-Valley and Rush Lake sub-basins are separated by a broad, northwest-trending buried intrabasin platform, and the Mid-Valley and Quichapa Lake sub-basins are separated by a more pronounced, northwest-trending intrabasin ridge. These intrabasin structural highs subsided more slowly than the adjacent sub-basins, but nonetheless accumulated sediment above them and may or may not have been positive topographic features at times during their evolution.

The isopach pattern for unit C also reflects the presence of the Rush Lake and Quichapa Lake sub-basins (figure 10d). Unit C likely accumulated during the early stages of displacement on the EBBFS.

Composition and Facies Distribution

Holocene basin-fill sediments in Cedar Valley include silt, sand, gravel, and clay (figure 13). These sediments

EXPLANATION

Map Units

Quaternary

| Qs | Sedimentary deposits |

Quaternary-Tertiary

| QTs | Sedimentary deposits |
| QTb | Basalt |

Tertiary to Triassic

Bedrock

Faults

——— . . Normal fault (dotted where concealed)

Folds

Cedar City-Parowan monocline (location approximate)

Contour of bouguer gravity anomaly, in mgal; contour interval 2 mgal. Tick marks point in direction of decreasing bouguer anomaly.

—— . —— . —— Cedar Valley drainage-basin boundary

|—704—| Seismic-reflection line

A |———| A' Cross section line

Wells (table B.3; letter is in ID column of table B.3)

USS
⊕   U.S. Steel borehole

OW1 ⊕   Oil Well
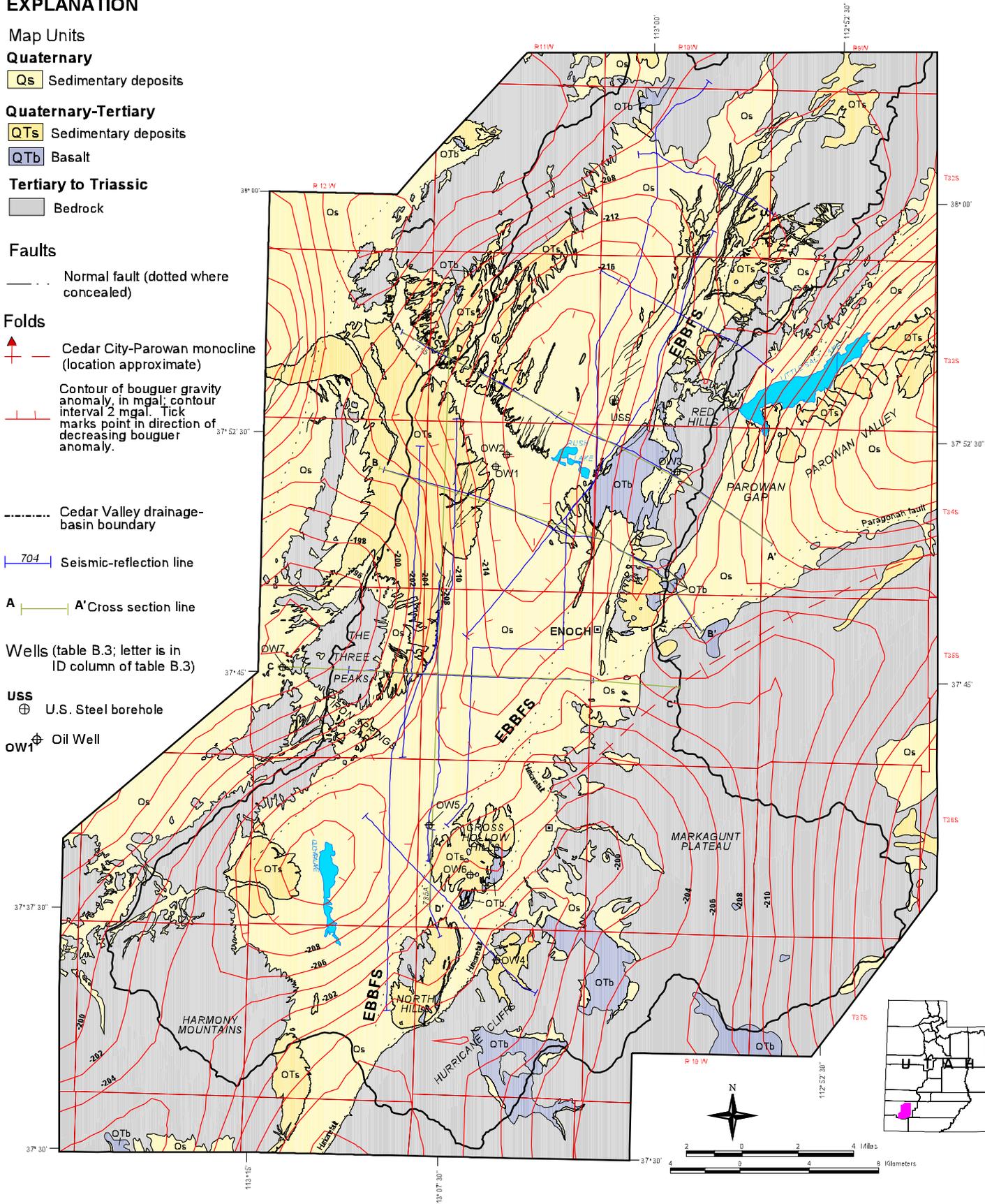
Figure 11A. *Bouguer gravity and aeromagnetic anomaly data for Cedar Valley and adjacent areas. Data from Bankey and others (1998). EBBFS is eastern basin-bounding fault system. A. Bouguer gravity-anomaly map.*

EXPLANATION

Map Units

Quaternary

| Qs | Sedimentary deposits

Quaternary-Tertiary

| QTs | Sedimentary deposits

| QTb | Basalt

Tertiary to Triassic

Bedrock

Faults

Normal fault (dotted where concealed)

Folds

Cedar City-Parowan monocline (location approximate)

Contour of aeromagnetic anomaly, in nanotesla; contour interval 25 nanotesla. Tick marks point in direction of decreasing anomaly value.

Interpreted subsurface margin of Three Peaks laccolith

This study

Blank and Mackin (1967)

Cedar Valley drainage-basin boundary

704 Seismic-reflection line

A ———— A' Cross section line

Wells (table B.3; letter is in ID column of table B.3)

USS
⊕ U.S. Steel borehole

OW1 ⊕ Oil Well
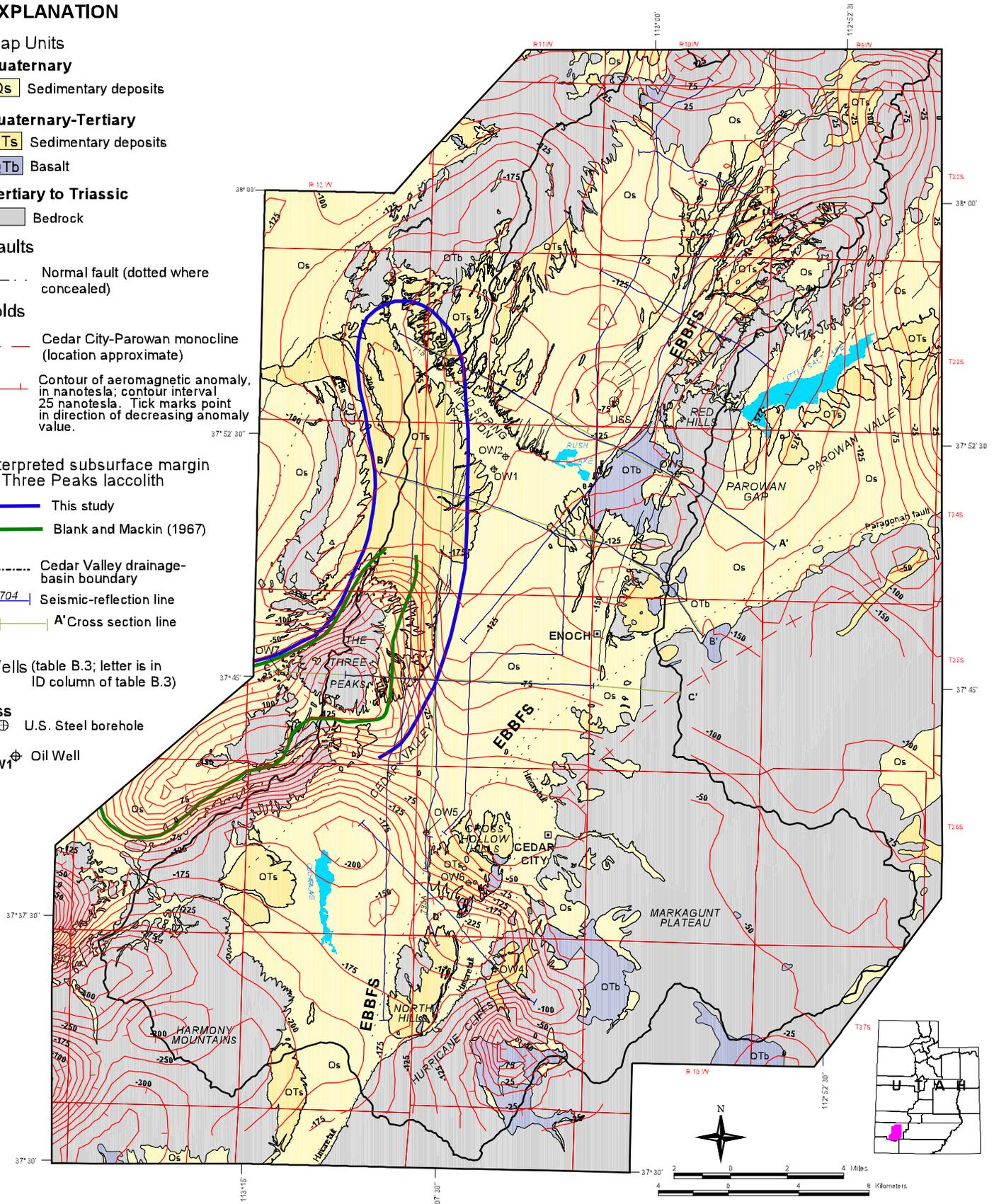
Figure 11B. Aeromagnetic-anomaly map.
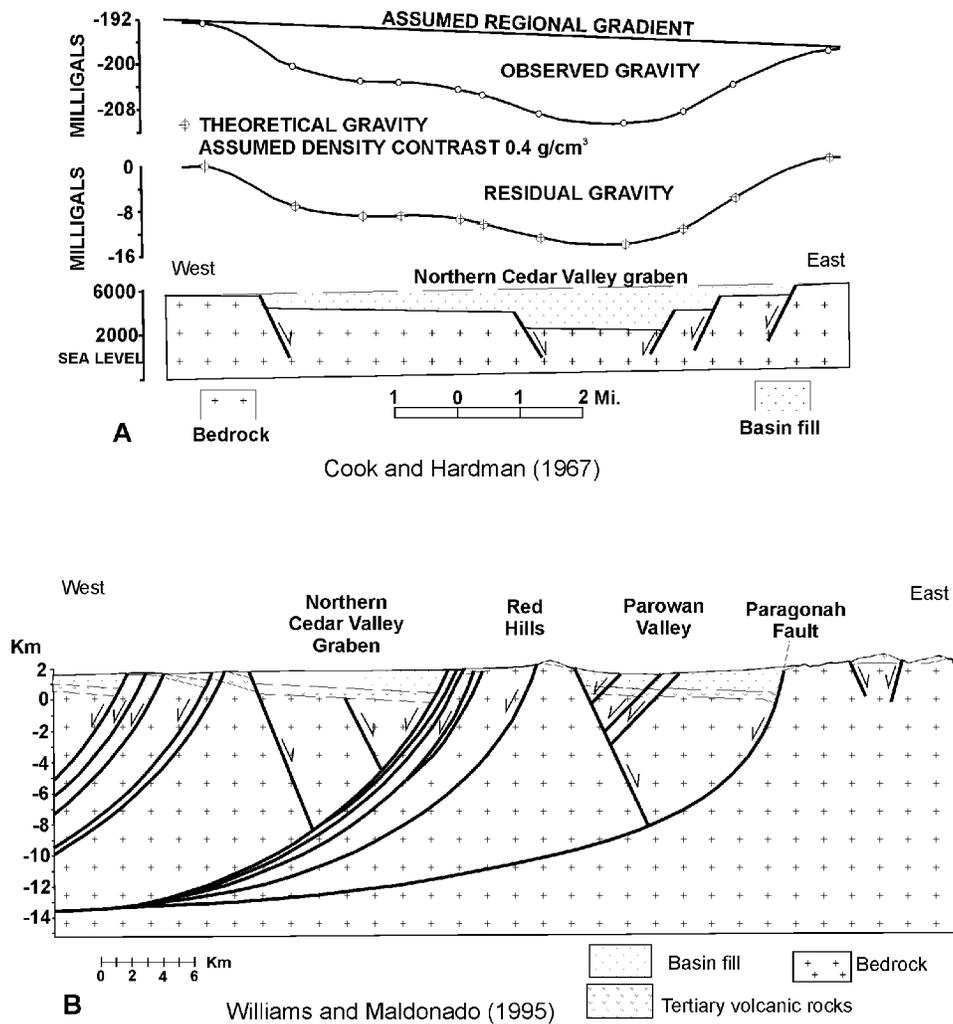
Figure 12. *Previous interpretations of the structure of northern Cedar Valley basin.* **A.** *Redrawn from figure 2 of Cook and Hardman (1967, p. 1,067).* **B.** *Redrawn from figure 2 of Williams and Maldonado (1995, p. 259).*

accumulated in fluvial and distal alluvial-fan (map unit Qa, plate 1), proximal to medial alluvial-fan (map unit Qaf, plate 1), and playa (map unit Qp, plate 1) environments. Proximal alluvial-fan deposits are present along the valley margins and are poorly sorted with poorly defined layering. Medial to distal alluvial-fan deposits show decreasing grain size and increasing sorting and layering toward the valley interior, and grade into fluvial deposits characterized by comparatively finer average grain size and greater sorting and layering. Playa deposits consist of fine-grained, locally gypsiferous sand, silt, and clay. Holocene deposits in Cedar Valley are probably up to 150 feet (46 m) thick along the eastern valley margin and in the Coal Creek alluvial fan below and northwest of Cedar City, and 25 to 100 feet thick (8-31 m) between Mud Spring Canyon and the southern part of the North Hills, although these values are not well constrained. North of Mud Spring Canyon, Holocene deposits form a gravel veneer above older alluvial-fan deposits (unit QTa) (Rowley, 1976; Rowley and Threet, 1976) and thin deposits in active washes, except along the western margin of the Red Hills where they are at least 100 feet (31 m) thick (Maldonado and Williams, 1993a, 1993b). Map units Qa, Qaf, and Qp correlate with the upper part of seismically defined basin-

fill unit A (figures 5 and A.1).

Pleistocene and Pliocene basin-fill deposits (map unit QTs; figure 13) include weakly consolidated to unconsolidated sand, silt, and clay, interbedded along the valley margins with semi-consolidated to consolidated gravel and sedimentary breccia, all deposited in alluvial-fan and fluvial environments (Rowley, 1976; Rowley and Threet, 1976; Maldonado and Williams, 1993b). Average grain size decreases and the degree of sorting and layering increases toward the valley center. As in other Tertiary extensional basins in the Basin and Range Province, the alluvial deposits are likely interbedded with lacustrine deposits in the central and eastern part of the valley (Anderson and others, 1983; Leeder and Gawthorpe, 1987). Map unit QTa likely correlates with the middle to lower part of seismically defined basin-fill unit A (figures 5 and A.1).

Three schematic cross sections constructed from well drillers' logs (figure 15) show that the Cedar Valley basin-fill deposits consist of interbedded medium- to coarse- and fine-grained deposits at scales of tens to several tens of feet. No individual deposit extends laterally for more than about a mile (1.6 km), although the imprecision of the drillers' logs may obscure the identification of some laterally persistent

A

B
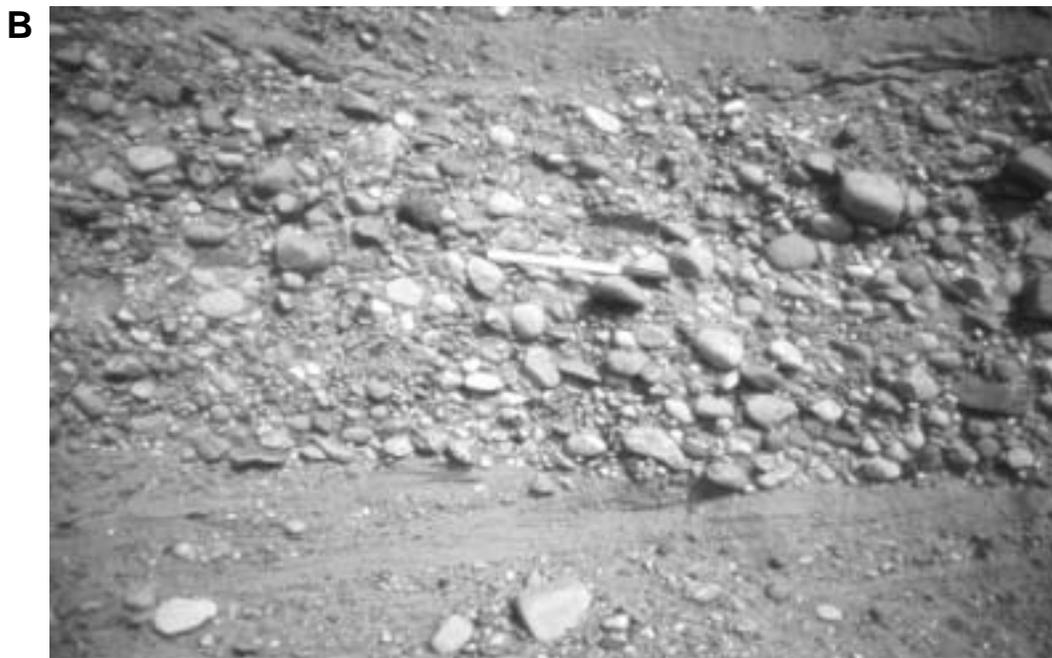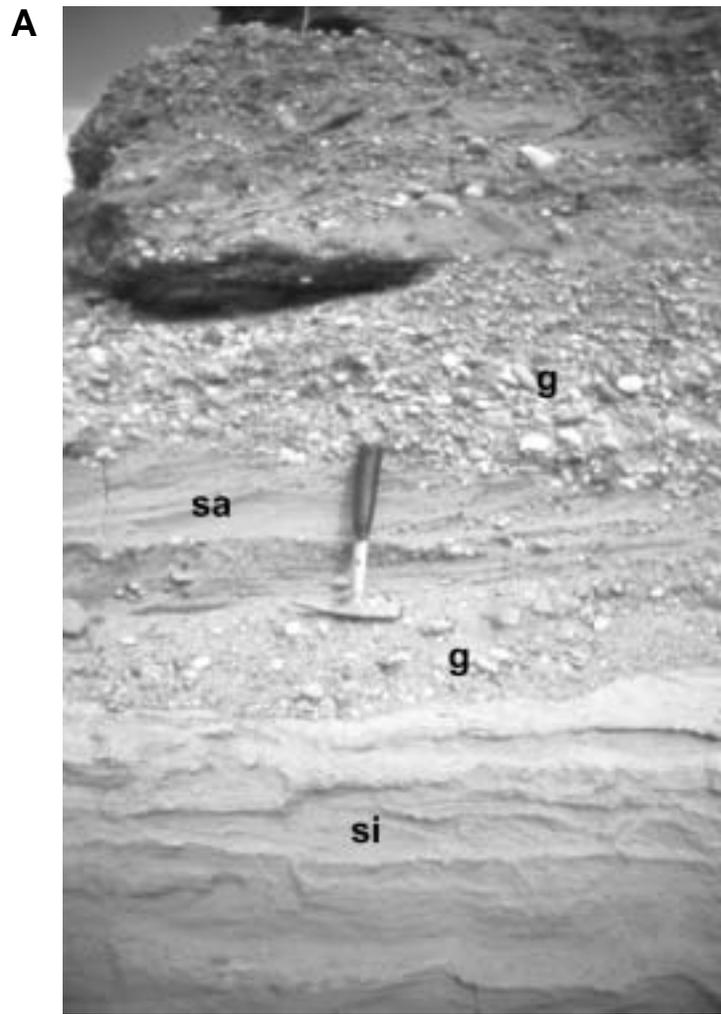
Figure 13AB. *Photographs of basin-fill deposits in Cedar Valley. **A.** Alluvial-fan deposits of Coal Creek, exposed in a quarry on the southwest corner of Cedar City Municipal Airport. Deposits are unconsolidated, interlayered gravel (g), sand (sa), and silt (si) of map unit Qaf. Hammer is 11 inches (23 cm) long. **B.** Closer view of interlayered gravel and sand, exposed in same quarry as figure 13A. Pen is 6 inches (15 cm) long.*

C

D
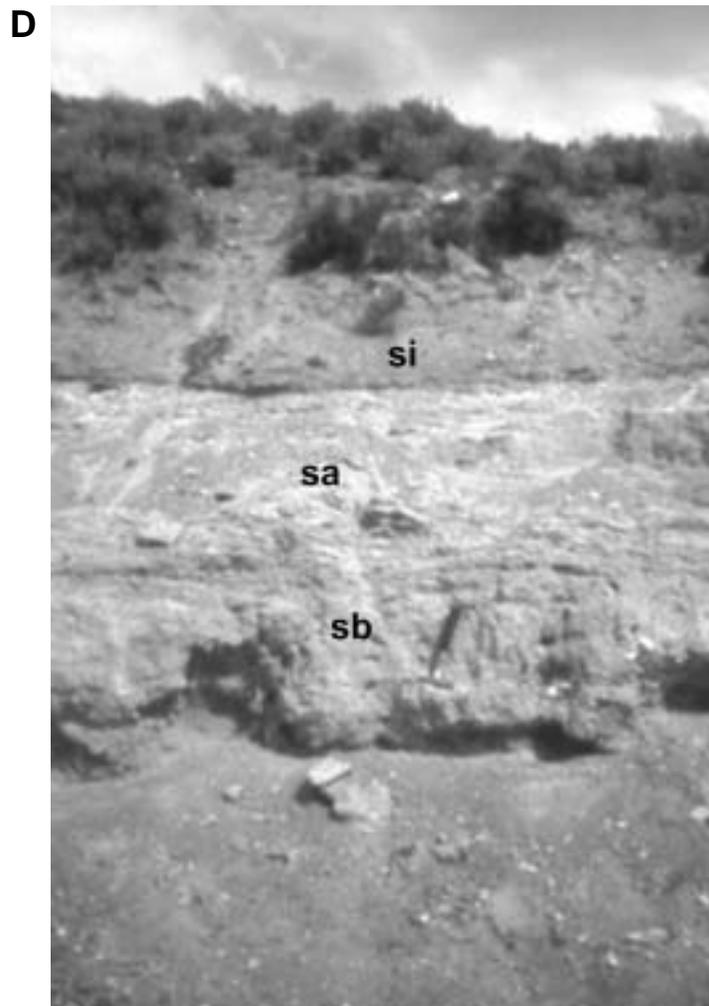
Figure 13CD. C. *Weakly consolidated to unconsolidated boulder gravel of map unit QTa, exposed in south-draining wash in the southeastern part of the North Hills in southeastern Cedar Valley. Clasts include monzonite of Pine Valley, Claron and Iron Springs Formations, and quartzite pebbles. Hammer is 11 inches (23 cm) long.* ***D.*** *Moderately to weakly consolidated silt (si), sand (sa) sedimentary breccia (sb) of map unit QTa, exposed on the eastern wall of upper Lost Spring Hollow, in northern Cedar Valley. Hammer is 11 inches (23 cm) long.*

Figure 13EF.   E. Silty sand of map unit QTa, exposed on the eastern wall of upper Lost Spring Hollow, in northern Cedar Valley. Hammer is 11 inches (23 cm) long. F. Moderately consolidated to cemented pebble gravel overlying moderately consolidated sedimentary breccia, both of map unit QTa. Exposed along the southwestern margin of Mud Spring Canyon in northwestern Cedar Valley. Hammer is 11 inches (23 cm) long.

EXPLANATION

Map Units

Quaternary

Qs Sedimentary deposits

Quaternary-Tertiary

QTs Sedimentary deposits

QTb Basalt

Tertiary to Triassic

Bedrock

Faults

— · · Normal fault (dotted where concealed)

Folds

Cedar City-Parowan monocline (location approximate)

E ——— E' Cross-section line (figures 15a-d)

— · · — · · Cedar Valley drainage-basin boundary

Wells (number is in ID column of corresponding data table)

J2 ● Well logged by Wallace (2001) (see table B.3)

E3 ● Well used to construct cross section (see table B.4)
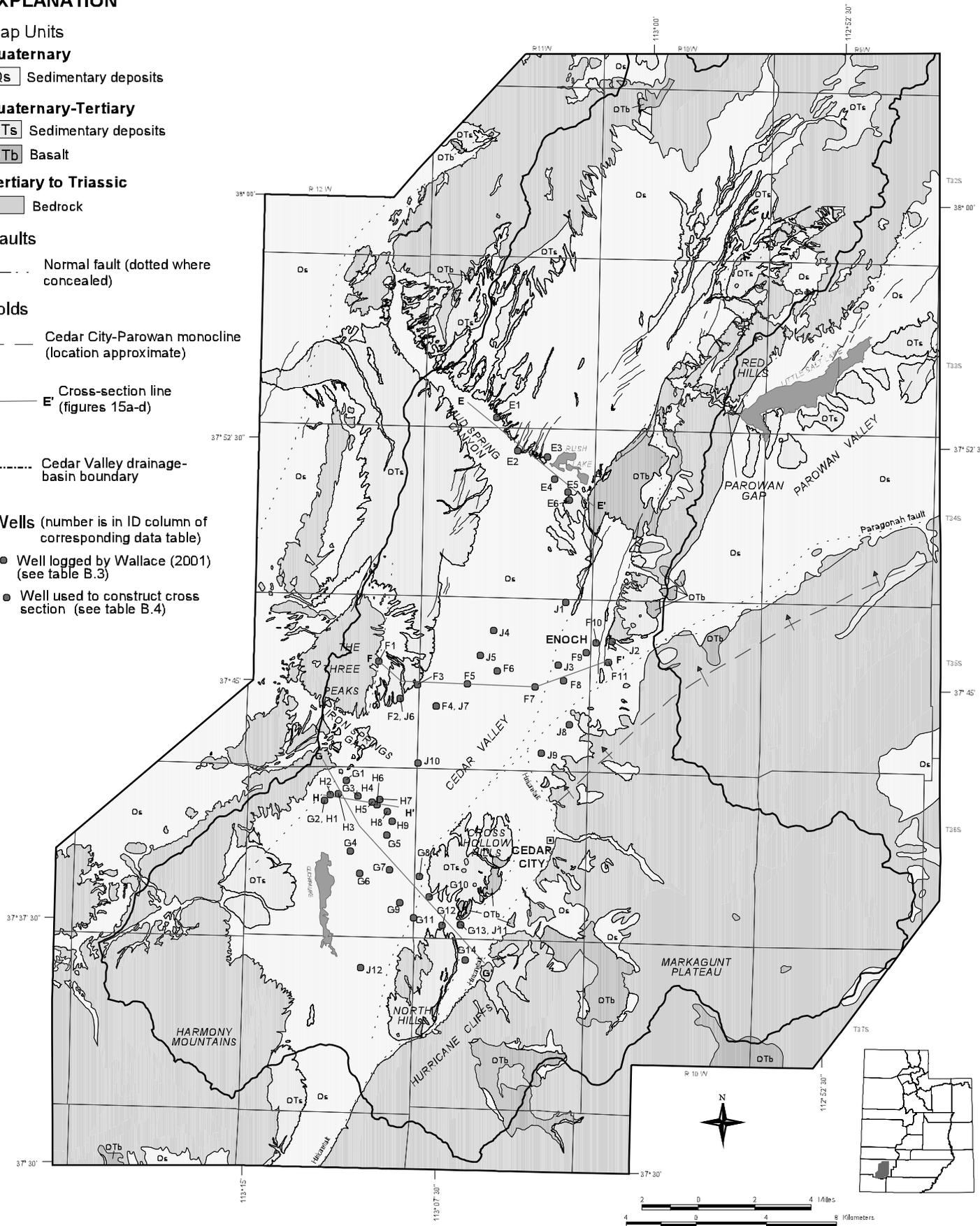
Figure 14. Location of cross sections (see figure 15) through Cedar Valley basin fill and wells used to construct them.
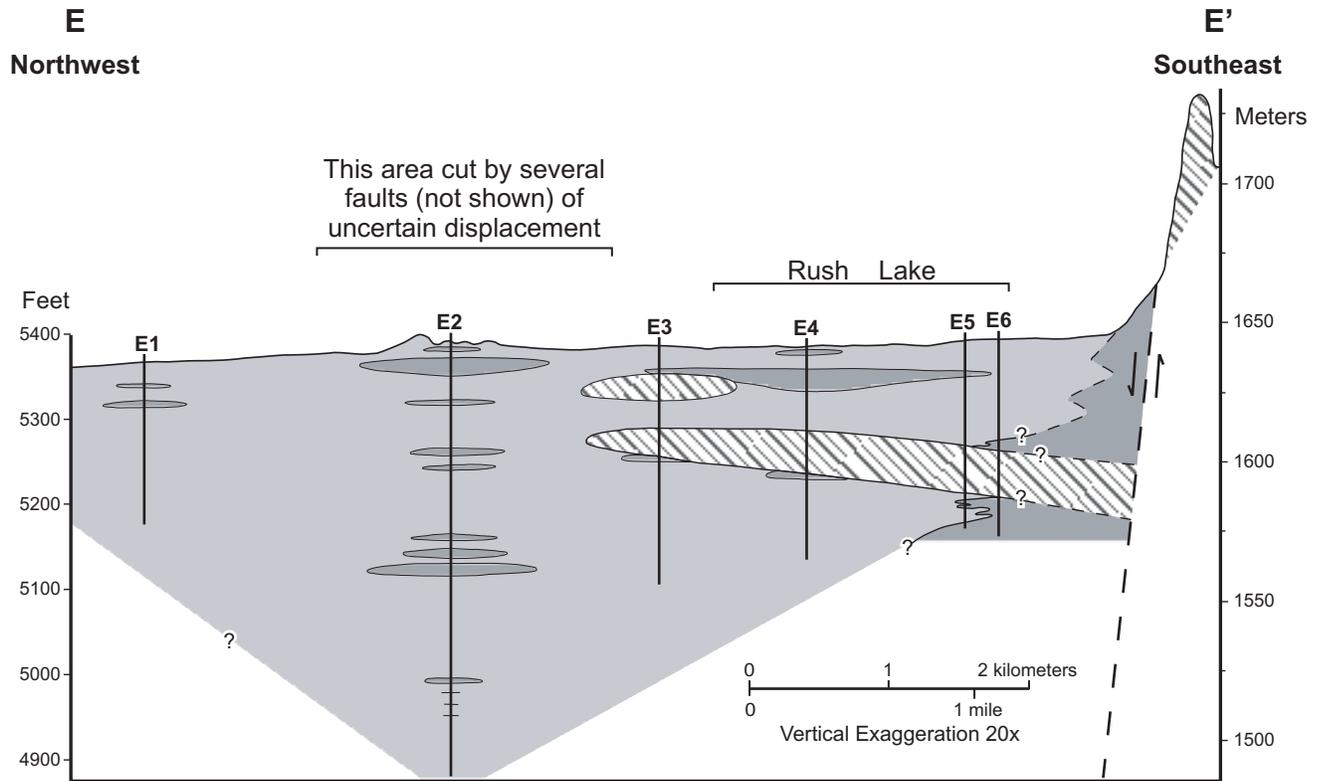
A. Northern Cedar Valley.
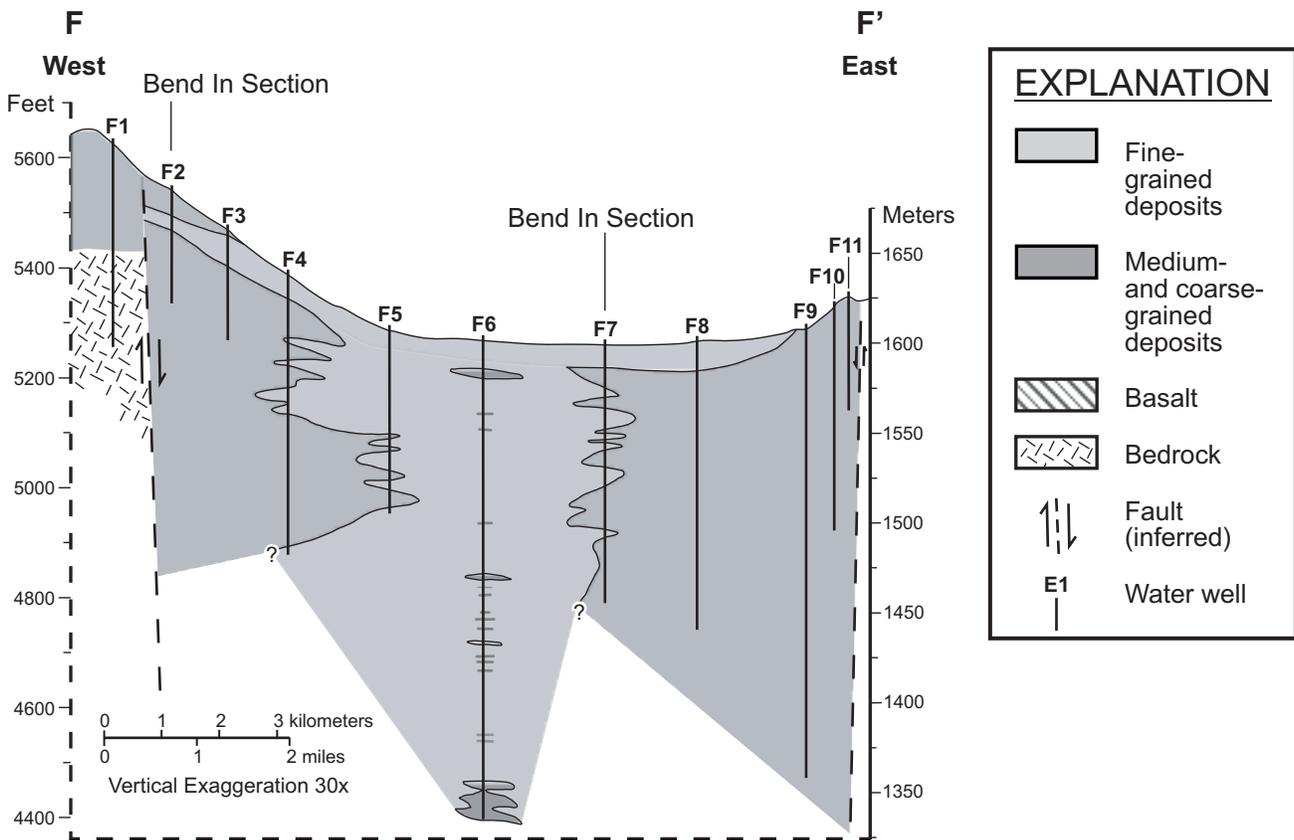
B. Central Cedar Valley.

Figure 15. Schematic cross sections of basin-fill deposits in Cedar Valley. See figure 14 for location and table B.4 for well data.
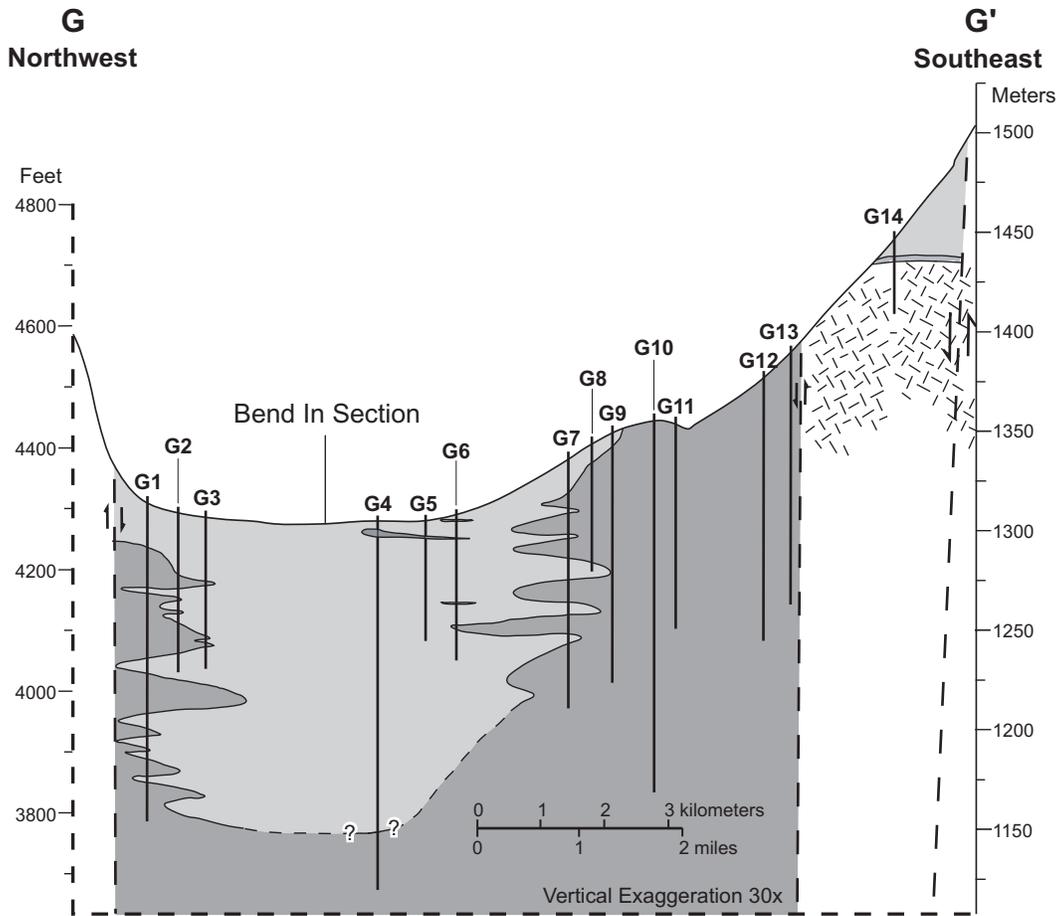
C. *Southwestern Cedar Valley.*
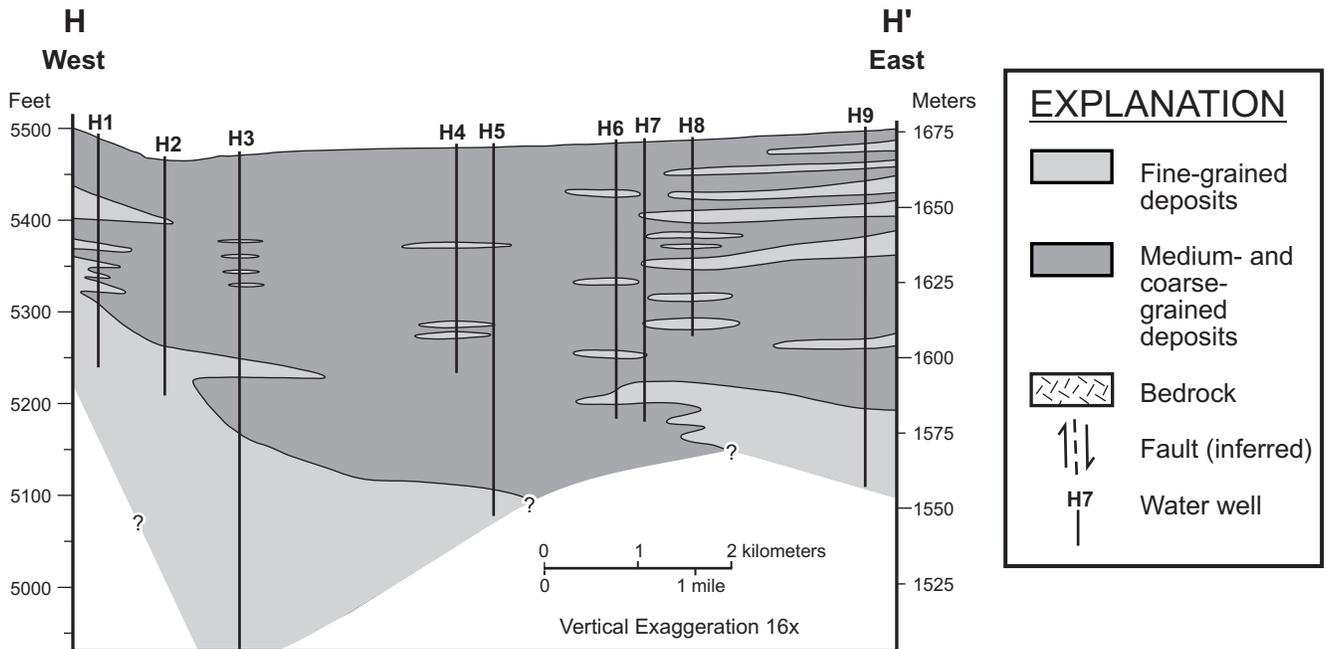
D. *Near west-central margin.*

Figure 15. *(continued)*

beds. The relative proportion of medium- and coarse-grained deposits to fine-grained deposits decreases from the valley margins toward the valley center, and the upper 25 to 100 feet (7-30 m) is commonly finer grained than underlying deposits, similar to trends observed in surface exposures.

Evolution of Cedar Valley Depositional Basin and Related Faults

The geometry and contact relations of the basin-fill deposits, older rock units, and faults interpreted from the Mobil seismic-reflection profiles, coupled with map relations and regional chronology, elucidate the depositional and structural evolution of Cedar Valley, as summarized in the following paragraphs and figure 16. Based on limited constraints on the timing and nature of faulting events in the region, and on the interpretive nature of the Cedar Valley basin-fill stratigraphy, the following history of the Cedar Valley depositional basin and related normal faults should be considered preliminary.

Prior to about 21 Ma, a topographically subdued volcanic plain characterized the land surface of southwestern Utah, and Cedar Valley did not exist, as indicated by the uniform regional distribution and gradual thickness changes of Miocene ash-flow tuffs erupted from eastern Nevada and southwestern Utah (Mackin, 1960; Rowley and others, 1979). Intrusion of the quartz monzonite laccoliths of the Iron Axis created a northeast-trending topographic ridge defined by the axes of the intrusions (Hacker, 1998). This ridge became the western margin of the Cedar Valley depositional basin after normal faulting commenced. Basin-fill unit C is interpreted to represent sediment derived from the Iron Axis topographic high.

Formation of the Cedar Valley depositional basin commenced with initiation of the EBBFS, causing hanging-wall subsidence and footwall uplift. Material eroded from the footwall and from the Iron Axis topographic ridge accumulated in the hanging-wall basin, forming seismically defined basin-fill units B and C. The geometry of units B and C and their relation to the basin-bounding faults are very similar to other published seismic-reflection profiles of Tertiary synextensional basins in the Basin and Range Province (Anderson and others, 1983; Effimoff and Pinezich, 1986).

The development of sub-basins within a larger synextensional depositional basin is common throughout the Basin and Range (Anderson and others, 1983; Effimoff and Pinezich, 1986; Schlische and Anders, 1996), and can be interpreted in terms of a model expressing the relation between faulting and basin development by Schlishce and Anders (1996) (figure 17). In this model, the sub-basin structure is related to initiation of the main basin-bounding fault system as a series of approximately co-linear, unconnected faults (figure 17, stage 1). The initial faults lengthen parallel to their strikes as displacement continues (figure 17, stage 2). This style of fault growth produces longitudinal basins adjacent to each fault, characterized by maximum cumulative hanging-wall subsidence and basin-fill thickness at the geometric center of the fault, and by an oval shape in plan view with the long axis parallel to the fault. Longitudinal sub-basins separated by transverse intrabasin highs characterize the early synextensional basin structure (figure 17,

stage 2). The intrabasin has a low subsidence rate due to its position between the fault centers, and may be bounded by displacement-transfer fault zones (Schlische and Anders, 1996; Faulds and Varga, 1998). After the propagating faults intersect, the two sub-basins are unified into one basin bounded by a single fault system, and the intrabasin high acquires the greatest subsidence rate within the basin by virtue of its position at the new geometric center of the basin-bounding fault system (figure 17, stage 3). This leads to burial of the intrabasin high and topographic leveling of the basin, concealing the sub-basin topography.

Applying the above model to the Cedar Valley depositional basin, the Rush Lake sub-basin originated in the hanging wall of a northeast-striking normal fault along the western margin of the present-day Red Hills, the Mid-Valley sub-basin originated in the hanging wall of a now concealed normal fault south and slightly east of the fault bounding the Rush Lake sub-basin, and the Quichapa Lake sub-basin originated in the hanging wall of a northeast-striking normal fault northwest of the present-day North Hills and Cross Hollow Hills (figure 16). Deposition of seismically defined basin-fill unit B accompanied faulting and related basin subsidence. A northwest-trending, transverse intrabasin high separated the Quichapa Lake and Mid-Valley sub-basins, and a northwest-trending, broad topographic bench separated the Mid-Valley and Rush Lake sub-basins (figure 16). It is uncertain when the initial basin-bounding faults became linked. The Paragonah fault, the main basin-bounding fault of the Parowan Valley depositional basin east-northeast of Cedar Valley (figure 6), likely initiated at about the same time as the Cedar Valley EBBFS (Williams and Maldonado, 1995; Maldonado and others, 1997).

The timing of initial motion on the Cedar Valley EBBFS is not well defined. Rowley and others (1979) and Anderson and Mehnert (1979) noted that on the northwestern margin of Cedar Valley, basalt flows dated at about 9 to 10 Ma are interbedded with basin-fill deposits overlying Miocene volcanic rocks, and deduced that motion on the EBBFS began around 10 Ma. The interpretations presented above suggest, however, that faulting and basin formation began prior to 10 Ma. The deposits described by Anderson and Mehnert (1979) and Rowley and others (1979) are not the earliest basin-fill deposits of Cedar Valley, but are part of seismically defined basin-fill unit A, which overlies synextensional basin-fill units B and C. Major displacement on Basin and Range normal faults began around 12 Ma in northern Utah and southeastern Nevada (Stewart, 1998), implying a similar time of initiation of the Cedar Valley EBBFS.

The Enoch graben and Mid-Valley sub-basins initiated during deposition of unit B, in a structurally complex zone between the faults bounding the Quichapa Lake and Rush Lake sub-basins (figure 16). The northern boundary of this zone trends northwest, and is co-linear with the northern boundary of the Rush Lake sub-basin. The northern boundary of the Enoch graben is also coincident with the southern boundary of exposures of the Jurassic Navajo Sandstone in the footwall of the EBBFS. These exposures may represent a local culmination of Cretaceous-Paleocene thrust-related structures that is probably bounded on the north and south by northwest-trending transverse faults and/or ramps. The southern ramp or fault is interpreted here to localize the northern boundaries of the Enoch graben and Rush Lake sub-basin.
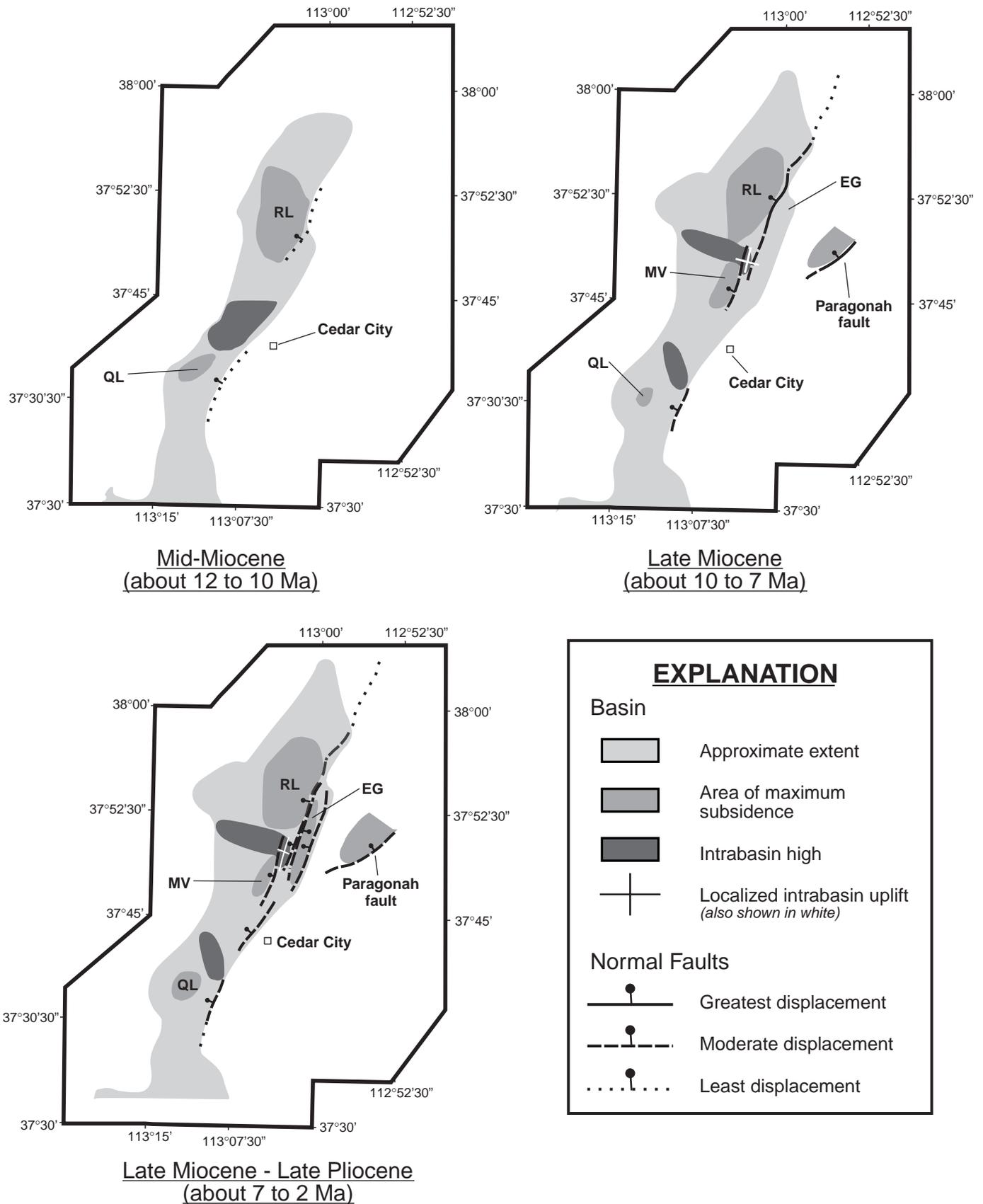
Figure 16. *Schematic diagrams depicting Tertiary to Quaternary evolution of basin subsidence and faulting in Cedar Valley, based on isopach maps in figure 10 and geologic data discussed in text. RL - Rush Lake sub-basin; QL - Quichapa Lake sub-basin; MV - Mid-Valley sub-basin; EG - Enoch graben; CHH - Cross Hollow Hills; NH - North Hills; CC - Cedar City sub-basin.*

Late Pliocene - early Quaternary
(about 2 to 1 Ma)

Mid-Quaternary - Holocene
(about 1 Ma to present)

EXPLANATION

Basin

Approximate extent

Area of maximum subsidence

Intrabasin high

Localized intrabasin uplift

Cedar City - Parowan monocline

Normal Faults

Greatest displacement

Moderate displacement

Least displacement
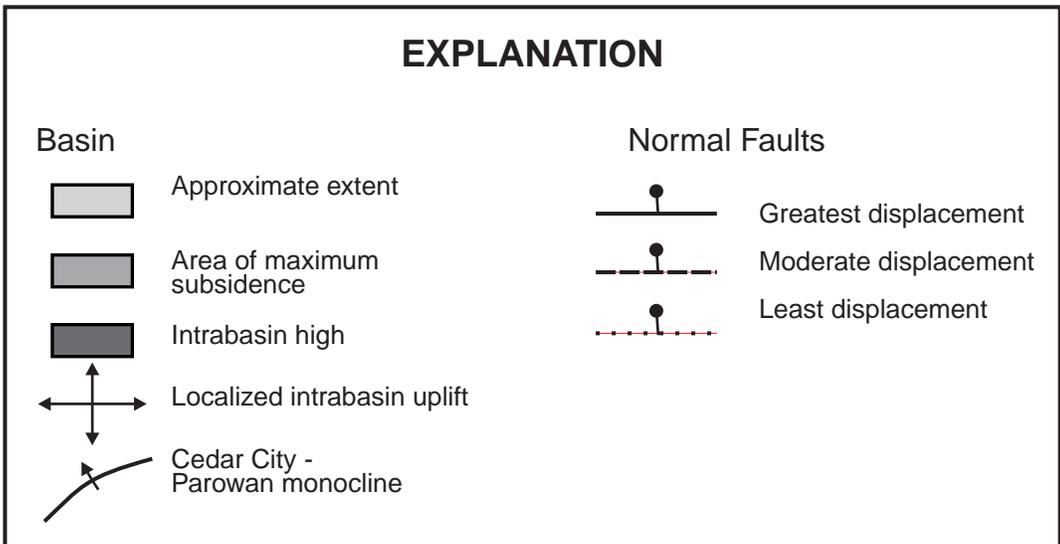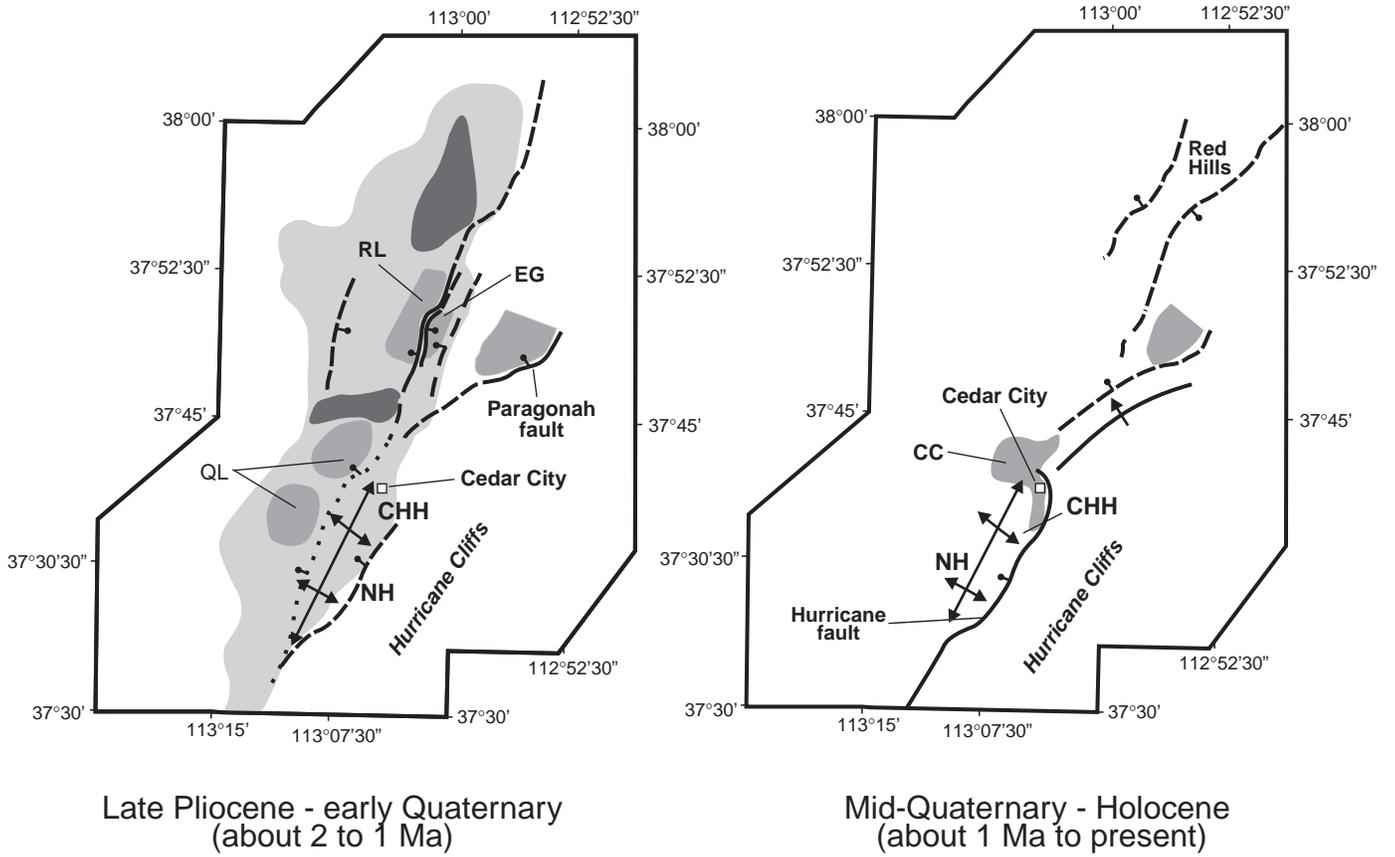
Figure 16. *(continued)*
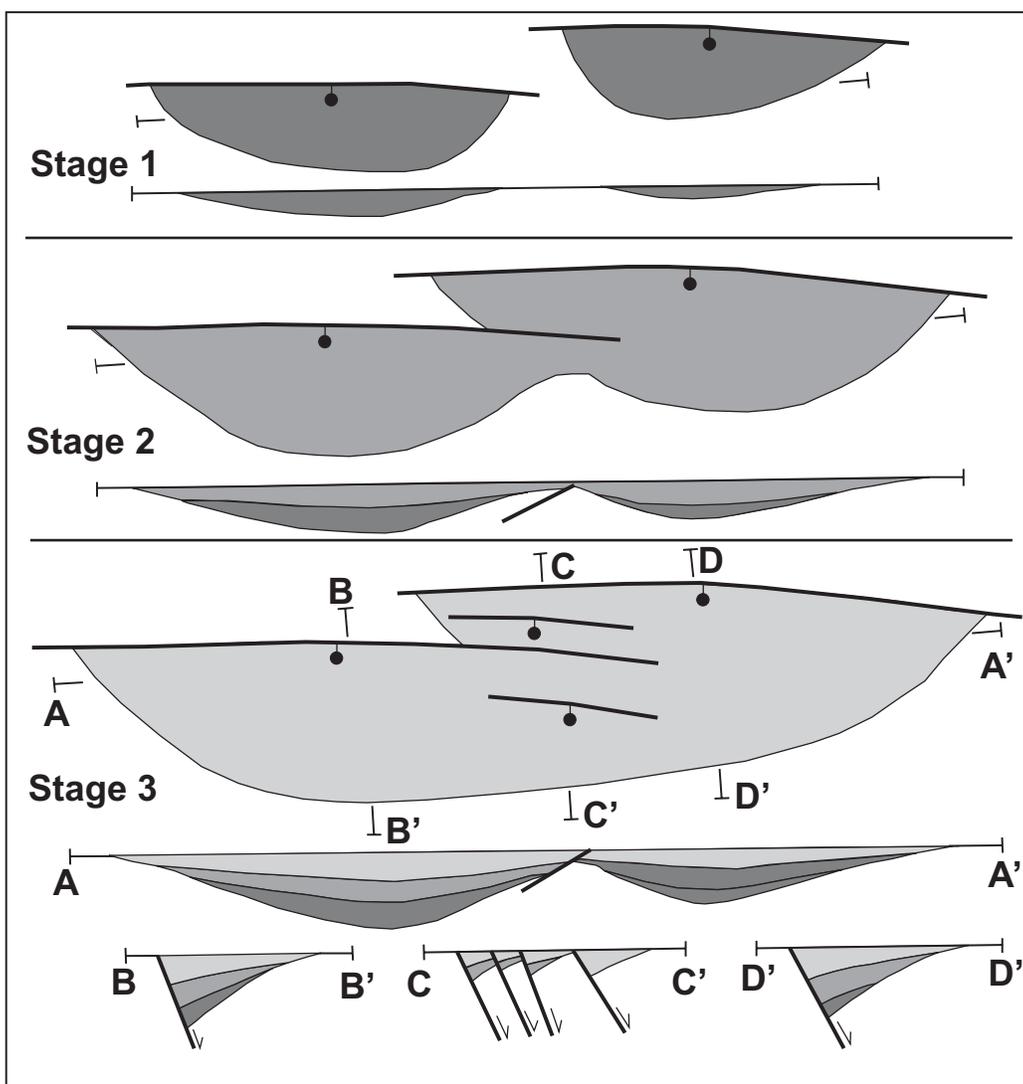
Figure 17. *Basin growth and filling model for two closely overlapping fault segments. From Schlishce and Anders (1996).*

Uplift of the North Hills, Cross Hollow Hills, and the buried culmination east of the Mid-Valley sub-basin likely began during deposition of unit A (figure 16). The North Hills and Cross Hollow Hills are complexly faulted antiforms in the footwall of the fault bounding the eastern margin of the Quichapa Lake sub-basin, and are in the hanging wall of the Hurricane fault (Anderson and Mehnert, 1979). The structural culmination below Enoch is in the footwall of the normal fault bounding the eastern margin of the Mid-Valley sub-basin, and in the hanging wall of the fault that forms the western boundary of the Enoch graben. The mechanisms causing the uplift of these localized culminations are unclear, though deposition of the Tertiary Claron Formation on the Jurassic Navajo Sandstone in the North Hills (plate 1; Averitt, 1967) indicates that this area was a structural high during Cretaceous to Paleocene contractional deformation.

Subsidence in the Cedar Valley depositional basin changed during the early stages of deposition of unit A (figure 16). The locus of maximum subsidence in the Quichapa Lake sub-basin and the associated intrabasin high both moved northeastward. The Quichapa Lake sub-basin moved

to a position above the transverse intrabasin high formerly bounding its northern margin, and the intrabasin high encroached on the Mid-Valley sub-basin, which ceased active subsidence. This northeastward movement may have been caused by impingement of the southwest-propagating Paragonah fault on the central part of the Cedar Valley EBBFS (figure 16). Such impingement would have reduced the net horizontal displacement rate across the EBBFS by placing its footwall in the hanging wall of the Paragonah fault. The Rush Lake sub-basin continued to subside and expand, and subsidence along the western margin of the Enoch graben increased during this time.

The structural and depositional setting of Cedar Valley also changed during the late stages of deposition of unit A, after early Pleistocene time (figure 16). Displacement on the southwestern part of the EBBFS ceased, but continued along the segment bounding the western Red Hills (figure 16) (Williams and Maldonado, 1995). South of the Red Hills, active normal faulting shifted east, due to initiation of movement on the Hurricane fault (figure 16) (Anderson and Mehnert, 1979). North of Cedar City, displacement on the Hurricane fault apparently transfers into the Cedar City-

Parowan monocline (figure 6; plate 1) (Threet, 1963; Andeson and Mehnert, 1979). Subsidence of the Cedar Valley land surface slowed, as did the deposition rate of unit A. Subsidence in the hanging wall of the Hurricane fault created the Cedar City sub-basin east of the Cross Hollow Hills, and uplift of its footwall formed the Hurricane Cliffs (figure 16). Deformation of the Cross Hollow Hills and North Hills antiforms in the hanging wall of the Hurricane fault continued after 1 Ma, as demonstrated by tilting and faulting of dated basalt flows in these areas (Anderson and Mehnert, 1979). Onlap of the upper part of unit A over the basin margins and continued deposition in the basin center concealed some of the topography related to the complex sub-basin structure that had previously characterized the Cedar Valley depositional basin. The topographic depressions around present-day Rush Lake and Quichapa Lake, and the subtle, transverse intrabasin high that separates them are interpreted here as relics of earlier topography and sub-basin structure in Cedar Valley.

TRANSMISSIVITY ESTIMATES FOR THE BASIN-FILL AQUIFER

Introduction

Bjorklund and others (1978, their plate 2 and pages 21-23) calculated and illustrated the transmissivity of the Cedar Valley basin-fill aquifer. Transmissivity estimates for post-1978 water wells are calculated here and combined with the results of Bjorklund and others (1978) to improve the spatial distribution and accuracy of transmissivity estimates for Cedar Valley.

Previous Work

Bjorklund and others (1978) estimated the transmissivity of the Cedar Valley basin-fill aquifer from specific-capacity data for 51 wells, using

(1) $T = Q/(h_0-h) \times (2.3/4\pi) \times \log(2.25Tt/r^2S)$ (Theis, 1963)

where:

h_0 = Pre-test water level in the well.
h = Post-test water level.
$Q(h_0-h)$ = Specific capacity of the well, in cubic feet per day per foot of drawdown.
t = Test duration, in hours.
r = Radius of the pumping well, in feet.
T = Aquifer transmissivity, in square feet per day.
S = Aquifer storativity (dimensionless).

Solution of equation (1) is iterative; an initial value for T is used in the right side of the equation, and is adjusted until the solution and the initial value converge. The equation also requires an independent estimate for S, assumes 100 percent well efficiency, and does not account for well-bore storage (Fetter, 1994, p. 256).

Transmissivity estimates using equation (1) were 40 to 60 percent lower than estimates from more rigorous aquifer tests in which the discharge rate and ground-water levels in the pumped well and up to three observation wells were

monitored (Bjorklund and others, 1978). To adjust for this systematic difference, Bjorklund and others (1978, p. 23) increased their transmissivity estimates from equation (1) by an unspecified amount, presumably 50 percent. Their results showed that transmissivity of the Cedar Valley basin-fill aquifer is greatest in alluvial-fan deposits on the east-central (near Cedar City), southwestern, and north-central valley margins. Bjorklund and others (1977) provided specific capacity values for the wells used in their calculations, but did not document (1) their resultant transmissivity estimates, (2) the pumping duration of the tests, or (3) the storativity values they used. Because the calculations of Bjorkland and others (1977, 1978) cannot be reproduced without the data listed above, new transmissivity estimates for the same wells were calculated for this study.

Methods

The new transmissivity estimates for wells used by Bjorkland and others (1977, 1978) employ the equation of Razack and Huntley (1991, in Fetter, 1994, p. 257),

(2) $T = 33.6(Q/[h_0-h])^{0.67}$

where:

T = Transmissivity, in square feet per day.
Q = Pumping rate, in cubic feet per day.
h_0-h = Drawdown in feet.

Equation (2) is based on an empirical relation between specific capacity and transmissivity for 215 water wells in an alluvial ground-water basin in Morocco. Table 1 presents transmissivity estimates using equation (2) for water wells used by Bjorklund and others (1977, 1978).

For post-1977 wells, transmissivity estimates from specific-capacity tests of eight hours or longer were calculated using the algorithm TGUESS (Bradbury and Rothschild, 1985). This algorithm is more accurate than equations (1) and (2) because it accounts for partial penetration of the aquifer, perforation of less than the entire casing, removal of water stored in the well bore during the early stages of the tests, and less than 100 percent well efficiency (Bradbury and Rothschild, 1985). Table 2 presents transmissivity estimates using TGUESS for specific-capacity test data from post-1978 water wells in Cedar Valley.

Specific-capacity test data from drillers' logs of six of the wells used by Bjorklund and others (1977, 1978) are sufficient to use in TGUESS (table 3). These corrected values are used in the following analysis.

Results from the two methods of estimating transmissivity from specific-capacity tests described above must be combined to increase the density and spatial distribution of data points in Cedar Valley over those presented by Bjorklund and others (1978). Figure 18a and tables 1 and 2 show that transmissivity estimates using equation (2) are systematically greater than those using TGUESS for the same wells, and figure 18b shows that the percent difference between the two methods decreases with increasing transmissivity values. Linear regression of the natural logs of transmissivity estimates from the two methods (figure 19) yields the equation:

(3) $\ln(T1) = 1.6(\pm0.01)x(\ln T2) - 6.2(\pm0.09)$

where:

T1 = Transmissivity estimate using TGUESS.
T2 = Transmissivity estimate using equation (2).

The goodness-of-fit (R^2) of equation (3) is 0.997, indicating an excellent fit to the data.

The transmissivity estimates for wells used by Bjorklund and others (1977, 1978), derived using equation (2), were adjusted using equation (3) to make them more consistent with transmissivity estimates for post-1978 wells derived using TGUESS (table 1).

Table 4 shows data and results from aquifer tests reported by Bjorklund and others (1978) and from six more recent aquifer tests. These estimates are considered more accurate than those derived using equations (1) through (3). Transmissivity estimates from different observation wells from the same test may be fairly consistent, or may vary considerably (compare tests T-2, T-4, and T-10, table 4). This variability is likely a function of both the heterogeneity of the basin-fill aquifer and imperfect test conditions (variable pumping rate, for example).

Results

Table 4 and figure 20 compare transmissivity estimates derived using TGUESS with estimates from the same wells derived from more sophisticated analysis of the aquifer-test data. The estimates from TGUESS are within 30 percent of those from aquifer tests for drawdown data indicating transmissivity of less than about 10,000 square feet per day (930 m^2/d). For recovery data and for tests indicating transmissivity of greater than about 10,000 square feet per day (930 m^2/d), TGUESS provides a poor match to aquifer-test results. Transmissivity estimates from specific-capacity data in this study may be either higher or lower than those from aquifer-test data from the same wells, in contrast with the results of Bjorklund and others (1978, p. 23) noted above.

Figure 21 shows the distribution of transmissivity estimates for the Cedar Valley basin-fill aquifer determined in this study, as described above. Transmissivity values range from over 20,000 square feet per day (1,860 m^2/d) near the eastern and southeastern valley margins to less than 5,000 square feet per day (465 m^2/d) in the valley center. The distribution of estimated transmissivity in figure 21 is more complicated than, but generally consistent with, the results of Bjorklund and others (1978). These results show variations and approximate magnitudes of the transmissivity of the basin-fill aquifer at a valley-wide scale, but should not be used to estimate or predict hydrologic properties at specific locations.

HYDROGEOLOGIC IMPLICATIONS OF BASIN-FILL GEOLOGY

Relations Among Transmissivity, Facies Distribution, and Stratigraphy

Figure 21 shows that transmissivity varies systematically with sediment type in Cedar Valley, as Bjorklund and oth-

ers (1978) concluded. The transmissivity values generally range from 10,000 to 20,000 square feet per day (930-1,860 m^2/d) in proximal to medial alluvial-fan deposits (map unit Qaf) along the eastern and southwestern valley margins, and are less than 10,000 square feet per day (930 m^2/d) in stream, distal alluvial-fan, and playa deposits in the valley center. The variations in both sediment characteristics and average transmissivity values are gradual and irregular. Proximal to medial alluvial-fan deposits have greater average grain size, lower degrees of sorting and layering, and fewer clay-rich layers than distal alluvial-fan, stream, and playa deposits. These characteristics likely result in higher average and more homogeneously distributed transmissivity in the proximal to medial alluvial-fan deposits than in the distal deposits. Transmissivity values are likely more heterogeneously distributed in the valley-center deposits, and the transmissivity of individual, well-sorted sand and gravel layers may greatly exceed the average values of the alluvial-fan deposits. As noted by Bjorklund and others (1978), clay-rich layers likely create the leaky confined conditions that predominate in the valley-center deposits by retarding upward flow of ground water in underlying sand and gravel layers, whereas unconfined conditions exist in the poorly layered deposits along the valley margins.

The transmissivity values in figure 21 and tables 1 through 4 are derived from wells screened over a wide range of depths, from about 50 to over 1,000 feet (15-305 m). These wells draw water predominantly from Holocene to middle Quaternary deposits of map units Qa, Qaf, and QTa of plate 1, corresponding to the upper part of seismically defined basin-fill unit A. The Holocene to early Quaternary stream and alluvial-fan deposits of units Qa and Qaf likely have greater transmissivity than the middle Quaternary to Pliocene alluvial deposits of unit QTa, based on field observations described above. The thicknesses of units Qa and Qaf are poorly known, so an isopach map for these deposits cannot be made. The transmissivity of the Cedar Valley basin-fill deposits likely decreases with depth due to increasing compaction and diagenesis.

Influence of Faults and Basin Geometry

Ground water may flow across the EBBFS, from bedrock in the footwall to basin fill in the hanging wall, depending on several factors. Cross-fault flow may be greater where bedrock having moderate to high permeability, such as the Navajo Sandstone, abuts the basin fill than where low-permeability units, such as the upper part of the Chinle Formation, are present. In general, the development of fine-grained fault material along the fault plane and cementation of adjacent rock due to circulation of ground water or geothermal fluids may significantly reduce or eliminate cross-fault permeability (Caine and others, 1996), but the degree of development of such features along the faults bounding the Cedar Valley basin is unknown.

Based on differences in ground-water chemistry across the projected traces of faults in the Enoch graben, Thomas and Taylor (1946) suggested that these faults formed hydrologic barriers within the basin fill. In contrast, Bjorklund and others (1978, p. 26) reported that an aquifer test in Parowan Valley indicated no measurable effects from two faults whose projections passed between the pumping well and

Table 1. *Transmissivity estimates for wells used by Bjorklund and others (1977, 1978) to calculate transmissivity of Cedar Valley basin-fill aquifer, and corrections to these values based on equation (3) in text.*

	LOCATION[b]				RESULTS			
ID[a]	T	R	Sec	Point	SC[c] (gpm/ft)	Transmissivity[d] (ft^2/d)	Corrected Transmissivity[e] (ft^2/d)	T from TGUESS (ft^2/d)[f]
1	33S	10W	31	ada-1	88.0	22900	25900	-
2	33S	10W	31	adb-1	60.0	17700	17000	-
3	33S	12W	14	dda-1	2.0	1810	400	350
4	34S	11W	1	daa-1	17.0	7610	4300	-
5	34S	11W	14	aad-1	100.0	24900	29800	-
6	34S	11W	23	bad-1	9.0	4970	2100	2200
7	34S	11W	36	dcc-2	45.0	14600	12400	-
8	35S	10W	18	cca-1	33.0	11900	8900	-
9	35S	10W	18	ccb-1	20.0	8500	5100	-
10	35S	11W	5	bbc-1	0.7	900	130	-
11	35S	11W	8	dcc-1	3	2380	640	620
12	35S	11W	9	ccc-1	35.0	12300	9400	-
13	35S	11W	12	dcd-1	3.0	2380	640	-
14	35S	11W	12	ddd-1	19.0	8200	4800	-
15	35S	11W	13	cbc-1	16.0	7310	4000	4200
16	35S	11W	13	ddb-1	22.0	9040	5600	-
17	35S	11W	14	aac-1	7.0	4200	1600	1500
18	35S	11W	17	dcd-1	20.0	8480	5100	-
19	35S	11W	21	cdc-1	15.0	7000	3700	-
20	35S	11W	21	dbd-1	17.0	7610	4300	-
21	35S	11W	24	aab-1	83.0	22000	24300	-
22	35S	11W	27	acc-1	14.0	6680	3500	-
23	35S	11W	27	bbc-1	60.0	17700	17000	-
24	35S	11W	27	cdd-1	66.0	18900	19000	-
25	35S	11W	27	dbb-1	33.0	11900	8900	-
26	35S	11W	29	acd-1	21.0	8770	5400	-
27	35S	11W	31	acd-1	18.0	7900	4500	-
28	35S	11W	32	abd-1	24.0	9590	6200	-
29	35S	11W	32	acd-1	22.0	9040	5600	-
30	35S	11W	32	dba-1	6.0	3790	1400	-
31	35S	11W	33	aac-1	51.0	15900	14300	-
32	35S	11W	33	bad-1	18.0	7910	4500	-
33	35S	11W	33	bbd-1	68.0	19300	19600	-
34	35S	11W	34	bad-1	80.0	21500	23400	-
35	35S	12W	27	bbd-1	3.0	2380	640	-
36	35S	12W	27	bca-1	2.0	1810	400	-
37	35S	12W	27	bcb-1	3.0	2380	640	-
38	35S	12W	36	dad-1	3.0	2380	640	-
39	35S	12W	36	dba-1	20.0	8480	5100	-
40	36S	11W	5	cac-1	46.0	14800	12700	-
41	36S	11W	5	cba-1	28.0	10600	7300	-
42	36S	11W	8	abd-1	4.0	2890	880	-
43	36S	11W	8	bba-1	59.0	17500	16700	-
44	36S	11W	18	bca-1	12.0	6030	2900	-
45	36S	12W	20	acc-1	15.0	7000	3700	-
46	36S	12W	25	bdd-1	23.0	9320	5900	-
47	36S	12W	32	ccb-1	45.0	14600	12400	-
48	36S	12W	32	ccc-1	47.0	15000	13000	-
49	37S	12W	5	bbb-1	19.0	8200	4800	-
50	37S	12W	5	bcb-1	18.0	7910	4500	-
51	37S	12W	14	abc-1	24.0	9590	6200	-
52	37S	12W	14	dbd-1	12.0	6030	2900	-
53	37S	12W	23	acb-1	12	6030	2900	-
54	38S	12W	4	cdc-1	0.3	510	50	40

Notes

a. Wells 47, 51, and 53 also have transmissivity estimates from aquifer-test data, included in table 4
    as IDs T2 (= well 47, table 1), T3 (=well 51, table 1), and T4 (= well 53, table 1). For these wells,
    figures 18 and 19 include the transmissivity values from table 1, and figure 20 includes
    the transmissivity values from table 4.
b. Well locations use U.S. Geological Survey (USGS) convention (figure B.1).
    T = Township, R = Range, Sec = Section, relative to Salt Lake 1855 Base Line and Meridian.
c. SC = specific capacity in gallons per minute per foot of drawdown,
    from Bjorklund and others (1977).
d. Transmissivity calculated using equation (2), as described in text.
e. Transmissivity corrected using equation (3), as described in text.
f. Data from table 2.

Table 2. *Transmissivity estimates from specific-capacity tests of Cedar Valley water wells postdating Bjorklund and others (1978).*

	LOCATION[b]				SPECIFIC-CAPACITY TEST DATA[c]							Transmissivity from TGUESS (ft²/sec)[d]	Transmissivity from equation (2) (ft²/sec)[e]
ID[a]	T	R	Sec	POD	Well Diameter (in)	Static Water Level (ft)	Drawdown (ft)	Duration (hr)	Yield (gpm)	Well Depth (ft)	Total Open Interval (ft)		
55	34S	11W	22	S 250 W150 NE	8	102	15	65	17	130	30	250	1240
56	34S	11W	36	S250 E100 W4	6	72	111	168	45	320	80	90	620
57	35S	10W	30	S295 E100 NW	8	302	90	34	142	400	120	330	1550
58	35S	11W	1	N135 E 215 SW	12	53	150	48	151	830	530	200	1150
59	35S	11W	3	N1320 E1320 SW	12	40	230	168	350	690	300	340	1510
60	35S	11W	4	S60 W60 E4	8	62	136	10	125	457	42	170	1080
61	35S	11W	4	S1890 W680 N4	8	50	18	8	30	300	80	310	1600
62	35S	11W	4	N400 W640 E4	8	33	90	10	300	368	33	680	2550
63	35S	11W	9	N1516 W540 SE	8	42	3	14	15	400	120	1080	3350
64	35S	11W	10	S1320 N4	8.63	22	12	18	160	145	25	3150	6470
65	35S	11W	10	N194 E42 SW	8	40	20	15	100	400	200	1090	3350
66	35S	11W	10	S250 S2310 E4	8	29	123	15	200	455	20	320	1580
67	35S	11W	12	S150 W840 E4	8	55	120	8	80	246	11	120	870
68	35S	11W	13	N1367 E138 SW	12	40	90	40	1400	510	65	4180	7170
69	35S	11W	16	N200 W2023 SE	6	35	40	12	75	300	80	390	1740
70	35S	11W	17	S1110 W745 NE	8	70	100	8	50	171	6	80	720
71	35S	11W	19	N1100 E500 S4	8	50	150	13	200	528	46	260	1380
72	35S	11W	19	S720 E1320 W4	12	50	25	34	400	800	600	3910	7300
73	35S	11W	21	N2130 W766 S4	6	70	3	12	50	420	40	4050	7500
74	35S	11W	21	S430 W3827 NE	9	120	40	16	20	450	70	90	720
75	35S	11W	21	S10 E10 NE	16	70	80	40	2000	400	300	8010	9850
76	35S	11W	21	N2675 W2048 S4	8	88	106	11	250	461	20	470	2030
77	35S	11W	24	N80 E80 W4	12	115	180	30	950	286	94	1170	3480
78	35S	11W	26	N823 E1582 W4	8	93	57	10	450	206	76	1750	4550
79	35S	11W	27	N150 E120 W4	10	60	110	17	1500	335	135	3460	6560
80	35S	11W	27	N1771 W50 S4	12	80	120	25	800	261	141	1490	4060
81	35S	11W	30	S1800 W900 NE	8	55	65	10.5	60	278	3	170	1080
82	35S	12W	36	N620 E1320 E4	10	53	52	15	1042	392	240	5220	8500
83	36S	11W	8	S295 E580 W4	16	72	113	12	900	501	300	1630	4580
84	36S	11W	17	S63 E76 NW	10	71	40	12	750	505	140	4610	8130
85	36S	11W	18	S2640 E2640 NW	16	67	130	72	1500	390	280	2960	5870
86	36S	12W	3	S66 E2699 W4	8	55	16	10	172	517	160	2410	5600
87	36S	12W	20	S2364 W700 NE	16	45	200	200	3200	802	640	5570	7300
88	36S	12W	29	S1134 E260 NW	8	145	50	12	70	502	15	270	1430
89	36S	12W	29	S625 W185 NE	8	25	10	48	24	392	16	540	2050
90	36S	12W	30	N660 W330 E4	6	140	20	18	40	203	20	430	1810
91	36S	12W	31	S860 W1100 N4	6	160	10	20	25	305	40	550	2110
92	36S	12W	31	N460 E1853 SW	6	180	40	8	30	360	80	140	940
93	36S	12W	34	N1683 W2458 SE	6	20	50	12	150	550	7	640	2380
94	36S	13W	27	N168 E765 SW	8	80	240	48	16	405	120	10	190
95	36S	13W	28	N1000 W1220 SE	6	219	240	36	3	401	80	2	60
96	37S	12W	1	S100 E1170 NW	8	82	160	20	1000	500	200	1450	3890
97	37S	12W	3	S2452 W197 N4	6	10	20	24	15	356	20	150	940
98	37S	12W	22	N1230 E211 S4	8	41	110	8	100	220	9	160	1070
99	37S	12W	26	N1000 E10 SW	8	58	20	22	50	212	80	530	2110
100	37S	12W	26	N692 E540 SW	6	84	2	12	18	200	80	2090	4970
101	37S	12W	26	S618 W150 NE	8	88	230	20	7.5	390	80	4	120
102	37S	12W	28	N200 E1200 SW	6	126	200	8	100	400	100	90	720
103	38S	12W	5	N1280 W2013 SE	6	170	10	8	25	297	40	510	2110

Notes

a. Wells 82 and 86 also have transmissivity estimates from aquifer-test data, included in table 4 as IDs T7 (=well 82, table 2) and T5 (=well 86, table 2). For these wells, figures 19 and 20 include the transmissivity values from table 2, and figure 20 incudes the transmissivity values from table 4.

b. Well locations use Point of Diversion (POD) (figure B.2) convention. T = Township, R = Range, Sec = Section, relative to Salt Lake 1855 Base Line and Meridian.

c. Data are from well-drillers' logs, available from the Utah Division of Water Rights, online (http://www.waterrights.utah.gov) or as paper files.

d. Methods are discussed in text.

e. Data from table 1.

Table 3. *Wells Bjorklund and others (1977, 1978) used to estimate transmissivity from specific-capacity test data, for which sufficient data are available to also use TGUESS.*

	LOCATION[a]				SPECIFIC-CAPACITY TEST DATA[b]							RESULTS		
ID	T	R	Sec	Point	Well Diameter (in)	Static-Water Level (ft)	Drawdown (ft)	Duration (hr)	Yield (gpm)	Well Depth (ft)	Total Open Interval (ft)	Specific Capacity (gpm/ft)	Transmissivity from TGUESS (ft²/sec)[c]	Transmissivity from equation (2) (ft²/sec)[d]
3	33S	12	14	dda-1	6	48	10	1.5	20	145	7	2	350	1810
6	34S	11	23	bad-1	14	90	160	23	1500	596	396	9	2190	4970
11	35S	11	8	dcc-1	10	45	158	10	500	300	100	3	620	2380
15	35S	11	13	cbc-1	12	22	90	40	1400	516	65	16	4180	7310
17	35S	11	14	aac-1	12	18	100	10	700	660	40	7	1450	4200
54	38S	12	4	cdc-1	8	32	133	2	40	404	37	0.3	40	510

Notes

a. Well locations use U.S. Geological Survey (USGS) convention (figure B.1). T = Township, R = Range, Sec = Section, relative to Salt Lake 1855 Base Line and Meridian.

b. Data are from well-drillers' logs, available from the Utah Division of Water Rights, online (http://www.waterrights.utah.gov) or as paper files.

c. Methods are discussed in text.

d. Data from table 1, shown for comparison with results from TGUESS.

Table 4. *Aquifer-test data for Cedar Valley water wells and comparison of methods of estimating transmissivity.*

IDa	Typeb	LOCATIONc T	R	Sec	USGS	POD	Distance from Pumped Well (ft)	Well Diameter (in)	Static Water Level (ft)	AQUIFER-TEST DATA Drawdown (ft)	Time (hr)	Yield (gpm)	Total Screened Interval	Transmissivity (ft2/day)d	RESULTS Storage Coefficient	Transmissivity from TGUESS (ft2/day)e	Corrected Transmissivity from equation (2) (ft2/day)e
Data from Bjorklund and others (1978)f																	
T1	P	35S	10W	18	cca-1		0	16	97	26.15	95	863	188	5200R	0.2	8000	8800
T2	P	36S	12W	32	ccb-1		0	16	70	30	30	1350	507	-	-	16900	12400
	o	36S	12W	32	ccc-1		652	16	53	28.62	30	1345	249	42000	0.0013	-	-
	o	37S	12W	5	bbb-1		1372	16	90	70.79	30	1345	207	52000	0.01	-	-
	o	37S	12W	5	bcb-1		3100	16	70	74.72	30	1345	182	15000	0.0015	-	-
	o	36S	12W	32	ccc-1		652	16	85	29.79	44	1400	249	46000R	0.0015	-	-
T3	P	37S	12W	14	abc-1		0	14	33	25	14	600	226	10000R	-	5790	6200
T4	P	37S	12W	23	acb-1		0	16	44	70.42	86	845	254	-	-	3080	2900
	o	37S	12W	23	aca-1		1000	16	83	-	86	845	193	2540	0.0005	-	-
	o	37S	12W	23	cbd-1		2650	12	50	-	86	845	197	2700	0.013	-	-
Data from Bulloch Brothers Engineering, Inc.g																	
T5	P	35S	12W	3		S66 E2699 W4	0	8	33.42	16.08	24	165	160	3150	-	3220	2400
T6	P	35S	11W	9		S470 E310 N4	0	12	30.67	56.83	19	237	285	990	-	1170	870
T7	P	35S	12W	36		N620 W1320 E4	0	12	59.83	5.17	11.5	108	240	3630	-	6280	5400
T8	P	36S	12W	7		N209 E845 W4	0	8	60	22.25	21	270	100	4110	-	3840	2900
Data From Lowe and others (2000)h																	
T9	P	36S	12W	25		N1310 W50 S4	0	8	105.25	1.5	1.67	892	480	20900	-	-	-
Data From Utah Division of Water Rights (1980)i																	
T10	P	35S	11W	26	acd-1		0	16	-	-	358	1420	260	-	-	-	-
	o	35S	11W	26	bca		2330	6	-	-	358	-	40	18600	0.048	-	-
	o	35S	11W	26	cba		2370	10	-	-	358	-	145	15400	0.042	-	-

Notes

a. Corresponds to label on figures 20 and 21. T2 = well 47, table 1; T3 = well 51, table 1; T4 = well 53, table 1; T5 = well 86, table 2; and T7 = well 82, table 2.

b. P = pumped well, 0 = observation well.

c. Well locations are in U.S. Geological Survey (USGS) (figure B.1) or Point of Diversion (POD) (figure B.2) notation. T = Township, R = Range, Sec = Section, relative to Salt Lake 1855 Base Line and Meridian.

d. Figures 20 and 21 show these values. R = recovery data; all others are drawdown data.

e. Methods discussed in text.

f. From table 4, page 23 of Bjorkland and others (1978). For aquifer test T2, figure 21 uses a transmissivity of 38,333 square feet/day, the arithmetic mean of the four estimates shown.

g. From S. Finstick, Bulloch Brothers Engineering, Inc., written communication, 1999. Transmissivity values are the average of estimates from drawdown and recovery phases of a single test.

h. From pages 20-21 of Lowe and others (2000). TGUESS could not provide a transmissivity estimate for this test because it could not converge on a solution within 25 iterations.

i. Static water level and drawdown data are unavailable, precluding use of TGUESS.

A

B
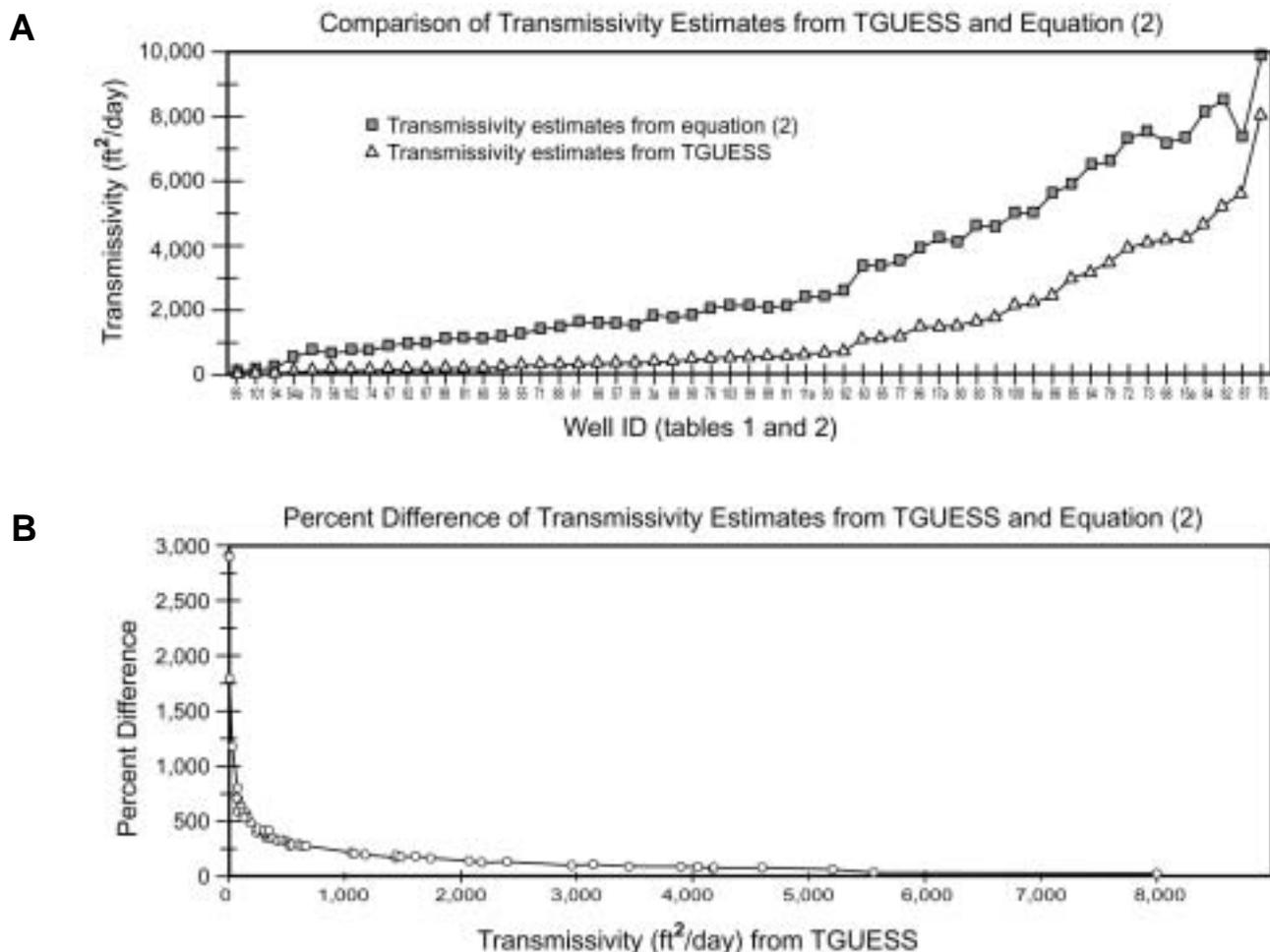
Figure 18AB. *Comparison of transmissivity estimates from TGUESS and equation (2).* **A.** *Plot of transmissivity estimate versus well ID (tables 1 and 2), arranged in order of increasing transmissivity. Transmissivity estimates from TGUESS (Bradbury and Rothschild, 1985) are considered more accurate and are consistently lower than those from equation (2).* **B.** *Plot of percent difference between transmissivity estimates using TGUESS and equation (2) against transmissivity calculated from TGUESS. Transmissivity estimates from the two methods are highly disparate for low transmissivity values, but converge with increasing transmissivity. Percent difference calculated from data in tables 1, 2, and 3.*
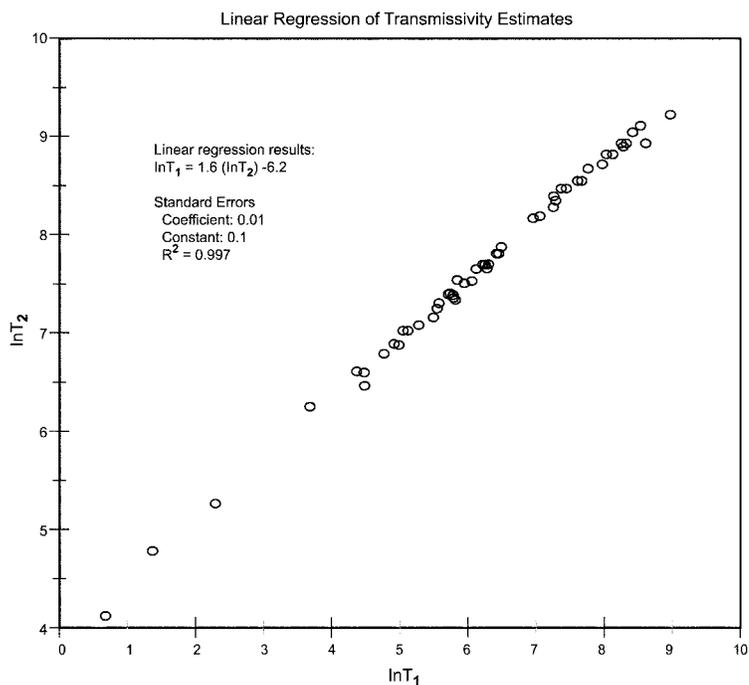
Figure 19. *Linear regression of transmissivity estimates from TGUESS (T_1) and equation 2 (T_2).*
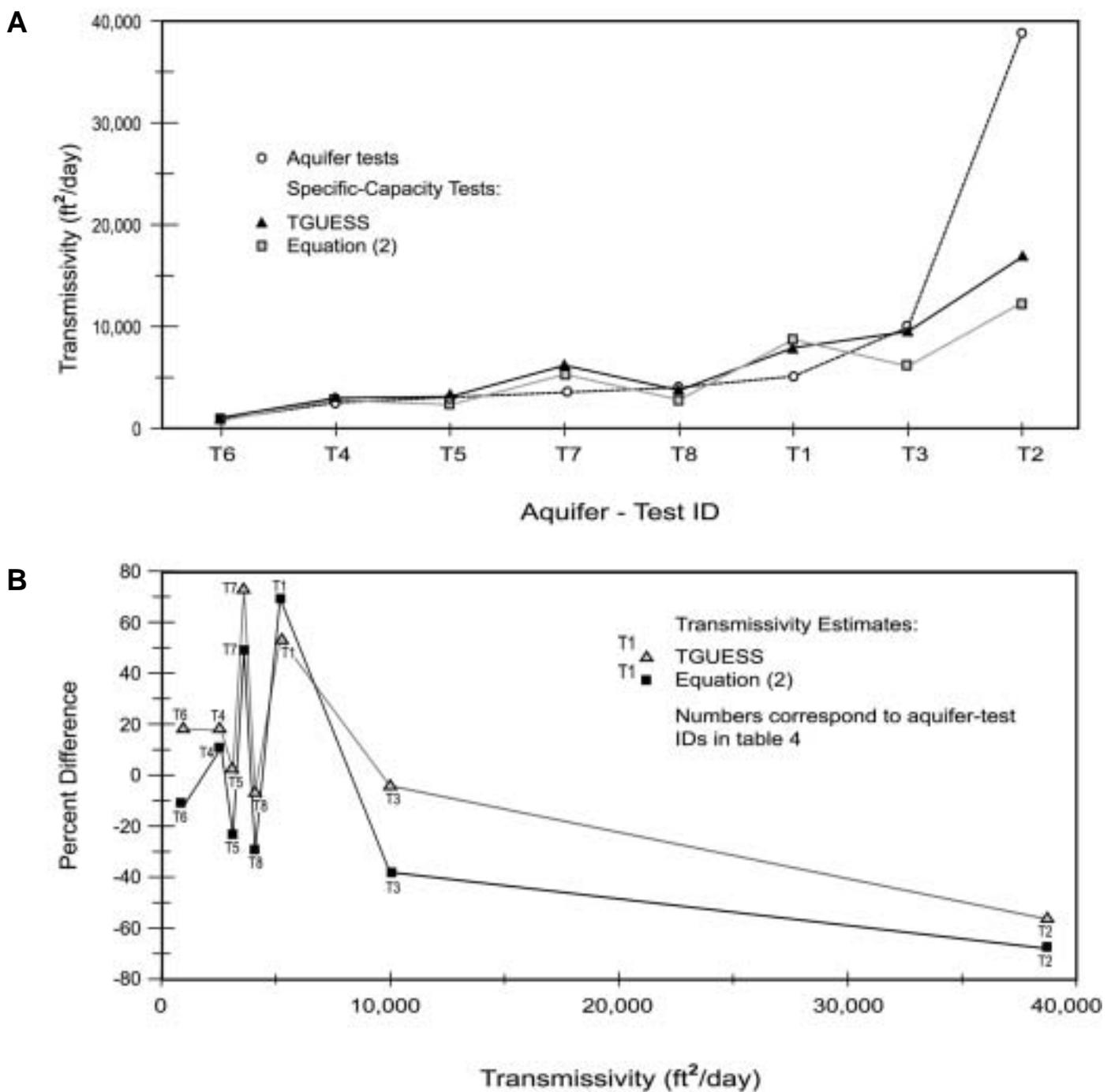
Figure 20AB. *Comparison of methods of estimating transmissivity.* ***A.*** *Plot of transmissivity estimates from aquifer-test analysis, TGUESS, and equation (2). Estimates from aquifer-test analyses are considered most accurate. Aquifer-test value for test T2 is the averaged estimates from four observation wells. Data are in table 4.* ***B.*** *Plot of percent difference between transmissivity estimates from TGUESS and equation (2), as compared to transmissivity estimates from analysis of aquifer-test data. No systematic trends apparent. Percent differences calculated from data in table 4.*

several of the observation wells. No trend in recent measurements of ground-water levels and chemistry in Cedar Valley, including the southern part of the Enoch graben, supports the hypothesis that intrabasin faults act as barriers to ground-water flow (J. Mason, U.S. Geological Survey, written communication, 2000).

The sub-basin structure of Cedar Valley may influence the present-day ground-water regime of the valley. The potentiometric surface in the southwestern part of the valley forms a closed low around Quichapa Lake (figure 1) which, as discussed above, occupies a relic topographic low inherited from the Quichapa Lake sub-basin. The effect of the Rush Lake sub-basin is less pronounced; the potentiometric surface there is not a closed low but is nearly flat (figure 1). In contrast, underflow through Iron Springs Gap and Mud Spring Canyon may be guided by their present-day topography, which is largely erosional and developed during Pleistocene time when they acted as drainage paths for Quichapa and Rush Lakes, respectively (Williams and Maldonado, 1995). The canyons were likely deeper during Pleistocene time than at present, and have since been partly backfilled by alluvial and eolian deposits.

South of Mud Spring Canyon, the potentiometric surface slopes uniformly to the northwest near the contact between the buried northeastern lobe of the Three Peaks laccolith and the basin fill (compare figures 1 and 11b). The quartz monzonite at that location may be highly permeable due to fractures, as observed in a quarry on the southeastern margin of Granite Mountain (figure 22), causing the decrease in the potentiometric surface (J. Mason, U.S. Geological Survey, verbal communication, 2000).

HYDROGEOLOGY OF BEDROCK UNITS

Introduction

Consolidated-rock aquifers are an important secondary component of the Cedar Valley drainage basin's ground-water system, but are currently of relatively minor importance for water supply (Bjorklund and others, 1978; J. Mason, U.S. Geological Survey, verbal communication, 2000). The majority of precipitation within the Cedar Valley drainage basin falls on bedrock (figure 1), and the basin-fill aquifer is recharged primarily by infiltration of stream flow from Coal Creek (Bjorklund and others, 1978), which represents a combination of runoff from precipitation and discharge of shallow ground water from bedrock and overlying colluvium. Underflow from bedrock to the basin-fill aquifer likely occurs, but is difficult to quantify (Bjorklund and others, 1978; J. Mason, U.S. Geological Survey, verbal communication, 2000). Water-budget analyses suggest that the amount of underflow is minor compared to other sources of recharge to the basin-fill aquifer (Bjorklund and others, 1978).

Several springs emanating from bedrock are used for culinary supply (figure 1; table B.2), but public-supply systems increasingly rely on wells, and the number of wells screened in bedrock is likely to increase as residential development continues. Cedar City, Enoch City, and a privately held subdivision in the western part of the valley have recently completed water supply wells screened in volcanic rocks on the valley margins (wells 3, 13, and 11, respectively, table B.1).

Hydrostratigraphy

Figure 23 shows a proposed hydrostratigraphy for bedrock units in the Cedar Valley drainage basin, based on qualitative evaluation of production to wells and springs and lithologic characteristics, chiefly degree and nature of cementation and fracturing. Hydrostratigraphic units in figure 23 are classified as (1) aquifer or potential aquifer, (2) heterogeneous, or (3) aquitard.

Established and prospective bedrock aquifers in the Cedar Valley drainage basin include Tertiary volcanic rocks, Tertiary quartz monzonite, and the Jurassic Navajo Sandstone. These units likely accommodate significantly greater underflow to the basin-fill aquifer than the other hydrostratigraphic units in the drainage basin.

Exposures of densely welded ash-flow tuffs of the Quichapa Group (map unit Tq) in and along the margins of the Harmony Mountains are highly fractured (figure 24), implying high hydraulic conductivity. The constituent formations of the Quichapa Group and the underlying Isom Formation and Needles Range Group (combined as map unit Tin on plate 1) form roughly tabular deposits of uniform lithology (Mackin, 1960), so flow of ground water through these units is not likely disrupted by facies variations present in many other volcanic rocks. Quichapa Group rocks crop out in the Harmony Mountains southwest of Cedar Valley, and likely continue into the subsurface of southwestern Cedar Valley without disruption by major faults. The Cedar City Quichapa #7 well (well 13, table B.1), the Buena Vista subdivision well (well 11, table B.1), and several private wells draw water from volcanic rocks, most likely the Quichapa Group. Withdrawal from volcanic rocks beneath southwestern Cedar Valley is likely to increase as development continues.

Quartz monzonite of the Iron Axis laccoliths also displays high to moderate fracture density (figure 22). According to records from the Utah Division of Water Rights, few wells are presently screened in quartz monzonite. Outcrops of this unit along the western valley margin receive only about 10 to 12 inches (25-38 cm) of precipitation annually, so likely contain little developable water. Basin-fill sediments in that area are relatively thin, so ground water may preferentially enter the more highly permeable quartz monzonite; this geometry is illustrated on the western part of cross section B-B′, plate 2.

The Navajo Sandstone, the principal bedrock aquifer of southwestern Utah (Heilweil and Freethey, 1992; Heilweil and others, 2000), crops out east of Cedar City along the Hurricane Cliffs (figure 6; plate 1) and is present below the Carmel, Dakota, and Straight Cliffs Formations east of its outcrop area. Cedar City drilled several wells in the Navajo Sandstone in Coal Creek Canyon, without successful water production due to caving and other mechanical problems (Utah Division of Water Rights, unpublished report).

Heterogeneous hydrostratigraphic units in the study area include all formations older than the Tertiary volcanics, except for the Navajo Sandstone (figure 23). The heterogeneous units consist of sandstone, siltstone, and mudstone interlayered at scales too small to depict in this report, and the hydrologic properties of both the individual layers and the formations as a whole are poorly known. Individual layers range from about 6 inches to 20 feet (15 cm-6 m) thick and about 100 feet to one mile (30 m-1.6 km) in lateral

EXPLANATION

Wells used for transmissivity estimates

Aquifer tests - table 4. Number is in ID column of table 4.

- ◦ 2 - 4,999 square feet/day
- ◎ 5,000 - 9,999 square feet/day
- ◉ 10,000 - 19,999 square feet/day
- ◯ 20,000 - 29,999 square feet/day
- T2 ◯ 30,000 - 39,999 square feet/day

Tguess algorithm and corrected values from equation (2) - tables 1-3

- · 2 - 4,999 square feet/day
- ● 5,000 - 9,999 square feet/day
- ● 10,000 - 19,999 square feet/day
- ● 20,000 - 29,999 square feet/day

Contour of transmissivity, in thousands of square feet/day; contours at 5,000, 10,000, 20,000, and 30,000 square feet/day; hachures point in direction of increasing transmissivity.

Map Units

Quaternary

- Qs Sedimentary deposits

Quaternary-Tertiary

- QTs Sedimentary deposits
- QTb Basalt

Tertiary to Triassic

- Bedrock

Faults

—— · · Normal fault (dotted where concealed)

Folds

⊥ Cedar City-Parowan monocline (location approximate)

Figure 21. *Distribution of transmissivity estimates for Cedar Valley basin-fill aquifer. See text for discussion and tables 1 - 4 for data.*

extent. Few water wells are developed in these units in the study area. The best water production from the heterogeneous hydrostratigraphic units would likely come from clustered sandstone sequences at least 100 feet (30 m) thick.

Aquitards in the study area are so designated based on their fine grain size, substantial thickness, and tendency to flow plastically rather than fracture. The lower two-thirds of unit Taf consists of about 1,000 feet (305 m) of predominantly fine-grained, volcaniclastic sandstone to mudstone overlying semiconsolidated sedimentary breccia (Hurlow, 1998). The Dakota Formation and the upper part of the Chinle Formation both consist of bentonitic mudstone ranging from about 100 to 400 feet (30-122 m) thick.

Hydrologic Connection Between Bedrock and Valley Fill

Although the amount of underflow from bedrock to basin fill is apparently small, as discussed above, the nature of this boundary is an important feature of the regional ground-water system because (1) ground water in the footwall and hanging wall of the EBBFS is hydrologically connected, and (2) cross-fault flow may be greater where the more permeable bedrock units abut the basin fill. Figure 10a illustrates the subsurface shape of the boundary between bedrock and basin fill in the Cedar Valley basin. Along the eastern basin margin, the EBBFS forms a steeply dipping boundary to about 500 to 3,500 feet (152-1,067 m) depth. The western, southwestern, and northern basin margins are characterized by a shallower, more gently sloping boundary

between bedrock and basin fill. The gentle slope of the western boundary may be locally punctuated by east-side-down normal faults of relatively small displacement not shown on the cross sections on plate 2.

Suggestions for Future Water-Supply Wells

The Utah Governor's Office of Planning and Budget (2001b) projects that Iron County's population will nearly double during the next 30 years. Greater water demand and the increasing proportion of domestic to agricultural use accompanying this growth may require the development of additional water-supply wells in Cedar Valley. Based on the geology and hydrogeology described above, this section suggests three geologic targets and general areas to explore for new water-supply well sites. These suggestions are based solely on geologic and hydrologic data, without consideration of important issues such as water rights, infrastructure, and environmental impacts. Plans for any new water-supply well should proceed only under the guidance of comprehensive, site-specific studies.

The most promising target unit and location in Cedar Valley are the fractured Tertiary volcanic rocks below the valley fill in the southwestern pat of the valley. At least two public-supply wells are screened in these volcanic rocks (wells 12 and 14, table B.1) which, as described above, are moderately to highly fractured (figure 24), and likely have high transmissivity but low storativity compared to the valley-fill aquifer. The valleyward projections of faults in bedrock in the northeastern Harmony Mountains are espe-
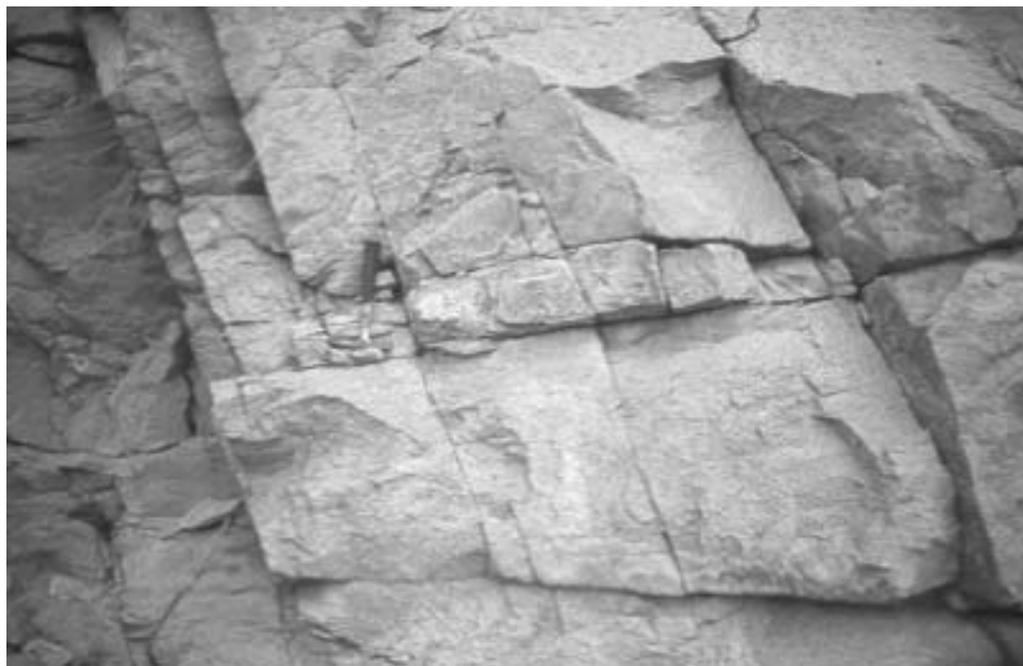
Figure 22. Fractured quartz monzonite (map unit Tqm) exposed in an open-pit mine on the southeastern side of Granite Mountain west of Cedar Valley. Hammer is 11 inches (23 cm) long.

Age (Ma)	Period	Epoch	Formation	Symbol(s)	Thickness in feet (m)	Hydro-stratigraphy	Porosity & Permeability
0.01	Q	Holocene	Sedimentary deposits	Qa,Qaf,Qp, Qct,Qm	0-150 (0-45)		PF
1.6		Pleistocene	Basalt	Qb,Tb	0-430 (0-130)		PV, SF
	QUATERNARY-TERTIARY	Pleistocene and Pliocene	Basin-fill deposits	QTa,QTs, Ts	0-1,530 (0-465)		PF
5	TERTIARY	Pliocene and Miocene	Alluvial-fan deposits	Taf	700 (215)		PF
		Miocene	Quartz monzonite	Tqm			SF
24			Tertiary volcanic rocks	Trcr,Thv, Tmd,Tbr, Ta,Tms, Tin	0-4,000 (0-1,220)		PV, SF
38		Oligocene ─?─ Eocene	Brian Head and Claron Formations	Tbh,Tc	1,440-1,570 (440-480)		PF, SF, SD
55 66		Paleocene	Grand Castle Formation	Tgc	750 (230)		SF
	CRETACEOUS	Late	Iron Springs Formation, Wahweap Sandstone, Straight Cliffs Formation, and Dakota Formation	Kis,Kws, Kd	2,700-3,600 (820-1,100)		SF
138	JURASSIC	Middle	Carmel Formation	Jc	1,130-1,360 (345-415)		SF, SD
		Early	Navajo Sandstone	Jn	1,700 (520)		PF, SF
205			Kayenta and Moenave Formations	Jk,Jm	1,080-2,110 (330-645)		SF
	TRIASSIC	Middle	Chinle Formation	Ŧc	240-490 (75-150)		SF
		Late	Moenkopi Formation	Ŧmu, Ŧmv, Ŧml, Ŧmt	1,880 (575)		SF

Figure 23. Suggested hydrostratigraphy for Cedar Valley drainage basin. Note that the units are from plate 1, and some units with similar hydrostratigraphic properties have been grouped. Period abbreviation: Q = Quaternary. Porosity and permeability abbreviations: PF = primary framework, PV = primary volcanic, SF = secondary fracture, SD = secondary dissolution. These refer to the types of porosity and permeability most likely to contribute to storage and flow of ground water in the formation. ▨ *Aquifer or potential aquifer.* ▨ *Heterogeneous lithology, porosity, and permeability (see text).* ■ *Aquitard (low permeability).*
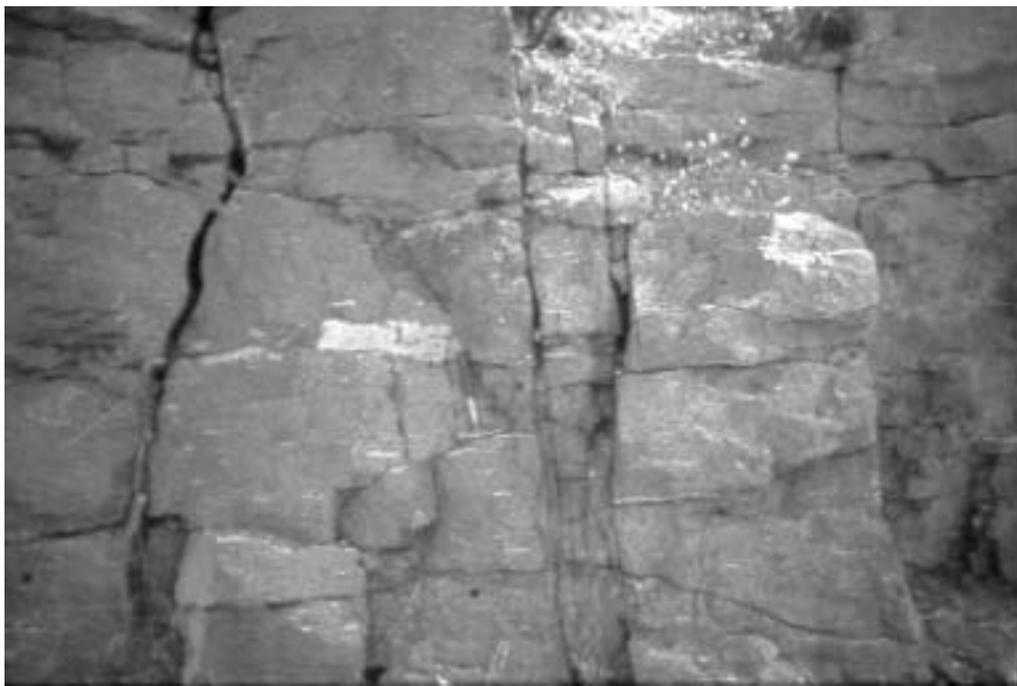
Figure 24. *Fractured ash-flow tuff deposits of the Bauers Tuff Member of the Condor Canyon Formation, part of the Quichapa Group (map unit Tq). Exposure is on the north side of Highway 56, just west of Cedar Valley. Hammer is 11 inches (23 cm) long.*

cially attractive targets. Ground-water quality in the area is good (Bjorklund and others, 1978), and recharge is most likely from snowmelt on the Harmony Mountains.

The quartz monzonite intrusions of Granite Mountain and The Three Peaks are potential geologic targets for water wells, based on moderate to high fracture density observed in outcrops and open-pit mines (figure 22). Little is known about the water-production characteristics of the intrusions, and water levels in the western part of the valley may be relatively deep (100 feet [30 m] or greater). An oil-exploration well in the Red Mountains (well C, table B.3) that penetrated a buried quartz monzonite intrusion was converted to a water well, according to UGS unpublished records, but production details are unavailable.

As noted above, Cedar City was unsuccessful in its attempts to establish two water-supply wells in the Navajo Sandstone in Coal Creek Canyon but not because of a lack of ground water in the formation (Utah Division of Water Resources, unpublished report). The Navajo Sandstone remains a potential target if these mechanical problems can be overcome by careful siting and improved drilling technology.

CONCLUSIONS

The principal aquifer in the Cedar Valley drainage basin consists of Quaternary and Tertiary basin-fill deposits below the topographic valley. Holocene to mid-Pleistocene surficial deposits are relatively thin, comprising only the upper 25 to 150 feet (8-46 m) of the Cedar Valley aquifer. The remainder of the Cedar Valley basin-fill aquifer consists of Miocene to mid-Quaternary basin fill that forms a fault-bounded, east-thickening subsurface wedge containing three unconformity-bounded units, as determined by interpretation of seismic-

reflection profiles of the valley collected by Mobil Exploration and Production Services U.S., Inc. These deposits accumulated in a composite depositional basin produced by normal faulting. The eastern basin-bounding fault system (EBBFS) initiated as a series of subparallel, roughly co-linear segments that may have reactivated thrust faults of the Cretaceous- to Paleocene-age Cordilleran fold and thrust belt. The normal faults grew and linked together with increasing displacement, producing a complicated internal basin structure characterized by four sub-basins and several intrabasin uplifts.

The basin-fill deposits consist of interbedded gravel, sand, silt, and clay deposited in alluvial-fan, fluvial, and lacustrine/playa environments. The alluvial-fan deposits, characterized by coarse average grain size and poorly developed layering and sorting, dominate the valley margins and grade to overall finer grained, well-layered, well-sorted fluvial deposits toward the valley center. Transmissivity of the basin-fill aquifer is greatest near the valley margins and gradually decreases toward the valley center, ranging from over 20,000 to less than 5,000 square feet per day (>1,860 to <465 m^2/d). This variation in transmissivity closely tracks the change from dominantly alluvial-fan to fluvial and lacustrine deposits in the basin fill.

Most precipitation in the Cedar Valley drainage basin falls on Triassic through Tertiary-age bedrock exposed on the steep cliffs and high plateaus to the southeast (figure 1). This precipitation either runs off or percolates through bedrock to Coal Creek, which forms the principal source of recharge to the Cedar Valley aquifer as it flows into the valley. Bedrock is important to the hydrogeology of Cedar Valley, not only because it transmits water to Coal Creek, but also because (1) it is hydrologically connected to the basin fill across the basin-bounding faults, although the amount of cross-fault flow is probably small, and (2) it is a likely target of future

water development. Most bedrock units in the study area consist of interlayered sandstone and mudstone, forming heterogeneous potential aquifers of uncertain extent, transmissivity, and chemical quality. The best established and potential bedrock aquifers in the study area are fractured Tertiary volcanic rocks and quartz monzonite exposed in the hills bounding the southwestern, western, and northeastern valley margins, and the Jurassic Navajo Sandstone in the subsurface east of the valley.

ACKNOWLEDGMENTS

REFERENCES

Allmendinger, R.W., 1992, Fold and thrust tectonics of the western United States exclusive of the accreted terranes, *in* Burchfiel, B.C., Lipman, P.W., and Zoback, M.L., editors, The Cordilleran orogen - Coterminous U.S.: Boulder, Colorado, Geological Society of America, The Geology of North America, v. G-3, p. 583-607.

Anderson, J.J., Rowley, P.D., Fleck, R.J., and Nairn, A.E.M., 1975, Cenozoic geology of southwestern high plateaus of Utah: Geological Society of America Special Paper 160, p. 1-51.

Anderson, R.E., and Mehnert, H.H., 1979, Reinterpretation of the history of the Hurricane fault in Utah, *in* Newman, G.W., and Goode, H.D., editors, 1979 Basin and Range symposium: Rocky Mountain Association of Geologists, p. 145-165.

Anderson, R.E., Zoback, M.L., and Thompson, G.A., 1983, Implications of selected subsurface data on the structural form and evolution of some basins in the northern Basin and Range Province, Nevada and Utah: Geological Society of America Bulletin, v. 94, p. 1,055-1,072.

Armstrong, R.L., 1968, Sevier orogenic belt in Nevada and Utah: Geological Society of America Bulletin, v. 79, p. 429-458.

—1970, Geochronology of Tertiary igneous rocks, eastern Basin and Range Province, western Utah, eastern Nevada, and vicinity, U.S.A.: Geochimica et Cosmochimica Acta, v. 34, p. 203-232.

Averitt, Paul, 1962, Geology and coal resources of the Cedar Mountain quadrangle, Iron County, Utah: U.S. Geological Survey Professional Paper 389, 71 p., 3 plates, scale 1:24,000.

—1967, Geology of the Kanarraville quadrangle, Iron County, Utah: U.S. Geological Survey Map GQ-694, 1 plate, scale 1:24,000.

Averitt, Paul, and Threet, R.L., 1973, Geologic map of the Cedar City quadrangle, Iron County, Utah: U.S. Geological Survey Map GQ-1120, scale 1:24,000.

Bankey, Viki, Grauch, V.J.S., and Kucks, R.P., 1998, Utah aeromagnetic and gravity maps and data - A web site for distribution of data: Online, U.S. Geological Survey Open-File Report 98-761, http://greenwood.cr.usgs.gov/pub/open-file-reports/ofr-98-0761/utah.html.

Best, M.G., and Christiansen, E.H., 1991, Limited extension during peak Tertiary volcanism, Great Basin of Nevada and Utah: Journal of Geophysical Research, v. 96, p. 13,509-13,528.

Best, M.G., Christiansen, E.H., and Blank, R.H., Jr., 1989, Oligocene caldera complex and calc-alkaline tuffs and lavas of the Indian Peak volcanic field, Nevada and Utah: Geological Society of America Bulletin, v. 101, p. 1,076-1,090.

Best, M.G., and Grant, S.K., 1987, Stratigraphy of the volcanic Oligocene Needles Range Group in southwestern Utah and eastern Nevada: U.S. Geological Survey Professional Paper 1433-A, 28 p.

Best, M.G., McKee, E.H., and Damon, P.E., 1980, Space-time-composition patterns of late Cenozoic mafic volcanism, southwestern Utah and adjoining areas: American Journal of Science, v. 280, p. 1,035-1,050.

Bjorklund, L.J., Sumsion, C.T., and Sandberg, G.W., 1977, Selected hydrologic data – Parowan and Cedar City drainage basin, Iron County, Utah: U.S. Geological Survey Utah Basic-Data Release 28, 55 p., 1 plate, scale 1:250,000.

—1978, Ground-water resources of the Parowan-Cedar City drainage basin, Iron County, Utah: Utah Department of Natural Resources Technical Publication 60, 93 p., 4 plates, scale 1:250,000.

Blank, H.R., 1959, Geology of the Bull Valley district, Washington County, Utah: Seattle, University of Washington, Ph.D. thesis, 177 p.

Blank, H.R., and Mackin, J.H., 1967, Geologic interpretation of an aeromagnetic survey of the Iron Springs District, Utah: U.S. Geological Survey Professional Paper 516-B, 14 p., 1 plate.

Blank, H.R., Rowley, P.D., and Hacker, D.B., 1992, Miocene monzonitic intrusions and associated megabreccia of the Iron Axis region, southwestern Utah, *in* Wilson, J.R., editor, Field quide to geologic excursions in Utah and adjacent areas of Nevada, Idaho, Wyoming: Utah Geological Survey Miscellaneous Publication 92-3, p. 399-420.

Bradbury, K., and Rothschild, E., 1985, TGUESS – A program to estimate aquifer transmissivity and hydraulic conductivity from specific capacity tests: Ground Water, v. 23, p. 240-246.

Burden, C.B., 2000, Ground-water conditions in Utah – Spring of 2000: Utah Division of Water Resources Cooperative Investigations Report 41, 140 p.

Caine, J.S., Evans, J.P., and Forster, C.B., 1996, Fault zone architecture and permeability structure: Geology, v. 24, p. 1,025-1,028.

Cook, E.F., 1960, Geologic atlas of Utah – Washington County: Utah Geological and Mineralogical Survey Bulletin, v. 70, 119 p., 1 plate, scale 1:125,000.

Cook, K.L., and Hardman, Elwood, 1967, Regional gravity survey of the Hurricane fault area and Iron Springs District, Utah: Geological Society of America Bulletin, v. 78, p. 1,063-1,076.

Daly, Christopher, and Weisburg, Jenny, 1997, Average annual precipitation – Utah: Reno, Nevada, Western Regional Climate Center: Online, http://www.wrcc.dri.edu/pcpn/ut.gif, accessed June 6, 2000.

Eakin, T.E., Price, Don, and Harrill, J.R., 1976, Summary appraisals of the nation's ground-water resources – Great Basin region: U.S. Geological Survey Professional Paper 813-G, 37 p.

Eaton, G.P., 1982, The Basin and Range Province – Origin and tectonic significance: Annual Review of Earth and Planetary Science, v. 10, p. 409-440.

Effimoff, Ivan, and Pinezich, A.R., 1986, Tertiary structural development of selected basins – Basin and Range Province, northeastern Nevada, *in* Mayer, Larry, editor, Extensional tectonics of the southwestern United States – A perspective on processes and kinematics: Boulder, Colorado, Geological Society of America Special Paper 208, p. 31-42.

Eppinger, R.G., Winkler, G.R., Cookro, T.M., Shubat, M.A., Blank, H.R., Jr., Crowley, J.K., Kucks, R.P., and Jones, J.L., 1990, Preliminary assessment of the mineral resources of the Cedar City 1° x 2° quadrangle, Utah: U.S. Geological Survey Open-File Report OF 90-034, 146 p., 1 plate, scale 1:250,000.

Evans, J.P., and Oaks, R.Q., Jr., 1996, Three-dimensional variations in extensional fault shape and basin form – The Cache Valley basin, eastern Basin and Range province, United States: Geological Society of America Bulletin, v. 108, p.

1,580-1,593.

Faulds, J.E., and Varga, R.J., 1998, The role of accommodation and transfer zones in the regional segmentation of extended terranes, *in* Faulds, J.E., and Stewart, J.H., editors, Accommodation zones and transfer zones – The regional segmentation of the Basin and Range Province: Boulder, Colorado, Geological Society of America Special Paper 323, p. 1-45.

Fetter, C.W., 1994, Applied hydrogeology: New York, Macmillan College Publishing Company, 691 p.

Fillmore, R.P., 1991, Tectonic influence on sedimentation in the southern Sevier foreland, Iron Springs Formation (Upper Cretaceous), southwestern Utah, *in* Nations, J.D., and Eaton, J.G., editors, Stratigraphy, depositional environments, and sedimentary tectonics of the western margin, Cretaceous Western Interior Seaway: Geological Society of America Special Paper 260, p. 9-25.

Fleck, R.J., Anderson, J.J., and Rowley, P.D., 1975, Chronology of mid-Tertiary volcanism in high plateaus region of Utah: Geological Society of America Special Paper 160, p. 53-61.

Goldstrand, P.M., 1994, Tectonic development of Upper Cretaceous to Eocene strata of southwestern Utah: Geological Society of America Bulletin, v. 106, p. 145-154.

Goldstrand, P.M., and Mullett, D.J., 1997, The Paleocene Grand Castle Formation – A new formation on the Markagunt Plateau of southwestern Utah, *in* Maldonado, Florian, and Nealey, L.D., editors, Geologic studies in the Basin and Range-Colorado Plateau transition zone in southeastern Nevada, southwestern Utah, and northwestern Arizona, 1995: U.S. Geological Survey Bulletin 2153, p. 61-77.

Hacker, D.B. 1998, Catastrophic gravity sliding and volcanism associated with the growth of laccoliths – Examples from early Miocene hypabyssal intrusions of the Iron Axis magmatic province, Pine Valley Mountains, southwestern Utah: Kent, Ohio, Kent State University, Ph.D. thesis, 258 p., 5 plates.

Hansen, W.R., 1991, Suggestions to authors of the reports of the United States Geological Survey, Seventh Edition: Washington, D.C., U.S. Government Printing Office, 289 p.

Heilweil, V.M., and Freethey, G.W., 1992, Hydrology of the Navajo aquifer in southwestern Utah and northwestern Arizona, including computer simulation of ground-water flow and water-level declines that could be caused by proposed withdrawals, *in* Harty, K.M., editor, Engineering and environmental geology of southwestern Utah: Utah Geological Association Publication 21, p. 213-223.

Heilweil, V.M., Freethey, G.W., Stolp, B.J., Wilkowske, C.D., and Wilberg, D.E., 2000, Geohydrology and numerical simulation of ground-water flow in the central Virgin River basin of Iron and Washington Counties, Utah: Utah Department of Natural Resources Technical Publication 116, 139 p.

Hintze, L.F., 1988 (reprinted 1993), Geologic history of Utah: Brigham Young University Geology Studies Special Publication 7, 202 p.

Hintze, L.F., Willis, G.C., Laes, D.Y.M., Sprinkel, D.A., and Brown, K.D., 2000, Digital geologic map of Utah: Utah Geological Survey Map 179DM, CD-ROM.

Hurlow, H.A., 1998, The geology of the central Virgin River basin, southwestern Utah, and its relation to ground-water conditions: Utah Geological Survey Water-Resources Bulletin 26, 53 p., 6 plates.

Hurlow, H.A., and Biek, R.F., 2000, Interim geologic map of the Pintura quadrangle, Washington County, Utah: Utah Geological Survey Open-File Report 375, 67 p, 1 plate, scale 1:24,000.

Imlay, R.W., 1980, Jurassic paleobiogeography of the co-terminous United States in its continental setting: U.S. Geological Survey Professional Paper 1062, 134 p.

Jackson, J.A., 1997, Glossary of geology: Alexandra, Virginia, American Geological Institute, fourth edition, 769 p.

Leeder, M.R., and Gawthorpe, R.L., 1987, Sedimentary models for extensional tilt-block/half-graben basins, *in* Coward, M.P., Dewey, J.F., and Hancock, P.L., editors, Continental extensional tectonics: Geological Society of London Special Publication 28, p. 139-152.

Liberty, L.M., Heller, P.L., and Smithson, S.B., 1994, Seismic reflection evidence for two-phase development of Tertiary basins from east-central Nevada: Geological Society of America Bulletin, v. 106, p. 1,621-1,633.

Lowe, Mike, and Wallace, Janae, 2001, Evaluation of potential geologic sources of nitrate contamination in ground water, Cedar Valley, Iron County, Utah with emphasis on the Enoch area: Utah Geological Survey Special Study 100, 50 p., 1 plate, scale 1:48,000.

Lowe, Mike, Wallace, Janae, and Bishop, C.E., 2000, Analysis of septic-tank density for three areas in Cedar Valley, Iron County, Utah – A case study for evaluations of proposed subdivisions in Cedar Valley: Utah Geological Survey Water-Resources Bulletin 27, 66 p.

Mackin, J.H., 1960, Structural significance of Tertiary volcanic rocks in southwestern Utah: American Journal of Science, v. 258, p. 81-131.

Mackin, J.H., Nelson, W.H., and Rowley, P.D., 1976, Geologic map of the Cedar City NW quadrangle, Iron County, Utah: U.S. Geological Survey Geologic Quadrangle Map GQ-1295, scale 1:24,000.

Mackin, J.H., and Rowley, P.D., 1976, Geologic map of The Three Peaks quadrangle, Iron County, Utah: U.S. Geological Survey Geologic Quadrangle Map GQ-1297, scale 1:24,000.

Maldonado, Florian, Sable, E.G., and Nealey, L.D., 1997, Cenozoic low-angle faults, thrust faults, and anastomosing high-angle faults, western Markagunt Plateau, southwestern Utah, *in* Maldonado, Florian, and Nealey, L.D., editors, Geologic studies in the Basin and Range-Colorado Plateau transition zone in southeastern Nevada, southwestern Utah, and northwestern Arizona, 1995: U.S. Geological Survey Bulletin 2153, p. 129-149.

Maldonado, Florian, and Williams, V.S., 1993a, Geologic map of the Paragonah quadrangle, Iron County, Utah: U.S. Geological Survey Map GQ-1713, scale 1:24,000.

—1993b, Geologic map of the Parowan Gap quadrangle, Iron County, Utah: U.S. Geological Survey Map GQ-1712, scale 1:24,000.

Maxey, G.B., 1964, Hydrostratigraphic units: Journal of Hydrology, v. 2, p. 124-129.

McKee, E.H., Blank, H.R., and Rowley, P.D., 1997, Potassium-argon ages of Tertiary igneous rocks in the eastern Bull Valley Mountains and Pine Valley Mountains, southwestern Utah, *in* Maldonado, Florian, and Nealey, L.D., editors, Geologic studies in the Basin and Range-Colorado Plateau transition zone in southeastern Nevada, southwestern Utah, and northwestern Arizona, 1995: U.S. Geological Survey Bulletin 2153, p. 243-252.

Moore, D.W., and Nealey, L.D., 1993, Preliminary geologic map of Navajo Lake quadrangle, Kane and Iron Counties, Utah: U.S. Geological Survey Open-File Report 93-190,

19 p., 1 plate, scale 1:24,000.

Palmer, A.R., 1983, The decade of North American geology 1983, geologic time scale: Geology, v. 11, p. 503-504.

Pearthree, P.A., Lund, W.R., Stenner, H.D., and Everitt, B.L., 1998, Paleoseismologic investigations of the Hurricane fault in southwestern Utah and northwestern Arizona – final project report: National Earthquake Hazards Reduction Program, External Research, 125 p.

Razack, M., and Huntley, D., 1991, Assessing transmissivity from specific capacity data in a large and heterogeneous alluvial aquifer: Ground Water, v. 29, p. 856-861.

Rowley, P.D., 1975, Geologic map of the Enoch NE quadrangle, Iron County, Utah: U.S. Geological Survey Geologic Quadrangle Map GQ-1301, scale 1:24,000.

—1976, Geologic map of the Enoch NW quadrangle, Iron County, Utah: U.S. Geological Survey Geologic Quadrangle Map GQ-1302, scale 1:24,000.

—1978, Geologic map of the Thermo 15-minute quadrangle, Beaver and Iron Counties, Utah: U.S. Geological Survey Geologic Quadrangle Map GQ-1493, scale 1:24,000.

Rowley, P.D., and Barker, D.S., 1978, Geology of the Iron Springs mining district in Utah, *in* Shawe, D.R., and Rowley, P.D., editors, Guidebook to mineral deposits of southwestern Utah: Utah Geological Association Publication 7, p. 49-58.

Rowley, P.D., Mehnert, H.H., Naeser, C.W., Snee, L.W., Cunningham, C.G., Steven, T.A., Anderson, J.J., Sable, E.G., and Anderson, R.E., 1994, Isotopic ages and stratigraphy of Cenozoic rocks of the Marysvale volcanic field and adjacent areas, west-central Utah: U.S. Geological Survey Bulletin 2071, 35 p.

Rowley, P.D., Nealey, L.D., Unruh, D.M., Snee, L.W., Mehnert, H.H., Anderson, R.E., and Gromme, C.S., 1995, Stratigraphy of Miocene ash-flow tuffs in and near the Caliente caldera complex, southeastern Nevada and southwestern Utah, *in* Scott, R.B., and Swadley, W.C., editors, Geologic studies in the Basin and Range-Colorado Plateau transition zone in southeastern Nevada, southwestern Utah, and northwestern Arizona, 1992: U.S. Geological Survey Bulletin 2056, p. 47-88.

Rowley, P.D., Steven, T.A., Anderson, J.J., and Cunningham, C.G., 1979, Cenozoic stratigraphic and structural framework of southwestern Utah: U.S. Geological Survey Professional Paper 1149, 22 p.

Rowley, P.D., and Threet, R.L., 1976, Geologic map of the Enoch quadrangle, Iron County, Utah: U.S. Geological Survey Geologic Quadrangle Map GQ-1296, scale 1:24,000.

Royse, Frank, Jr., Warner, M.A., and Reese, D.L., 1975, Thrust belt structural geometry and related stratigraphic problems, Wyoming-Idaho-northern Utah, *in* Bolyard, D.W., editor, Deep drilling frontiers of the central Rocky Mountains: Rocky Mountain Association of Geologists, p. 41-54.

Sable, E.G., and Maldonado, Florian, 1997, The Brian Head Formation (revised) and selected Tertiary sedimentary rock units, Markagunt Plateau and adjacent areas, southwestern Utah, *in* Maldonado, Florian, and Nealey, L.D., editors, Geologic studies in the Basin and Range-Colorado Plateau transition zone in southeastern Nevada, southwestern Utah, and northwestern Arizona, 1995: U.S. Geological Survey Bulletin 2153, p.7-26.

Schlische, R.W., and Anders, M.H., 1996, Stratigraphic effects and tectonic implications of the growth of normal faults and extensional basins, *in* Beratan, K.K., editor, Reconstructing the history of Basin and Range extension using sedimentology and stratigraphy: Boulder, Colorado, Geological Society of America Special Paper 303, p. 183-203.

Scott, R.B., and Swadley, W.C., editors, 1995, Geologic studies in the Basin and Range-Colorado Plateau transition zone in southeastern Nevada, southwestern Utah, and northwestern Arizona, 1992: U.S. Geological Survey Bulletin 2056, 275 p.

Siders, M.A., 1991, Geologic map of the Mount Escalante quadrangle, Iron County, Utah: Utah Geological Survey Map 131, 9 p., scale 1:24,000.

Smith, R.B., and Bruhn, R.L., 1984, Intraplate extensional tectonics of eastern Basin-Range – Inferences on structural style from seismic reflection data, regional tectonics, and thermal-mechanical models of brittle-ductile deformation: Journal of Geophysical Research, v. 89, p. 5,733-5,762.

Steven, T.A., Morris, H.T., and Rowley, P.D., 1990, Geologic map of the Richfield 1° x 2° quadrangle, west-central Utah: U.S. Geological Survey Miscellaneous Investigations Series Map I-1901, scale 1:250,000.

Stewart, J.H., 1978, Basin-Range structure in western North America – A review, *in* Smith, R.B., and Eaton, G.P., editors, Cenozoic tectonics and regional geophysics of the western Cordillera: Boulder, Colorado, Geological Society of America Memoir 152, p. 1-31.

—1998, Regional characteristics, tilt domains, and extensional history of the late Cenozoic Basin and Range Province, western North America, in Faulds, J.E., and Stewart, J.H., editors, Accommodation zones and transfer zones – The regional segmentation of the Basin and Range Province: Boulder, Colorado, Geological Society of America Special Paper 323, p. 47-74.

Taylor, W.J., 1993, Stratigraphic and lithologic analysis of the Claron Formation in southwestern Utah: Utah Geological Survey Miscellaneous Publication 93-1, 52 p.

Telford, W.M., Geldart, L.P., Sheriff, R.E., and Keys, D.A., 1976, Applied geophysics: Cambridge, U.K., Cambridge University Press, 859 p.

Theis, C.V., 1963, Estimating the transmissivity of a water table aquifer from the specific capacity of a well: U.S. Geological Survey Water Supply Paper 1536-I, p. 332-336.

Thomas, H.E., and Taylor, G.H., 1946, Geology and ground-water resources of Cedar City and Parowan Valleys, Iron County, Utah: U.S. Geological Survey Water-Supply Paper 993, 210 p.

Threet, R.L., 1963, Structure of the Colorado Plateau margin near Cedar City, Utah, *in* Heylmun, E.B., editor, Geology of the southwestern transition between the Basin-Range and Colorado Plateau, Utah: Intermountain Association of Petroleum Geologists 12th Annual Field Conference, Guidebook to the Geology of Southwestern Utah, p. 109-117.

Utah Division of Water Rights, 1982, Water use data for public suppliers in Utah – 1980: Water Use Report No. 3, 94 p.

—2000, Flow records – public water suppliers: Online, <http://www.waterrights.utah.gov, accessed 12/11/2000 and 5/4/ 2001.

Utah Governor's Office of Planning and Budget, 2001a, Demographic and economic analysis: Online, <http://www.governor.state.ut.us/dea/Demographics/2000_Census_Data/>, accessed July, 2001.

—2001b, Long term economic and demographic projections: Online, <http://www.qget.state.ut.us/projections/tables/table 8.htm>, accessed September 4, 2001.

van Kooten, G.K., 1988, Structure and hydrocarbon potential beneath the Iron Springs laccolith, southwestern Utah: Geological Society of America Bulletin, v. 100, p. 1,533-1,540.

Wallace, Janae, 2001, Geologic logs of water wells in Utah: On-line, http://www.waterrights.utah.gov/wellinfo/findwlog.htm, accessed numerous times during 2000 and 2001.

Wernicke, Brian, 1992, Cenozoic extensional tectonics of the U.S. Cordillera, *in* Burchfiel, B.C., Lipman, P.W., and Zoback, M.L., editors, The Cordilleran orogen – Coterminous U.S.: Boulder, Colorado, Geological Society of America, The Geology of North America, v. G-3, p. 553-581.

Williams, V.S., and Maldonado, Florian, 1995, Quaternary geology and tectonics of the Red Hills area of the Basin and Range-Colorado Plateau transition zone, Iron County, Utah, *in* Scott, R.B., and Swadley, W.C., editors, Geologic studies in the Basin and Range-Colorado Plateau transition zone in southeastern Nevada, southwestern Utah, and northwestern Arizona, 1992: U.S. Geological Survey Bulletin 2056, p. 257-275.

Willis, G.C., 1999, The Utah thrust system - An overview, *in* Spangler, L.E., and Allen, C.J., editors, Geology of northern Utah and vicinity: Utah Geological Association Publication 27, p. 1-9

GLOSSARY

Definitions are from Jackson (1997), with modification by the author. Many of the terms appear only in the Description of Map Units in appendix A. Italicized words in definitions may not appear in the text but are in the glossary.

Alkalic – Describing an igneous rock in which the molecular ratio [$(Na_2O + K_2O):Al_2O_3:SiO_2$] differs from 1:1:6 by deficiency in either Al_2O_3 or SiO_2.

Alluvial – Deposited by a stream or other body of running water. Alluvium is a general term for unconsolidated *detrital* material deposited during comparatively recent geologic time by a stream or other body of running water, as a sorted or semisorted sediment in the bed of a stream or on its flood plain or delta, or as a cone or fan at the base of a mountain slope.

Andesitic – Said of a dark-colored, fine-grained volcanic rock containing *phenocrysts* of Na-rich *plagioclase feldspar* and one or more of the following: *biotite*, *hornblende*, or *pyroxene*; in a *groundmass* composed generally of the same minerals as the *phenocrysts*.

Angular unconformity – An *unconformity* between two groups of rocks whose bedding planes are not parallel or in which the older, underlying rocks dip at a different angle (usually steeper) than the younger, overlying strata.

Anticline – A *fold*, the core of which contains stratigraphically older rocks, and is convex upward.

Aphanitic – Said of the texture of an igneous rock in which the grains are too small to distinguish with the unaided eye; both *microcystalline* and *cryptocrystalline* textures are included.

Aquifer - A body of rock or sediment that contains sufficient saturated permeable material to conduct ground water and to yield significant quantities of water to wells and springs.

Aquitard - An impermeable layer that creates confined ground-water conditions, in which ground water is under pressure significantly greater than that of the atmosphere.

Arkose - A *feldspar*-rich sandstone, commonly coarse grained and pink or reddish, that is typically composed of angular to subangular grains that may be either poorly or moderately well sorted; *quartz* is usually the dominant mineral, with *feldspars* constituting at least 25%; matrix commonly includes clay minerals, mica, iron oxide, and fine-grained rock fragments.

Ash-flow tuff – A density-current deposit, generally a hot mixture of volcanic gases and *tephra* that travels across the ground surface; produced by the explosive disintegration of viscous lava in a volcanic crater, or from a fissure or group of fissures. The solid materials contained in a typical ash flow are generally unsorted and ordinarily include volcanic dust, *pumice*, *scoria*, and blocks in addition to ash.

Bentonite – A soft, plastic, porous, light-colored rock composed essentially of clay minerals of the montmorillonite (smectite) group plus colloidal silica, and produced by devitrification and accompanying chemical alteration of a glassy igneous material, usually a tuff or volcanic ash.

Bentonitic – Containing *bentonite*.

Biotite – A widely distributed rock-forming mineral of the mica group: $K(Mg,Fe^{2+})_3(OH)_2[(Al,Fe^{3+})Si_3O_{10}]$.

Breccia – A coarse-grained clastic rock, composed of angular broken rock fragments held together by mineral cement or in a fine-grained matrix.

Bomb – A pyroclast ejected while viscous and shaped while in flight, larger than 64 mm in diameter.

Calc-alkalic – Said of a series of igneous rocks in which the weight percentage of silica is between 56 and 61 when the weight percentages of CaO and of $K_2O + Na_2O$ are equal.

Calcarenite – A limestone consisting predominantly of sand-size carbonate grains.

Caldera – A large, basin-shaped volcanic depression, more or less circular in form, the diameter of which is many times greater than that of the included vent or vents.

Carbonate strata – Sediment formed by the organic or inorganic precipitation from aqueous solution of calcium-, magnesium-, or iron-carbonate minerals.

Chert – A hard, dense, dull to semivitreous, *microcystalline* or *cryptocrystalline* sedimentary rock, consisting dominantly of interlocking crystals of quartz less than about 30 microns in diameter, that may also contain impurities such as calcite, iron oxide, and the remains of siliceous and other organisms. It has a tough, splintery to conchoidal fracture, and may be variously colored. Chert occurs as nodular or concretionary segregations (chert nodules) in limestones and dolomites, or as areally extensive layered deposits (bedded chert); it may be an original organic or inorganic precipitate, or a replacement product.

Clastic – Pertaining to a rock or sediment composed principally of broken fragments that are derived from preexisting rocks or minerals and that have been transported some distance from their places of origin.

Cognate inclusion – An inclusion in an igneous rock to which it is genetically related.

Concordant – Structurally conformable; said of strata displaying parallelism of bedding or structure; said of an igneous intrusion possessing contacts which are parallel to foliation or bedding in country rock.

Conglomerate – A coarse-grained clastic sedimentary rock, composed of rounded to subangular fragments larger than 2 mm in diameter typically containing fine-grained particles in the interstices, and commonly cemented by calcium carbonate, iron oxide, silica, or hardened clay; the consolidated equivalent of gravel.

Cordilleran fold and thrust belt – A gently arcuate, convex-east belt of thrust faults and related folds, extending from northern British Columbia to southeastern California and from the eastern boundary of the Cascade and Sierra Nevada Mountains to western Wyoming and central Utah, that formed during mid-Cretaceous through Paleocene time.

Cryptocrystalline – Said of a texture of a rock consisting of crystals that are too small to be recognized and separately distinguished even under the ordinary microscope (although crystallinity may be shown by the use of the electron microscope).

Dacitic – Said of a medium- to light-colored, fine-grained volcanic rock with similar composition to andesite, but having less calcic *plagioclase feldspar* and more *quartz.*

Detrital – Pertaining to or formed from *detritus.*

Detritus – A collective term for loose rock and mineral material that is worn off or removed by mechanical means, such as sand, silt, and clay, derived from older rocks and moved from its place of origin.

Diamictite – A nongenetic term for a nonsorted or poorly sorted, non-calcareous, terrigenous sedimentary rock that contains a wide range of particle sizes.

Dip - The inclination of a planar surface (for example, bedding or a fault), as measured relative to horizontal and in a vertical plane that is perpendicular to the *strike* of the surface.

Disconformity – An *unconformity* in which the bedding planes above and below the break are essentially parallel, indicating a significant interruption in the orderly sequence of sedimentary rocks, generally by a considerable interval of erosion or non-deposition, and usually marked by a visible and irregular or uneven surface.

Eolian – Pertaining to the wind; especially said of such deposits as dune sand and loess, of sedimentary structures such as wind-formed ripple marks, or of erosion and deposition accomplished by the wind.

Facies – The aspect, appearance, and characteristics of a rock unit, usually reflecting the conditions of origin; a mappable, areally restricted part of a *lithostratigraphic* body, differing in *lithology* from other beds deposited at the same time and in lithologic continuity.

Fault - A discrete surface or zone of discrete surfaces separating two rock masses across which one rock mass has slid past the other.

Feldspar – A group of abundant rock-forming minerals, generally divided into two compositional groups, (1) the *plagioclase feldspar* series: $CaAl_2Si_2O_8$ to $NaAlSi_3O_8$, and (2) the *alkali feldspar* series: $(K,Na)AlSi_3O_8$.

Fiamme – Vitric lenses in welded tuffs, averaging a few centimeters in length, perhaps formed by collapse of fragments of pumice.

Fluvial – Of or pertaining to a river; produced by the action of a stream or river.

Fold - A curve or bend of a planar structure such as rock strata or bedding planes.

Footwall - The lower block of a non-vertical fault.

Fracture - A general term for any surface within a material across which there is no cohesion; includes *joint* and *fault.*

Gamma-ray log – The radioactivity log curve of the intensity of broad-spectrum, undifferentiated natural gamma radiation emitted from the rocks in a cased or uncased borehole.

Graben – An elongate trough or basin, bounded on both sides by high-angle *normal faults* that dip toward the interior of the trough.

Groundmass – The finer grained and/or glassy material between the *phenocrysts* in a *porphyritic* (see *porphyry*) igneous rock.

Hanging wall - The upper block of a non-vertical fault.

Hornblende – The commonest mineral of the rock-forming amphibole group:

$(Ca,Na)_{2-3}(Mg,Fe^{2+}, Fe^{3+},Al)_5(OH)_2[(Si,Al)_8O_{22}]$

Hydraulic conductivity - A coefficient of proportionality describing the rate at which a fluid can flow through a permeable medium. Hydraulic conductivity is a function of the physical properties of the porous or fractured medium and of the density and viscosity of the fluid.

Hydrostratigraphy - Division of a rock mass into hydrostratigraphic units; a hydrostratigraphic unit is a body of rock distinguished and characterized by its porosity and permeability. Hydrostratigraphy is the classification of rocks and sediment based on their capacity to transmit water, and rocks are typically designated as either aquifers or aquitards (Maxey, 1964; Hansen, 1991). Hydrostratigraphic units may (1) coincide with lithostratigraphic units, (2) have boundaries corresponding to facies changes within a single lithostratigraphic unit, or (3) encompass several lithostratigraphic units with similar water-transmitting properties (Maxey, 1964; Hansen, 1991).

Joint - A planar or nearly planar fracture in rock, along which negligible relative movement has occurred.

Laccolith – A *concordant* igneous intrusion with a convex-up roof and known or assumed flat floor.

Lacustrine – Pertaining to, produced by, or formed in a lake.

Lava flow – The solidified body of rock formed from a surficial outpouring of molten lava from a vent or fissure; also the outpouring itself.

Limestone – A sedimentary rock consisting chiefly of calcium carbonate, principally in the form of the mineral calcite; formed by either organic or inorganic processes, and may be detrital, chemical, oolitic, crystalline, or recrystallized; many are highly fossiliferous and represent ancient shell banks or coral reefs; rock types include micrite, calcarenite, coquina, chalk, and

travertine.

Lithology - The description of rocks on the basis of such characteristics as color, mineralogic composition, and grain size.

Lithostratigraphic unit – A defined body of sedimentary, extrusive igneous, or metamorphosed sedimentary or volcanic strata that is distinguished and delimited on the basis of lithic characteristics and stratigraphic position. Boundaries of lithostrati-graphic units are placed at positions of lithic change, either at distinct contacts or arbitrarily within zones of gradation. The fundamental unit is the formation.

Magnetite – A black, cubic, strongly magnetic, opaque rock-forming mineral: $(Fe^{2+}Fe^{3+})[Fe^{3+}O_4]$.

Micrite - A rock or rock matrix composed of carbonate mud with crystals less than 4 micrometers in diameter.

Microcrystalline – Said of a texture of a rock, consisting of crystals that are small enough to be visible only under the micro-scope.

Mudstone - A fine-grained sedimentary rock in which the proportions of clay and silt are approximately equal.

Normal fault - A fault along which the *hanging wall* has moved downward relative to the *footwall*.

Olivine – An olive-green mineral common in magnesium-rich igneous rocks: $(Mg, Fe)_2SiO_4$.

Oncolite – A small, variously shaped, concentrically laminated, calcareous sedimentary structure, formed by the accretion of suc-cessive layered masses of gelatinous sheaths of blue-green algae.

Onlap – An overlap characterized by the regular and progressive pinching out, toward the margins or shores of a basin, of the sedimentary units within a conformable sequence of rocks.

Orthoclase – A member of the *alkali feldspar* group of rock-forming minerals: $KAlSi_3O_8$.

Pellet – A small, usually rounded aggregate of accretionary material, such as a fecal pellet; a spherical to elliptical homogeneous clast made up almost exclusively of clay-sized calcareous material, devoid of internal structure, and contained in a well-sort-ed carbonate rock.

Permeability - A coefficient describing the rate at which fluid can flow through a porous or fractured medium.

Phenocryst – A relatively large, conspicuous crystal in a *porphyritic* (see *porphyry*) igneous rock.

Plagioclase - A group of the *feldspar* minerals, including albite, $Na[AlSi_3O_8]$, and anorthite, $Ca[Al_2Si_2O_8]$, which form a com-plete solution series at high temperatures.

Plutonic – Pertaining to an igneous rock or intrusive body that formed below the land surface.

Porphyry – An igneous rock of any composition that contains conspicuous phenocrysts in a fine-grained groundmass.

Potentiometric surface - A surface representing the total head of ground water and defined by the levels to which water will rise in tightly cased wells.

Pumice – A light-colored, vesicular, glassy volcanic rock commonly having the composition of *rhyolite*.

Pyroclastic – Pertaining to clastic rock material formed by volcanic explosion or aerial expulsion from a volcanic vent.

Pyroxene – A group of dark-colored, rock-forming minerals with the general formula: $A_2B_2[Si_4O_{12}]$, where A = Ca, Na, Mg, or Fe^{2+}, and B = Mg, Fe^{2+}, Fe^{3+}, Cr, Mn, or Al.

Quartz – Crystalline silica, an important rock-forming mineral: SiO_2.

Quartzarenite - *Sandstone* that is composed of more than 95 percent quartz framework grains.

Quartzite - A metamorphic rock consisting mainly of quartz and formed by recrystallization of *sandstone* or *chert*.

Quartz monzonite – A plutonic rock whose felsic (Si-, Ca-, Na-, and K-rich) minerals consist of 10-50% *quartz*, and in which the *alkali feldspar*/total *feldspar* ratio is between 35% and 65%.

Reverse fault - A fault that dips greater than 30 degrees, along which the *hanging wall* has moved upward relative to the *foot-wall*.

Rhyodacitic – Said of a volcanic rock intermediate between rhyolite (see *rhyolitic*) and dacite (see *dacitic*).

Rhyolitic – Said of a group of light-colored volcanic rocks, typically *porphyritic* and exhibiting flow texture, with *phenocrysts* of *quartz* and *alkali feldspar* in a glassy to *cryptocrystalline groundmass*.

Sandstone - A medium-grained clastic sedimentary rock composed of abundant rounded or angular fragments of sand size and more or less firmly united by a cementing material.

Sanidine – A mineral of the *alkali feldspar* group, most commonly found in volcanic and rapidly cooled plutonic rocks: $KAlSi_3O_8$.

Scoria – A bomb-sized pyroclast that is irregular in form and generally very vesicular.

Shale - A laminated, indurated rock with >67 percent clay-sized minerals.

Siliciclastic strata – Sedimentary rocks which form by settling of grains from aqueous suspension, and which are almost exclu-sively silicon-bearing, either as forms of *quartz* or silicates.

Siltstone - An indurated silt having the texture and composition of shale but lacking its fine lamination or fissility.

Sonic log – An acoustic log showing the interval-transit time of compressional seismic waves in rocks near the well bore of a liquid-filled borehole.

Storativity – The volume of water an aquifer releases from or takes into storage per unit surface area of the aquifer per unit

change in head. Also called storage coefficient.

Stratigraphy - The science of rock strata, concerned with the original succession and age relations of rock strata and with their form, distribution, lithologic composition, fossil content, and geophysical and geochemical properties.

Strike - The angle a planar feature makes relative to north, as measured in a horizontal plane.

Syncline - A *fold*, the core of which contains stratigraphically younger rocks, and is convex downward.

Tephra – A collective term used for all *pyroclastic* material ejected during an explosive volcanic eruption.

Terrigenous – Derived from the land or continent.

Thrust fault - A *fault* that dips 30 degrees or less, along which the *hanging wall* has moved upward relative to the *footwall*.

Trachyandesitic – Said of a volcanic rock with composition similar to, but more *alkalic* than, an andesite (see *andesitic*).

Transmissivity – The rate at which a fluid is transmitted through a unit width of an aquifer under a hydraulic gradient.

Two-way travel time – The measured time for a seismic wave to travel down to a reflecting horizon in the subsurface, then back up to the surface where it is recorded by a geophone.

Unconformity - A substantial break or gap in the geologic record where a rock unit is overlain by another that is not next in stratigraphic succession.

Vesicular – Said of the texture of a lava rock characterized by abundant vesicles (cavities of variable shape, formed by the entrapment of a gas bubble during solidification of the lava).

Vitric – Said of *pyroclastic* material that characteristically contains more than 75 percent glass.

Vug – A small cavity in a vein or rock, usually lined with crystals of a different mineral composition from the enclosing rock.

APPENDIX A

Ancillary material to Plate 1

**Sources of Plate 1
Map Compilation**

| Baboon Peak | Dry Willow Peak | Jack Henry Knoll |

U.S.G.S. GQ-1493
(Thermo 15')
(Rowley, 1978)

U.S.G.S. I-1901
(Richfied 1° x 2°)
(Steven and others, 1990)

| Enoch NW | Enoch NE | Parowan Gap | Para-gonah |

U.S.G.S. GQ-1302
(Rowley, 1976)

U.S.G.S. GQ-1301
(Rowley, 1975)

U.S.G.S. GQ-1712
(Maldonado and
Williams,1993b)

U.S.G.S. GQ-1713
(Maldonado and
Williams,1993a)

| The Three Peaks | Enoch | Summit | Parowan |

**Plate 1
Boundary**

U.S.G.S. GQ-1297
(Mackin and
Rowley, 1976)

U.S.G.S. GQ-1296
(Rowley and
Threet, 1976)

| Desert Mound | Cedar City NW | Cedar City | Flanigan Arch | Brian Head |

U.S.G.S.
Prof. Pap. 516B
(Blank and
Mackin, 1967)

U.S.G.S. GQ-1295
(Mackin and
others, 1976)

U.S.G.S. GQ-1120
(Averitt and
Threet, 1973)

U.S.G.S.
Bulletin 2153
(Maldonado
and others, 1997)

| Stoddard Mt | Kanarraville | Cedar Mountain | Webster Flat | Navajo Lake |

U.S.G.S. OF 90-34
(Eppinger and
others, 1990)

U.S.G.S. GQ- 694
(Averitt, 1967)

U.S.G.S.
Prof. Pap. 389
(Averitt, 1962)

**Surface-
Drainage
Boundary**

Figure A.1. *Sources of plate 1 map compilation, with names and boundaries of 7¹/₂ minute quadrangles, and references.*

Age (Ma)
(not drawn to scale)

Plates 1 and 2

Figure 6

Basin-fill units,
shown only on cross sections

Holocene

Qa

Qaf

Qm

Qct

Qp

?

?

Qs

0.01

?

?

?

0.4 [1,9]

Qb

1.1 [4]

1.3 [4,5,6]

QTs

A

?

Pleistocene

?

QTa

QTs

QTb

1.6

Pliocene

?

Ts

?

?

5

Tm

?

B

Tb

9.0 9.8 [4]

?

?

?

?

Tamf

?

19.4 [8]

C

Miocene

Trcr

20.5

19 [2,3]

Tqm 20.9 [12]

Thv

21.5 [12]

Tms

21.8 [12]

Tq

22 [2,3]

22.6 [12]

?

Tv

23.6 [12]

Tmd

?

Tv

24

24 [2,9]

24.7

Tbv

Tmd

?

Oligocene

26 [2,3]

Tin

27-32.4 [2,6,7,11,12]

31.9 [13]

Tbh

38

TKs

(continued on next page)

(continued from previous page)

Figure A.2. *Correlation of map units. Radiometric ages, in Ma, with superscript(s) keyed to the following sources: (1) Armstrong (1970), (2) Fleck and others (1975), (3) Rowley (1978), (4) Anderson and Mehnert (1979), (5) Best and others (1980), (6) Best and Grant ((1987), (7) Best and others (1989), (8) Siders (1991), (9) Maldonado and Williams (1993a), (10) Maldonado and Williams (1993b), (11) Rowley and others (1994), (12) McKee and others (1997), and (13) Sable and Maldonado (1997).*

Age (Ma)	Period	Epoch	Formation	Symbol(s)	Thickness in feet (m)	Lithology
0.01	Q	Holocene	Sedimentary deposits	Qa,Qaf, Qp,Qct,Qm	0-150 (0-45)	
1.6		Pleistocene	Basalt	Qb	0-330 (0-100)	
	Quaternary -Tertiary	Pleistocene and Pliocene	Sedimentary deposits	QTs	0-100 (0-30)	
			Basin-fill deposits	QTa	0-1,330 (0-400)	
5		Quaternary -Miocene	Seismically defined basin-fill deposits	A	0-1,330 (0-400)	Shown only on cross sections (plate 2) and text illustrations
				B	0-1,830 (0-560)	
				C	0-980 (0-300)	
	Tertiary	Pliocene and Miocene	Sevier River Formation	Ts	0-100 (0-30)	
			Basalt	Tb	0-100 (0-30)	
			Alluvial-fan and mud flow deposits	Tamf	700 (215)	
		Miocene	Racer Canyon and Rencher Formations	Trcr	2,500 (760)	
			Quartz monzonite	Tqm		
			Horse Valley Formation	Thv	2,630 (800)	
			Mount Dutton Formation	Tmd	0-1,000 (0-305)	
			Bear Valley Formation	Tbv	0-260 (0-80)	
			Quichapa Group	Tq	0-1,850 (0-565)	
24			Flows of Mud Spring	Tms	0-150 (0-45)	
		Oligocene	Isom and Needles Range Formations	Tin	540-1,390 (165-425)	
38			Brian Head Formation	Tbh	720 (220)	
		?				
		Eocene	Claron Formation	Tc	720-850 (220-260)	

(continued on next page)

(continued from previous page)

Age (Ma)	Period	Epoch	Formation		Symbol	Thickness in feet (m)	Lithology
	T	Paleocene	Grand Castle Formation		Tgc	750 (230)	
66	Cretaceous	Late	Iron Springs Formation		Kis	2,700-3,600 (825-1,100)	
			Wahweap Sandstone and Straight Cliffs Formation		Kws	1,600-2,500 (490-760)	
			Dakota Formation		Kd	1,100 (335)	
138	Jurassic	Middle	Carmel Formation		Jc	1,130-1,360 (345-415)	
		Early	Navajo Sandstone		Jn	1,700 (520)	
			Kayenta Formation		Jk	730-1,570 (225-480)	
205			Moenave Formation			350-540 (110-165)	
	Triassic	Middle	Chinle Formation		Ꝑc	240-490 (75-150)	
		Early	Moenkopi Formation	Upper red member	Ꝑmu	1,200 (365)	
				Virgin Limestone Member	Ꝑmv	130 (40)	
				Lower red member	Ꝑml	250-315 (75-95)	
~240				Timpoweap Member	Ꝑmt	100 (30)	
	Paleozoic		Paleozoic sedimentary rocks		Pzs		Shown only on cross sections

Figure A.3. *Stratigraphic column. Sources: Rowley (1976), Rowley and Threet (1976), Rowley (1978), Hintze (1988), Blank and others (1992), Maldonado and Williams (1993a, 1993b), and Hurlow (1998). Thicknesses are approximate and are rounded to the nearest ten feet. Period abbreviations: Q=Quaternary, T=Tertiary.*

Table A.1. Comparison of map units on plate 1 and its sources.

This Report (plate 1)	Thermo 15' quadrangle (Rowley, 1978)	Richfield 1° x 2° quadrangle (Steven and others, 1990)	Parowan Gap 7 1/2-minute quadrangle (Maldonado and Williams, 1993b)	Paragonah 7 1/2-minute quadrangle (Maldonado and Williams, 1993a)	Enoch NE 7 1/2-minute quadrangle (Rowley, 1975)	Enoch NW 7 1/2-minute quadrangle (Rowley, 1976)	Enoch 7 1/2-minute quadrangle (Rowley and Threet, 1976)	The Three Peaks 7 1/2-minute quadrangle (Mackin and Rowley 1976)	Cedar City NW 7 1/2-minute quadrangle (Mackin and others, 1976)	Iron Springs District Scale 1:48,000 (Blank and Mackin, 1967)	Kanarraville 7 1/2-minute quadrangle (Averitt, 1967)	Cedar City 7 1/2-minute quadrangle (Averitt and Threet 1973)	Cedar Mountain 7 1/2-minute quadrangle (Averitt, 1962)	USGS Bulletin 2153-G (Maldonado and others, 1997)	Cedar City 1° x 2° quadrangle (Eppinger and others, 1990)
Qa	Qa	QTa	Qsc, Qsf, Qst	Qae, Qsf	Qal, Qv	Qal, Qv	Qal, Qv	Qal, Qv	Qal, Qv	Qs	Qal, Qs	Qal, Qs	Qal, Qs	QTac	n/a
Qaf (QTs)	Qf	QTa	Qfa, Qf, Qfo, Qp, Qpo	Qfa, Qf, Qfo, Qp	Qf	Qf	Qf	Qf	Qf	Qs	n/a	Qp	Qf, Qp, Qsw	QTac	TQu
Qp (QTs)	n/a	n/a	Ql, Qlm	Ql, Qlm	n/a	n/a	n/a	n/a	n/a	n/a	n/a	n/a	n/a	QTac	n/a
Qct (QTs)	n/a	QTa	Qt	Qt	n/a	n/a	n/a	Qc	Qc	Qs	Qt	Qt, Qct	Qt	QTac	n/a
Qm (QTs)	n/a	QTa	n/a	n/a	n/a	n/a	Qlb	n/a	n/a	Qs	Qlb	Qlb	qlb	QTl, QTli	n/a
Qb	n/a	n/a	Qbr	Qbw	n/a	n/a	n/a	n/a	n/a	n/a	Qb	Qb, Qa	Qb. Qa	Qb, Qbd	n/a
Tb	QTb	Tba	Tbd	n/a	Qtb	Qtb	Qtb	n/a	n/a	n/a	n/a	Tb	n/a	n/a	n/a
QTa	QTs	QTa	QTh, QTl, QTb	QTf, QTb	QTs	QTs	QTs	QTs	QTs	Qs	n/a	n/a	Tl, Tf, Ts	QTac	n/a
Tamf	n/a	n/a	n/a	n/a	n/a	n/a	n/a	n/a	n/a	n/a	Tf, Tau, Tal, Talg	Tf	n/a	n/a	Tmc
Ts	n/a	Ts	n/a	n/a	n/a	n/a	n/a	n/a	n/a	n/a	n/a	n/a	n/a	n/a	n/a
Trcr	n/a	n/a	n/a	n/a	n/a	n/a	n/a	n/a	n/a	Tpr	n/a	n/a	n/a	n/a	Tvr
Tm	n/a	n/a	Tm; Tbv, Tl, Tib, Tn where bounded by low angle faults	Tm; Tbv, Tl, Tib, Tn where bounded by low angle faults	n/a	n/a	n/a	n/a	n/a	Tb, Tbq, Tbc	n/a	n/a	n/a	Tm	n/a
Thv	Thv, Thn, Thm	Th	n/a	n/a	n/a	n/a	n/a	n/a	n/a	n/a	n/a	n/a	n/a	n/a	n/a

Table A.1 (continued)

This Report (plate 1)	Thermo 15' quadrangle (Rowley, 1978)	Richfield 1° x 2° quadrangle (Steven and others, 1990)	Parowan Gap 7 1/2-minute quadrangle (Maldonado and Williams, 1993b)	Paragonah 7 1/2-minute quadrangle (Maldonado and Williams, 1993a)	Enoch NE 7 1/2-minute quadrangle (Rowley, 1975)	Enoch NW 7 1/2-minute quadrangle (Rowley, 1976)	Enoch 7 1/2-minute quadrangle (Rowley and Threet, 1976)	The Three Peaks 7 1/2-minute quadrangle (Mackin and Rowley, 1976)	Cedar City NW 7 1/2-minute quadrangle (Mackin and others, 1976)	Iron Springs District Scale 1:48,000 (Blank and Mackin, 1967)	Kanarraville 7 1/2-minute quadrangle (Averitt, 1967)	Cedar City 7 1/2-minute quadrangle (Averitt and Threet 1973)	Cedar Mountain 7 1/2-minute quadrangle (Averitt, 1962)	USGS Bulletin 2153-G (Maldonado and others, 1997)	Cedar City 1° x 2° quadrangle (Eppinger and others, 1990)
Tmd	Tm, Tl	Td	Td	Td, Tdd	Tmd, Tmdt	Tmd	n/a	n/a	n/a	n/a	n/a	n/a	n/a	Tv	n/a
Tbv	n/a	Tbv	Tbv	Tbv, Tbvb	Tbv	n/a	n/a	n/a	n/a	n/a	n/a	n/a	n/a	Tv	n/a
Tqm	n/a	n/a	n/a	n/a	n/a	n/a	n/a	Tap, Tai, Tqsv	Tap, Tai, Tqs	Tpp, Tps, Tp, Tpl, Tir, Tiv	n/a	n/a	n/a	n/a	n/a
Tv — Tq	Tcb, Tlc	Tq	Tl, Tcb	Tl	Tccb, Tl	Tccb, Tccs, Tl, Tlt, Tln	Th, Tccb, Tlt, Tln	Th, Tccb, Tccr, Tccs, Tl	Th, Tccb, Tccv, Tccs, Tl	Tq	Tqh, Tqb, Tql	Tql	Twt	Tv	Tvr
Tv — Tin	Tib, Tn	Ti	Tib, Tn, Tnl, Tnw	Tib, Tn, Tnl, Tnw	Tin, Tib, Tn	Tin, Tis, Tib, Tn	Tib, Tn	Tin, Tib, Tn	Tin, Tib	Tin	Tih	Tib	n/a	Tv	n/a
Tms	n/a	n/a	Trs, Trst	Trs	n/a	Tms	n/a	n/a	n/a	n/a	n/a	n/a	n/a	n/a	n/a
Tbh	n/a	n/a				n/a	n/a	n/a	n/a	n/a	n/a	n/a	n/a	Tbh	n/a
Tcgc — Tc	Tce	n/a	Tcl	Tcl	n/a	Tca, Tcb, Tcc, Tcd, Tce	Tca, Tcb, Tcc, Tcd, Tce	Tca, Tcb, Tcc, Tcd, Tce	Tca, Tcb, Tcc, Tcd, Tce	Tc	Tc, Tct	Tc	n/a	Tcg	Tcl, Tw
Tcgc — Tgc	n/a	n/a	Tpc	Tpc	n/a	n/a	n/a	n/a	n/a	n/a	n/a	n/a	n/a	Tcg	n/a
Kis	n/a	n/a	Kiu, Kil	n/a	n/a	n/a	Ksl	Kiu, Kim, Kil, Km	Kiu, Kim, Kil, Km	Kis	n/a	n/a	n/a	Ki	Kis
Kwsd — Kws	n/a	n/a	n/a	n/a	n/a	n/a	n/a	n/a	n/a	n/a	n/a	Kw, Ksu, Ksl, Ksb	Kws	Ku	n/a
Kwsd — Kd	n/a	n/a	n/a	n/a	n/a	n/a	n/a	n/a	n/a	n/a	Kd, Kt	Kd, Kdc, Kdb	Kt	Ku	n/a
Ku	n/a	n/a	n/a	n/a							n/a	n/a	n/a	Kiu	n/a

Table A.1 (continued)

This Report (plate 1)	Thermo 15' quadrangle (Rowley, 1978)	Richfield 1°x2° quadrangle (Steven and others, 1990)	Parowan Gap 7 1/2-minute quadrangle (Maldonado and Williams, 1993b)	Paragonah 7 1/2-minute quadrangle (Maldonado and Williams, 1993a)	Enoch NE 7 1/2-minute quadrangle (Rowley, 1975)	Enoch NW 7 1/2-minute quadrangle (Rowley, 1976)	Enoch 7 1/2-minute quadrangle (Rowley and Threet, 1976)	The Three Peaks 7 1/2-minute quadrangle (Mackin and Rowley 1976)	Cedar City NW 7 1/2-minute quadrangle (Mackin and Others, 1976)	Iron Springs District Scale 1:48,000 (Blank and Mackin, 1967)	Kanarraville 7 1/2-minute quadrangle (Averitt, 1967)	Cedar City 7 1/2-minute quadrangle (Averitt and Threet 1973)	Cedar Mountain 7 1/2-minute quadrangle (Averitt, 1962)	USGS Bulletin 2153-G (Maldonado and others, 1997)	Cedar City 1°x2° quadrangle (Eppinger and others, 1990)
Jc	n/a	n/a	Jc, Jt	n/a	n/a	n/a	n/a	Jcb, Jch, Jcs	Jcb, Jchc, Jch, Jcs	Jcc	Jcw, Jcg, Jcb, Jcl	Jcw, Jcg, Jcb, Jcl	Jw, Jcu, Je, Jca	Jc	n/a
Jn	n/a	n/a	Jn	n/a	n/a	n/a	n/a	n/a	n/a	n/a	JTRn	JTRn	JTRn	n/a	n/a
Jk	n/a	n/a	n/a	n/a	n/a	n/a	n/a	n/a	n/a	n/a	TRkc, TRkl, TRk, TRns	TRkc, TRkl, TRk, TRns	TRkc, TRkl, TRk, TRns	n/a	n/a
Jm	n/a	n/a	n/a	n/a	n/a	n/a	n/a	n/a	n/a	n/a	TRms, TRmd	TRms, TRmd	TRms, TRmd	n/a	n/a
TRc	n/a	n/a	n/a	n/a	n/a	n/a	n/a	n/a	n/a	n/a	TRcu, TRcs	TRcu, TRcs	TRcu, TRcs	n/a	n/a
TRmu	n/a	n/a	n/a	n/a	n/a	n/a	n/a	n/a	n/a	n/a	TRmu	TRmu	TRmu	n/a	n/a
TRmv	n/a	n/a	n/a	n/a	n/a	n/a	n/a	n/a	n/a	n/a	TRmv	TRmv	TRmv	n/a	n/a
TRml	n/a	n/a	n/a	n/a	n/a	n/a	n/a	n/a	n/a	n/a	TRml	TRml	TRml	n/a	n/a
TRmt	n/a	n/a	n/a	n/a	n/a	n/a	n/a	n/a	n/a	n/a	TRmt	TRmt	TRmt	n/a	n/a

DESCRIPTION OF MAP UNITS

NOTE: Most of the unit descriptions presented below are paraphrased from previously published work. Sources of paraphrased descriptions: Qp - Maldonado and Williams (1993b); Qb - Rowley (1975) and Rowley and Threet (1976); Tb – Rowley (1975, 1976); Ts – Steven and others (1990); Tm – Maldonado and Williams (1993a, 1993b); Trcr – Blank and others (1992); Tqm – Blank and Mackin (1967); Thv and Tmd – Rowley (1978); Tbv - Maldonado and Williams (1993a, 1993b); Tq – Blank and others (1992); Tin – Rowley (1976), Blank and others (1992), and Maldonado and Williams (1993a, 1993b); Tbh – Sable and Maldonado (1997); Tc - Mackin and Rowley (1976), Mackin and others (1976), and Taylor (1993); Tgc – Goldstrand and Mullett (1997); Kis - Maldonado and Williams (1993b); Kws – Moore and Nealey (1993); Kd – Averitt (1962); Jc – Averitt and Threet (1973); Jn through Tmt – Hurlow and Biek (2000).

QUATERNARY

Qa   **Stream deposits** – Moderately to well-sorted, moderately to well-layered, interbedded gravel, sand, silt, and clay; includes channel, flood-plain, terrace, and local small alluvial-fan and colluvial deposits in valley center and drainages in the surrounding hills and mountains; gradational with unit Qaf. Up to about 25 feet (8 m) thick.

Qaf   **Alluvial-fan deposits** – Poorly sorted, structureless to moderately layered gravel, sand, silt, and clay; clasts are pebble- to boulder-size; deposited along valley margins in debris-flow and alluvial environments where streams and ephemeral drainages enter the valley; gradational with unit Qa. Up to about 150 feet (46 m) thick.

Qp   **Playa deposits** – Clay, silt, sand, and pebble gravel deposited on playa floor and margins, and eolian sand and silt deposits on playa margins; some deposits are calcareous, saline, or gypsiferous. About 1 to 15 feet (0.3-5 m) thick.

Qct   **Colluvium and talus** – Colluvium is poorly to moderately sorted, locally derived gravel, sand, and soil obscuring bedrock; deposited by slope wash, soil creep, and minor debris flows. Talus is poorly sorted, angular boulders and fine-grained interstitial sediments; locally derived material deposited principally by rock fall on and at the base of steep slopes. Up to about 10 feet (3 m) thick.

Qm   **Mass-movement deposits** – Poorly sorted, clay- to boulder-sized, locally derived material deposited by rotational and translational processes; chiefly landslide and slump deposits, but also includes some talus and colluvium. Thickness varies from about 10 to 100? feet (3-30? m).

Qb   **Basalt** – Dark-gray to black, dense, vesicular flows with fine grained phenocrysts of olivine and/or plagioclase feldspar; local deposits of black and red, poorly consolidated scoria. Includes local cinder and ash deposits on the Markagunt Plateau east and southeast of Cedar City. Up to 330 feet (100 m) thick. Anderson and Mehnert (1979) reported K-Ar whole-rock ages of 1.09 ± 0.34 Ma for a flow in the North Hills south of Cedar City and 1.28 ± 0.4 Ma for a flow in the western Red Hills.

QUATERNARY-TERTIARY

QTa   **Quaternary-Tertiary alluvium** – Poorly to well-sorted, moderately to well-layered, interbedded, brown to tan gravel and sand, and tan to red-tan silt and clay; deposited near valley margins in alluvial-fan and stream environments; typical exposures include beds of massive, unsorted pebble to boulder gravel, silty sand, and clay in variable proportions, 1 to 10 feet (0.3-3 m) thick; correlates with middle to lower part of seismically defined basin-fill unit A. Thickness is not well known, but if this unit comprises all of unit A it ranges from 0 to about 1,330 feet (0-405 m) thick.

QTs   **Quaternary and Quaternary-Tertiary sediment, undivided** - Used where source maps do not subdivide the surficial deposits listed above.

TERTIARY

Tb   **Basalt** – Dark-gray, black, and red, dense vesicular flows with fine-grained olivine phenocrysts. Thickness 0 to 100 feet (0-30 m). Anderson and Mehnert (1979) reported K-Ar whole-rock ages of 9.04 ± 0.86 Ma and 9.86 ± 0.72 Ma for flows in northern Cedar Valley.

Tamf   **Alluvial and mudflow deposits** – Poorly to moderately sorted sedimentary breccia, gravel, sand, silt, and clay, deposited in a variety of alluvial environments in the southern part of the study area and adjacent areas to the south (Averitt, 1967; Hurlow, 1998). Lower part consists of consolidated, volcaniclastic diamictite (sedimentary breccia) likely deposited by mudflows, interbedded with variably consolidated alluvial(?) sand and silt. Middle part consists of tuffaceous, tan to red-tan sand, silt, clay, and gravel deposited in alluvial environments. Upper part consists of unconsolidated boulder gravel. Lower contact is unconformable above Quichapa Group rocks or, locally, interbedded with tuff similar to the 19 Ma Racer Canyon Formation, described below (P. Rowley, U.S. Geological Survey, written communication, 1996; Hurlow, 1998). Upper age limit is poorly constrained, but is older than about 1 Ma, the age of basalt flows overlying these deposits in the Cross Hollow Hills and North Hills (Anderson and Mehnert, 1979). About 700 feet (213 m) thick.

Ts   **Sevier River Formation and equivalent rocks** – Poorly to moderately consolidated conglomerate, sandstone, and siltstone, deposited in alluvial and lacustrine environments, with local interbeds of airfall tuff and basaltic lava flows. Shown only in northeastern part of map. Thickness up to about 100 feet (30 m).

Tm   **Megabreccia** – In Red Hills and on Markagunt Plateau, gravity-slide blocks emplaced during Tertiary faulting and composed of undivided Tertiary volcanic and sedimentary rocks (Maldonado and others, 1997). East of Iron Mountain, gravity-slide blocks emplaced during local topographic uplift related to emplacement of quartz monzonite intrusions and composed of Claron and Isom Formations and Quichapa and Needles Range Groups (Blank and Mackin, 1967).

Trcr   **Racer Canyon and Rencher Formations** — Racer Canyon Formation is white to pale gray or tan, moderately welded, variably resistant, rhyolitic to dacitic ash-flow tuff with biotite and abundant red to purple lithic fragments. About 1,500 feet (460 m) thick. Siders (1991) reported a K-Ar age of 19.2 ± 0.8 Ma on biotite from the Racer Canyon tuff. Rencher Formation is white to tan, brown, or reddish-purple, weakly to moderately welded, variably resistant, crystal-rich, andesitic to dacitic ash-flow tuff and tuff breccia, with biotite, hornblende, and pyroxene phenocrysts and abundant angular to subrounded cognate inclusions. Lower contact is unconformable above Quichapa Group rocks. About 985 feet (300 m) thick. McKee and others (1997) reported K-Ar ages on biotite of 21.5 ± 0.6 Ma from the upper member, 21.8 ± 0.7 Ma from the middle member, and 23.6 ± 0.7 Ma from the lower member of the Rencher Formation.

Tqm   **Quartz monzonite porphyry** – Light gray (fresh) or grayish-green to medium brown (altered), with phenocrysts of plagioclase feldspar, hornblende, biotite, and pyroxene in a fine-grained groundmass of orthoclase, quartz, and magnetite. The outer 100 to 300 feet (30-91 m) of the intrusions are relatively fresh, fine-grained quartz monzonite porphyry. The inner part of the intrusions are altered and contain black veins composed of magnetite, which have been mined extensively as a source of iron ore (Blank, 1959; Rowley and Barker, 1978). Includes The Three Peaks, Granite Mountain, Iron Mountain, and Stoddard Mountain intrusions (plate 1). These bodies form domed, flat-bottomed laccoliths that intruded upward along the Iron Springs thrust, then spread laterally along a weak bedding plane within the Jurassic Carmel Formation (Blank and Mackin, 1967; van Kooten, 1988). Interpretation of seismic-reflection data in this report indicates that buried intrusions northeast of The Three Peaks intrude the Tertiary Claron Formation (cross sections A-A′ and B-B′, plate 2). Armstrong (1970) reported K-Ar ages of about 20 Ma.

Thv   **Horse Valley Formation** – Gray, pink, red, black, purple, or brown, variably resistant, rhyodacitic to dacitic lava flows, volcanic mudflow breccia, shallow intrusions, and ash-flow tuff; and black dacitic to andesitic volcanic mudflow breccia and lava flows. Rhyodacite to dacite contains sparse plagioclase phenocrysts in a groundmass of glass with abundant, very fine-grained feldspar crystals. About 2,630 feet (800 m) thick in area of plate 1, and thicker to the north. Fleck and others (1975) reported K-Ar ages on whole-rock and biotite samples of 21.9 ± 0.4 and 19.0 ± 0.6 Ma, respectively.

Tmd   **Mount Dutton Formation** – Brown, medium- to dark-gray, green, red, black, purple, or yellow, poorly to moderately resistant, angular pebble- to boulder-sized clasts of aphanitic dacitic to andesitic volcanic rock, in a light-gray, tan, or pink muddy matrix; clasts contain phenocrysts of plagioclase, hornblende, pyroxene, and opaque minerals in a groundmass of plagioclase, mafic minerals, and glass; weathers to bouldery slopes. About 1,000 feet (305 m) thick in study area, but much thicker to the north and northeast. K-Ar ages on plagioclase, biotite, and hornblende phenocrysts and a whole-rock sample range from 26.0 ± 0.8 to 25.1 ± 0.7 Ma (Fleck and others, 1975).

Tbv   **Bear Valley Formation** — Olive-gray, yellow-gray, and medium-green, moderately to poorly resistant, tuffaceous sandstone; composed of subangular to well-rounded volcanic clasts, glass shards, and mineral grains including feldspar, pyroxene, hornblende, biotite, magnetite, and quartz; interbedded with pale yellowish-brown mudflow breccia composed of cobble-sized clasts of andesitic to dacitic volcanic rocks, tuff, and tuffaceous sandstone. About 260 feet (80 m) thick. Fleck and others (1975) reported K-Ar ages of 23.9 ± 0.5 for plagioclase and 24.0 ± 0.4 Ma for biotite from a tuff bed in the Bear Valley Formation.

Tq   **Quichapa Group** – Includes Harmony Hills Tuff (youngest), Condor Canyon Formation, and Leach Canyon Formation (oldest) (Cook, 1960; Mackin, 1960). Total thickness is about 1,850 feet (565 m). K-Ar ages range from 24.7 to 20.5 Ma (Armstrong, 1970; McKee and others, 1997).

     The Harmony Hills Tuff is reddish-pink to tan, moderately welded, moderately resistant, crystal-rich, trachyandesitic ash-flow tuff with phenocrysts of biotite, hornblende, pyroxene, quartz, and sanidine; contains cognate inclusions and flattened vesicles. About 560 feet (170 m) thick. Armstrong (1970) reported a K-Ar age of 20.5 Ma.

     The Condor Canyon Formation is dense, resistant, reddish-brown to pinkish-red welded ash-flow tuff, with medium- to fine-grained phenocrysts of plagioclase, biotite, and quartz; matrix is aphanitic, with conspicuous, pale gray fiamme. A dark, andesitic mudflow breccia is locally present in the middle part of the formation. About 860 feet (290 m) thick. McKee and others (1997) reported a K-Ar age of 22.6 ± 0.6 Ma on biotite from a sample from the lower part of the Condor Canyon Formation in the Bull Valley Mountains.

     The Leach Canyon Formation is pale pink to pinkish-gray welded ash-flow tuff with medium- to coarse-grained phenocrysts of plagioclase, quartz, and biotite; matrix is microcrystalline to cryptocrystalline with angular cognate inclusions of red, gray, and pale green tuff containing fine-grained phenocrysts of plagioclase, quartz, and biotite; vesicles range from roughly spherical to flattened, and are lined with white secondary minerals and surrounded by pale gray to white alteration halos. A 3- to 6-foot- (1-2 m) thick lacustrine limestone deposit is locally present in the middle part of the formation. About 950 feet (290 m) thick. Armstrong (1970) reported a K-Ar biotite age of 24.7 Ma from a sample of the Leach Canyon Formation.

     The Condor Canyon and Leach Canyon Formations erupted from the Caliente caldera complex in southeastern Nevada and southwestern Utah (see figure 4 for location), and are widespread in southwestern Utah, forming relatively flat-based, eastward-thinning, sheet-like deposits that are now cut by numerous normal faults (Mackin, 1960; Rowley and others, 1979). The source area of the Harmony Hills Tuff is uncertain (Blank and others, 1992).

Tms   **Flows of Mud Spring** – Dark reddish-brown or grayish-purple, resistant, crystal-poor, rhyodacitic lava flows and dikes; phenocrysts are fine-grained plagioclase, biotite, and magnetite; locally brecciated and altered. Thickness 0 to 150 feet (0-45 m).

MIOCENE-OLIGOCENE

Tv   **Tertiary volcanic rocks, undivided**

OLIGOCENE

Tin   **Isom Formation and Needles Range Group** – The Isom Formation is purplish gray, brick-red, or brown, densely welded, crystal-poor trachyandesitic ash-flow tuff with phenocrysts of plagioclase and pyroxene, and gray, flattened pumice fiamme. A tan, yellow, or pale green, medium- to coarse-grained sandstone is locally present in the middle part of the formation. Thickness ranges from about 400 to 800 feet (122-244 m). Fleck and others (1975) reported K-Ar ages of 25.0 ± 0.4 and 25.2 ± 0.4 on plagioclase from the lower part of the Isom Formation.

     The Needles Range Group is grayish- to orange-pink, moderately welded, dacititc ash-flow tuff; phenocrysts are medium- to fine-grained plagioclase, hornblende, biotite, quartz, magnetite, and sanidine. A 12-foot-thick (4 m) layer of pale greenish-yellow tuffaceous sandstone, conglomerate, and sandstone is locally present in the middle part of the formation. About 140 to 590 feet (43-180 m) thick. Best and Grant (1987) reported average K-Ar ages of 27.9 Ma for the Lund Formation and 29.5 Ma for the Wah Wah Springs Formation, which together comprise the Needles Range Group.

     The Isom Formation erupted from the Caliente caldera complex in southeastern Nevada and southwestern Utah, and the Needles Range Group erupted from the Indian Peak caldera complex in southwestern Utah (see figure 4 for location; Best and Grant, 1987; Best and others, 1989). Both units are widespread in southwestern Utah, forming relatively flat-based, eastward-thinning, sheet-like deposits that are now cut by numerous normal faults (Mackin, 1960; Rowley and others, 1979).

OLIGOCENE-EOCENE(?)

Tbh   **Brian Head Formation** – Contains volcanic, volcaniclastic, and siliciclastic deposits, from top to bottom. The volcanic deposits consist of interbedded, vertically and laterally heterogeneous mudflow breccia, volcaniclastic sandstone, conglomerate, volcanic breccia, mafic lava, and ash-flow tuff. The volcaniclastic deposits are interbedded gray to greenish-gray, clayey tuffaceous sandstone, conglomeratic sandstone, and clay. The siliciclastic deposits are reddish-brown, pink, and reddish-orange sandstone grading to pebble conglomerate, above interbedded siltstone, claystone, and micritic limestone. Conglomerate clasts include quartz, quartzite, chert, siltstone, and gray micritic to silty limestone. About 720 feet (220 m) thick. Sable and Maldonado (1997) reported $^{40}Ar/^{39}Ar$ ages of 33.0 ± 0.1 on plagioclase and 33.7 ± 0.1 on biotite from an ash-flow tuff in the upper part of the formation; the age of the base of the Brian Head Formation is poorly constrained and may vary regionally.

OLIGOCENE(?)-EOCENE

Tc   **Claron Formation** – The Claron Formation consists of an upper part composed of dominantly pale gray to white, interbedded limestone, claystone, and minor conglomerate; and a lower part composed of orange-red to reddish-brown, interbedded siltstone, claystone, sandstone, conglomerate, and gray-, lavender-, pink- and yellow-stained limestone. The Claron Formation was deposited in fluvial and lacustrine environments (Taylor, 1993), and overlies Grand Castle or Iron Springs Formations above a disconformity or angular unconformity. The Claron Formation is late Paleocene to late Eocene(?) or early Oligocene in age, based on paleontological and palynological data (Goldstrand, 1994). About 720 to 850 feet (219-259 m) thick.

     The upper part is white to pale gray, resistant limestone interbedded with pale gray to pinkish-gray, poorly resistant clay-rich mudstone; limestone has moderately to poorly defined bedding, and includes unfossiliferous micrite, fine-grained bioclastic calcarenite, and pelletal calcarenite; calcite-filled veins are common.

     The lower part is interbedded mudstone, siltstone, sandstone, conglomerate, and limestone. Mudstone is orange-red to red-brown and clayey to silty, and contains thin beds of resistant, reddish-brown siltstone; sandstone is tan to brown, medium- to coarse-grained, cross-bedded to structureless litharenite; sandstone grades into, or is locally incised by, limestone-quartzite-chert-clast pebble conglomerate that is clast-supported, and very thick bedded, in discrete channels about 3 feet (1 m) or less thick. Limestone is (1) orange, pink, tan, lavender, and yellow, very resistant micrite with poorly defined bedding, and calcite-filled veins and vugs, and (2) medium gray, resistant micrite to calcarenite with moderately to well-defined, medium to thin bedding with bivalve shell fragments, pellets, oncolites, and calcite-filled veins and vugs.

OLIGOCENE-CRETACEOUS

Tcgc   **Claron and Grand Castle Formations, undivided**

PALEOCENE-CRETACEOUS

Tgc   **Grand Castle Formation** – Pale orange-red to tan, resistant, interbedded conglomerate and sandstone; conglomerate is structureless to planar or trough-cross-bedded, clast-supported, with boulder- to pebble-sized clasts, grading locally to structureless to planar- or trough-cross-bedded, coarse- to medium-grained sandstone; clasts include quartzite, limestone, and minor sandstone

and chert; individual beds typically 1 to 3 feet (0.3-0.9 m) thick, varying to 10 feet (3 m); sandstone is fine grained, well stratified, planar or trough cross-bedded, and ripple laminated; individual beds vary from 3 to 11 feet (1-4 m) thick. Lower contact is a disconformity or angular unconformity above the Iron Springs Formation or, locally in the hanging wall of the Parowan Gap thrust, the Carmel Formation. Deposited in a fluvial environment. About 750 feet (230 m) thick. Imprecisely dated as latest Cretaceous to early Paleocene, based primarily on palynological data from adjacent and laterally correlative units (Goldstrand and Mullett, 1997).

CRETACEOUS

Kis   **Iron Springs Formation** – Yellowish-gray, tan, or pale brown, moderately resistant sandstone, with thin beds of conglomerate, siltstone, shale, oyster-shell and gastropod coquina, and coal (the latter two are rare). Sandstone is fine to medium-grained, well sorted quartzarenite; planar- or trough cross-bedded to structureless; soft-sediment deformation common; deposited in fluvial braid-plain and shallow-marine environments; lower contact is a disconformity above Carmel Formation. About 2,700 to 3,600 feet (820-1,100 m) thick. The Iron Springs Formation is Cenomanian to Santonian or early Campanian in age, based primarily on palynological data (Goldstrand, 1994).

Kws   **Wahweap Sandstone and Straight Cliffs Formation** – The Wahweap Sandstone is brownish-gray, light olive brown, and reddish-brown, pale red-weathering, poorly resistant mudstone, sandstone, clayey sandstone, and siltstone; present only in the southeastern corner of the map area (Moore and Nealey, 1993). The Straight Cliffs Formation is interbedded sandstone, mudstone, and siltstone. The sandstone and siltstone are pale tan, grayish-tan, or brown, moderately to weakly resistant, fine to medium grained, with planar laminations, planar cross-bedding, and silicified plant fragments; contains thin mud-pellet conglomeratic layers, and dark gray beds of oyster- and gastropod-shell coquina; deposited in shallow-marine environments; lower contact is conformable with Dakota Formation. Combined thickness about 1,600 to 2,500 feet (490-760 m).

Kd   **Dakota Formation** – Light- to dark-gray and reddish-brown, poorly resistant mudstone; pale gray to tan, moderately resistant, thin, lenticular, medium-grained, planar-bedded sandstone; and, about 20 to 30 feet (6-9 m) above the base, a 0- to 10-foot-thick (0-3 m), medium gray, structureless to weakly stratified pebble to cobble conglomerate with quartzite, chert, and limestone clasts. Deposited in shallow-marine, intertidal, and fluvial environments; lower contact is a disconformity above the Carmel Formation. About 1,100 feet (335 m) thick.

Kwsd   **Wahweap Sandstone, Straight Cliffs Formation, and Dakota Formation, undivided**

Ku   **Iron Springs Formation, Wahweap Sandstone, Straight Cliffs Formation, and Dakota Formation, undivided**

JURASSIC

Jc   **Carmel Formation** – Interbedded, pale to medium-gray, platy weathering, thin- to medium-bedded, silty to clayey micrite to fine-grained calcarenite containing sparse bivalve fossils; pale gray to greenish-gray, massive to poorly laminated silty micrite; pale yellowish-gray, calcareous mudstone; brown to reddish-brown, locally gypsiferous mudstone; tan, sandy bioclastic limestone to calcareous sandstone containing disarticulated bivalve, mollusk, and oyster shells and, locally, *Pentacrinus* sp. crinoid columnals; and pale greenish-gray calcareous mudstone to siltstone and clayey micrite; deposited in shallow-marine, intertidal, and sabkha environments (Imlay, 1980). Varies from about 1,130 to 1,360 feet (345-415 m) thick.

Jn   **Navajo Sandstone** – Pale reddish-orange, reddish-brown, or white, resistant, fine- to medium-grained eolian sandstone (quartzarenite); trough cross-bedded; well-rounded quartz grains have frosted surfaces due to abrasion. About 1,700 feet (520 m) thick.

Jk   **Kayenta Formation** – Interbedded, reddish-brown to orange-red, variably resistant, thin- to medium-bedded, fine-grained sandstone, siltstone, and mudstone with planar to ripple laminae; east of Cedar City, the middle 725 feet (221 m) of the formation is trough-cross-bedded eolian sandstone similar to the Navajo Sandstone. Deposited in fluvial, playa, and lacustrine environments. Varies from about 730 to 1,570 feet (220-480 m) thick.

Jm   **Moenave Formation** – Upper part is medium- to thick-bedded, resistant, fine-grained sandstone, with planar or low-angle cross bedding. Middle part is reddish-purple, greenish-gray, and blackish-red, moderately to poorly resistant mudstone and claystone, lesser reddish-brown, fine-grained sandstone and siltstone, and thin, cherty, dolomitic limestone beds. Lower part is reddish-brown, variably resistant, thin-bedded, fine-grained sandstone, siltstone, and mudstone with planar, low-angle, and ripple cross-stratification. Deposited in fluvial and lacustrine environments. Lower contact is a disconformity above the Chinle Formation. Varies from about 350 to 540 feet (105-165 m) thick.

Jkm   **Kayenta and Moenave Formations, undivided** – (shown only on cross sections).

TRIASSIC

Ŧc   **Chinle Formation** – Upper part is variably colored mudstone, claystone, siltstone, lesser sandstone and pebbly sandstone, and minor chert and nodular limestone; swelling mudstones and claystones are common throughout and weather to a popcorn surface. Lower part is resistant, fine- to coarse-grained sandstone, pebbly sandstone, and conglomerate with subrounded clasts of quartz,

quartzite, and chert; thick-bedded with both planar and low-angle cross-stratification. Deposited in fluvial and lacustrine environments. Varies from about 240 to 490 feet (75-150 m) thick.

Moenkopi Formation

Ŧmu   **Upper red member** – Reddish-orange to reddish-brown, thin- to medium-bedded, variably resistant siltstone, mudstone, and fine-grained sandstone with planar, low-angle, or ripple cross-stratification; thin-bedded, poorly resistant, gypsiferous, pale red to reddish-brown mudstone and siltstone; resistant, white to greenish-gray bedded gypsum; thin, laminated, light-gray dolomite beds; thin-bedded, variably resistant, reddish-brown siltstone, mudstone, and fine-grained sandstone with white to greenish-gray gypsum beds and veins. Deposited in tidal-flat to shallow-marine environments. Lower contact is conformable with Virgin Limestone Member. Averitt (1962, 1967) used this member; it has subsequently been subdivided into the middle red, Schnabkaib, and upper red members. About 1,200 feet (365 m) thick.

Ŧmv   **Virgin Limestone Member** – Yellowish-gray, resistant, finely crystalline limestone and silty limestone; light-gray, coarsely crystalline, fossiliferous limestone with crinoid columnals, gastropods, and brachiopods; and gray, yellowish gray, and grayish purple, poorly resistant siltstone and mudstone. Deposited in a shallow-marine environment. About 130 feet (40 m) thick.

Ŧml   **Lower red member** – Interbedded, variably resistant, laminated to thin-bedded, reddish-brown mudstone and siltstone with thin, laminated, light-olive-gray gypsum beds and veinlets. Deposited in a tidal-flat environment. About 250 to 315 feet (76-96 m) thick.

Ŧmt   **Timpoweap Member** – Upper part is grayish-orange, variably resistant, thin- to thick-bedded, calcareous, fine-grained sandstone, siltstone, and mudstone. Deposited in a shallow-marine environment. Lower part is light-brown weathering, light-gray, resistant, thin- to thick-bedded limestone and cherty limestone. About 100 feet (30 m) thick.

Ŧs   **Triassic sedimentary rocks, undivided** – (shown only on cross sections).

APPENDIX B

Water-well data

Sections within a township

R. 12 W.

6	5	4	3	2 ● Well	1
7	8	9	10	11	12
18	17	16	15	14	13
19	20	21	22	23	24
30	29	28	27	26	25
31	32	33	34	35	36

T. 36 S.

6 miles
9.7 kilometers

Section 2

NW   N4   NE

1,600 ft

Well ●   1,000 ft

W4   E4

Point of Diversion:
1,600 feet south and
1,000 feet west of the
northeast corner of
Section 2, T. 35 S., R. 12 W.

Listed in data tables as:

35S 12W 2 S1600 E1000 NE

SW   S4   SE

1 mile
1.6 kilometers

SALT LAKE   BASE LINE

Salt Lake City

SALT LAKE MERIDIAN

T. 36 S. R. 12 W.

Figure B.1. *Numbering system for wells in Utah - Point of Diversion convention.*

Sections within a township

Tracts within a section

R. 12 W.

Section 2

6	5	4	3	2 ● Well	1
7	8	9	10	11	12
18	17	16	15	14	13
19	20	21	22	23	24
30	29	28	27	26	25
31	32	33	34	35	36

T. 36 S.

b

a

b

a

c

a ● Well
b   a
d
c   d

c

d

6 miles
9.7 kilometers

1 mile
1.6 kilometers

(C-36-12) 2adb-1

B	A

SALT LAKE   BASE LINE
Salt Lake City

C   D

SALT LAKE MERIDIAN

■
T. 36 S. R. 12 W.
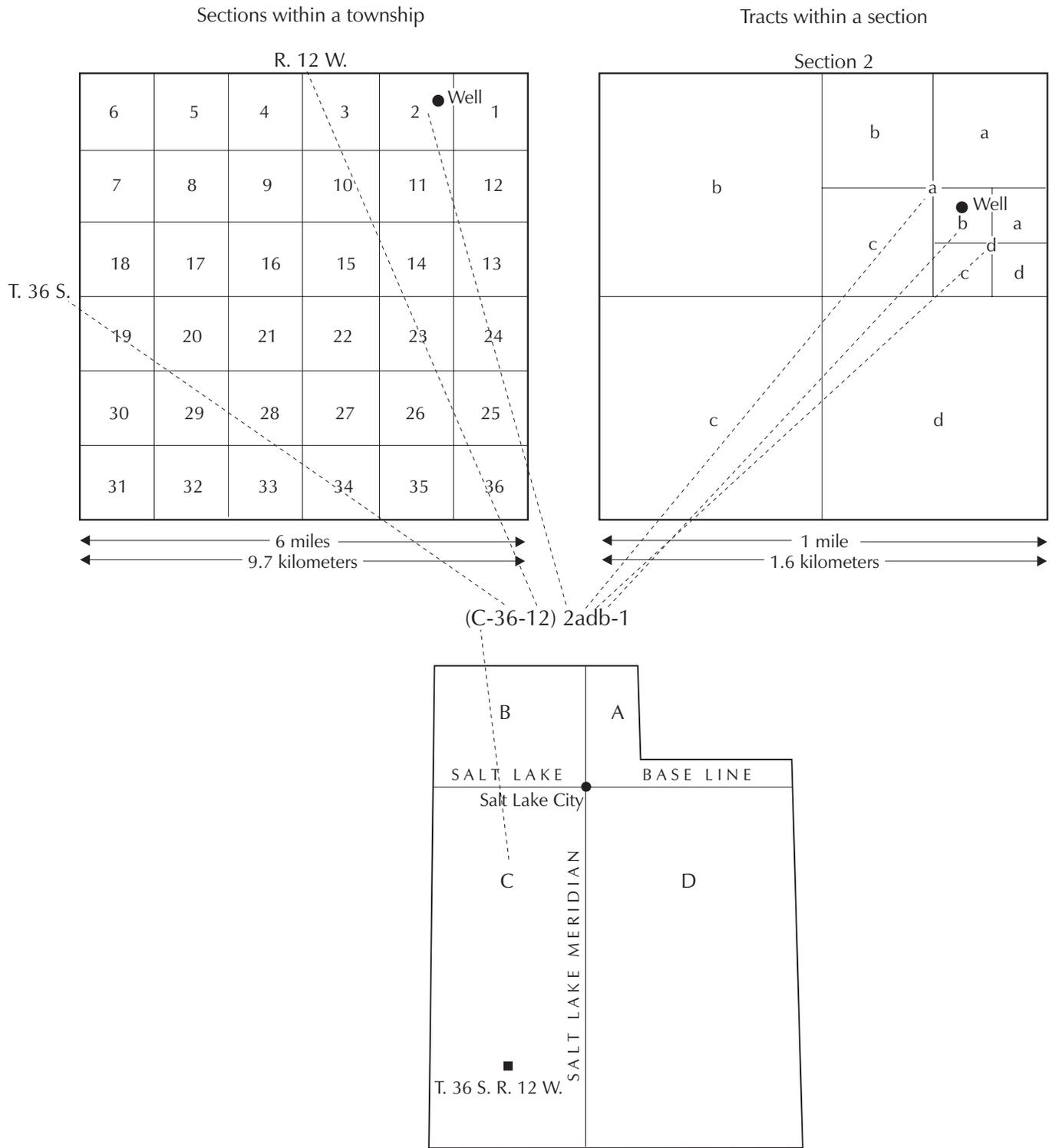
Figure B.2. *Numbering system for wells in Utah - U.S. Geological Survey convention.*

Table B.1. Public water-supply wells in Cedar Valley.

ID[1]	OWNER	Location[2] Point of Diversion	Sec	T	R	Source of Log[3]
1	Angus Water Co.	S470 E310 N4	9	35S	11W	http://www.waterrights.utah.gov/cgi-bin/docview.exe?Folder=WIN018226
2	Enoch City Corporation	S2210 E1170 N4	7	35S	10W	http://www.waterrights.utah.gov/cgi-bin/docview.exe?Folder=WIN018746
3	Enoch City Corporation	S95 E2615 W4	7	35S	10W	http://www.waterrights.utah.gov/cgi-bin/wellprt.exe?014400
4	Enoch City Corporation	N380 E700 SW	7	35S	10W	Utah Division of Water Rights paper files
5	Enoch City Corporation	S1478 E195 N4	18	35S	10W	Utah Division of Water Rights paper files
6	Cedar City Corporation	N1110 E880 SW	18	35S	10W	Utah Division of Water Rights paper files
7	Cedar City Corporation	S59 W1614 E4	24	35S	11W	Utah Division of Water Rights paper files
8	Cedar City Corporation	S1345 E1607 NW	11	36S	11W	http://www.waterrights.utah.gov/cgi-bin/wellprt.exe?004006
9	Monte Vista Water Co.	S575 W13 NE	7	36S	11W	http://www.waterrights.utah.gov/cgi-bin/wellprt.exe?014328
10	Park West Subdivision	N620 W1320 E4	36	35S	12W	Utah Division of Water Rights paper files
11	Mountain View SSD	S66 E2699 W4	3	36S	12W	Utah Division of Water Rights paper files
12	Desert Development LLC	N209 E845 W4	7	36S	12W	http://www.waterrights.utah.gov/cgi-bin/wellprt.exe?003066
13	Cedar City Corporation	N341 W213 SE	17	36S	12W	http://www.waterrights.utah.gov/cgi-bin/wellprt.exe?016153
14	Cedar City Corporation	S2364 W700 NE	20	36S	12W	http://www.waterrights.utah.gov/cgi-bin/wellprt.exe?013549
15	Cedar City Corporation	S263 W2467 NE	29	36S	12W	http://www.waterrights.utah.gov/cgi-bin/wellprt.exe?018295
16	Cedar City Corporation	N750 E100 SW	32	36S	12W	Utah Division of Water Rights paper files
17	Cedar City Corporation	N100 E100 SW	32	36S	12W	Utah Division of Water Rights paper files
18	Cedar City Corporation	S550 E50 NW	5	37S	12W	http://www.waterrights.utah.gov/cgi-bin/wellprt.exe?003982
19	Spring Creek Water Users	N1310 W50 S4	25	36S	12W	http://www.waterrights.utah.gov/cgi-bin/wellprt.exe?004169
20	Spring Creek Water Users	N795 W1078 E4	36	36S	12W	Utah Division of Water Rights paper files
21	Rainbow Ranchos Water Co.	S100 E1166 NW	1	37S	12W	http://www.waterrights.utah.gov/cgi-bin/wellprt.exe?004086
22	Kanarraville Town	S01°35' E851 NW	35	37S	12W	Utah Division of Water Rights paper files

Notes
1. Corresponds to number on figures 1 and 6 and plate 1.
2. Location is given in "Point of Diversion" notation - see figure B.1. Sec = Section, T = Township, R = Range.
3. Many water-well drillers' logs are available on the Utah Division of Water Rights, online (http://www.waterrights.utah.gov) - the specific link for available wells are provided. Other logs are available as paper files.

Table B.2. *Springs used for municipal supply in Cedar Valley drainage basin [1]. The rights to all of the springs listed are owned by Cedar City.*

ID[2]	Point of Diversion[3]			Sec	T	R	Spring Name	Unit[4]
S	S 760	W 1487	NE	23	37S	11W	Upper Posie Spring	Kd
S2	N 55	W 1377	SE	14	37S	11W	Lower Posie Spring	Jc
S3	S 265	W 590	NE	23	37S	11W	Birch Spring	Kd
S4	S 723	W 1488	NE	23	37S	11W	Upper Posie Spring #2	Kd
S5	S 1548	E 821	NW	24	37S	11W	3-Ledge Spring #1	Kd
S6	S 1535	E 810	NW	27	37S	11W	3-Ledge Spring #2	Kd
S7	S 1596	E 780	NW	27	37S	11W	3-Ledge Spring #3	Kd
S8	S 647	E 519	NW	24	37S	11W	West Big Spring	Kd
S9	S 791	E 760	NW	24	37S	11W	East Big Spring	Kd
S10	S 3035	W 2095	NE	23	37S	11W	Urie Spring	Kws
S11	S 250	E 60	N4	35	37S	10W	Cluff Spring	Kwsd
S12	Lot 3			5	37S	10W	Lower Will Williams Spring	Kd
S13	SE NW			5	37S	10W	Upper Barnson Spring	Kwsd
S14	SE SW			32	36S	10W	Dry Spring	Kd
S15	NW SE			32	36S	10W	Upper Black Rock Spring	Kws
S16	NW SE			32	36S	10W	Barnson Trail Spring	Kd
S17	NE SE			32	36S	10W	Lower Head House Spring	Kwsd
S18	SE NE			32	36S	10W	Raspberry Spring	Kd
S19	SE SW			32	36S	10W	White Rock Spring	Kws
S20	S 1930	W 2820	NE	11	37S	13W	Right Fork Quichapa	Tq
S21	S 1896	E 1502	NE	12	37S	13W	Quichapa confluence	Tq
S22	S 284	E 1858	NW	12	37S	13W	Left Fork Quichapa	Tq

Notes

1. Data from Utah Division of Water Rights (http://www.waterrights.utah.gov).
2. Corresponds to number on figures 1 and 6 and plate 1.
3. Location is given in "Point of Diversion" notation - see figure B.1. Sec = Section, T = Township, R = Range. Points of Diversion for springs 13 through 19 give the general location within the section. Example: spring 13 is located on the southeast quarter of the northwest quarter of section 32, in Township 36 South, Range 10 West.
4. Determined by the author by plotting the springs on plate 1. Units (see appendix A for descriptions): Jc - Carmel Formation; Kd - Dakota Formation; Kws - Wahweap Sandstone and Straight Cliffs Formation, undivided; Kwsd - Wahweap Sandstone and Straight Cliffs and Dakota Formations, undivided; Tq - Quichapa Group.

Table B.3. Exploration wells in Cedar Valley[1].

ID[2]	Operator	Well Name	API No.[3]	Location[4]							Compl.	Elevation	TD[5]	Formation Tops[6]
				Point				Sec	T	R	Year			
OW1	Jenkins & McQueen	2 Adams	4302160001	990	1980	FNL	FEL	9	34S	11W	1950	5300	690	No log available
OW2	Jenkins & McQueen	1 Adams	4302120100	2310	2310	FSL	FWL	9	34S	11W	1950	5300	3968	Pc 2600
OW3	Mountain Fuel Supply Co.	LSL–Gov't	4302110758	2310	330	FSL	FEL	9	34S	10W	1963	6113	4400	Ju 2929, Tqm 3490
OW4	Mountain Fuel Supply Co.	Shurtz Creek	4302130002	580	780	FNL	FEL	9	37S	11W	1973	6497	5996	Ŧrmt 540, Pk 746, Pt 905, Pc 2477, Pp 3418, Mc 4664, Mr 5070, Du 5784
OW5	Odessa Natural Corp.	Cedar City	4302130003	2010	2031	FNL	FWL	18	36S	11W	1975	5515	11700	Jk 3585, Ŧrc 4830, Ŧrm 5166, Pk 7110, Pt 7560, Pc 8030, Pp 8980, PPc 9720, Mu 10450, Du 11250
OW6	Cabot Corp.	Cedar City	4302130004	660	660	FNL	FEL	29	36S	11W	1978	5932	5740	Ŧrmt 4776, Pk 4969, Pt 5223
OW7	ARCO Oil & Gas Co.	Three Peaks	4302130006	1005	350	FSL	FWL	17	35S	12W	1985	5390	15590	Kis 130, Jc 840, Tqm 4232, Jc 4908, Jn 6286, Jk 9310, Ŧrc 10937, Ŧrm 10937, Pk 11597, Pt 12130, Pc 12662, Pp 13758, PPc 14535, Mr 15451
USS	U.S. Steel	n/a	n/a	500	3000	FNL	FWL	31	33S	10W	n/a	5455	3,011	All in basin fill

Notes

n/a: not applicable or data unknown

1. Oil-well data from U.S. Bureau of Reclamation. U.S. Steel well information from Rowley (1975).

2. Corresponds to letters on figure 6 and plate 1.

3. Petroleum Information (PI) database number.

4. Location is given as distance in feet frm section lines. FNL = from north line, FSL = from south line,   FEL = from east line, FWL = from west line.
    Sec = Section, T = Township, R = Range, relative to 1855 Salt Lake Base Line and Meridian.

5. TD = total depth

6. Data from Utah Division of Oil, Gas and Mining and UGS unpublished records. Formation of tops are in feet. Unit abbreviations: Tqm = quartz monzonite;
    Kis - Iron Springs Formation; Jc - Carmel Formation; Jn - Navajo Sandstone; Jk - Kayenta Formation; Ŧrc - Chinle Formation; Ŧrm - Moenkopi Formation;
    Ŧrmt - Timpoweap Member of Moenkopi Formation; Pk - Kaibab Limestone; Pt - Toroweap Formation; Pc - Pakoon Formation; PPc - Callville Limestone;
    Mr - Redwall Limestone; Mu - Mississippian rocks, undivided; Du - Devonian rocks, undivided. See Hintze (1988) for information about pre-Triassic units.

Table B.4. *Wells used to construct schematic cross sections of basin-fill deposits [1].*

ID[2]	Point of Diversion			Location[3]		
				Sec	T	R
E1	N2235	W150	S4	33	33S	11W
E2	N1175	E1300	SW	3	34S	11W
E3	N75	W1230	S4	2	34S	11W
E4	N1320		S4	11	34S	11W
E5	S1152	E5	NW	13	34S	11W
E6	N50	E250	W4	13	34S	1W
F1	N3349	E345	S4	14	35S	12W
F2	S400	E1845	W4	24	35S	12W
F3	S165	W540	NE	24	35S	12W
F4	N1100	E500	S4	19	35S	11W
F5	N100	W1665	SE	17	35S	11W
F6	N20	W1385	E4	16	35S	11W
F7	S5	E250	NW	23	35S	11W
F8	N1367	E138	SW	13	35S	11W
F9	N1188	W1159	NE	13	35S	11W
F10	S20	E920	W4	7	35S	10W
F11	S935	E633	N4	18	35S	10W
G1	S66	E2699	W4	3	36S	12W
G2	S1240	W1340	NE	9	36S	12W
G3	S198	W363	NE	10	36S	12W
G4	N194	E1150	S4	15	36S	12W
G5	S2156	W182	NE	14	36S	12W
G6	N1290	E460	SW	23	36S	12W
G7	N2060	E500	SW	24	36S	12W
G8	N1195	E910	SW	19	36S	11W
G9	N1310	W50	S4	25	36S	12W
G10	N2740	E2740	SW	30	36S	11W
G11	S1550	W25	NE	36	36S	12W
G12	S301	W135	E4	31	36S	11W
G13	S2660	E670	N4	32	36S	11W
G14	N1600	W1000	SE	5	37S	11W
H1	S1240	W1340	NE	9	336S	12W
H2	S60	W130	N4	9	36S	12W
H3	N155	E1365	SW	3	36S	12W
H4	S198	W363	NE	10	36S	12W
H5	N1270	E2360	W4	11	36S	12W
H6	S1750	W2050	NE	11	36S	12W
H7	S710	E1070	N4	11	36S	12W
H8	N2299	W140	SE	11	36S	12W
H9	S2150	E900	W4	12	36S	12W

Notes

1. Logs are available from Utah Division of Water Rights, online (http://www.waterrights.utah.gov) or paper files.

2. Corresponds to number on figure 14.

3. Location is given in "Point of Diversion" notation - see figure B.1. Sec = Section, T = Township, R = Range.

Table B.5. *Cedar Valley water wells logged by Wallace (2001).*

ID[1]	USGS	Point of Diversion			Sec	T	R	Source of Log[3]
J1	bbb	S500	E400	NW	1	35S	11W	UGS paper files
J2	acd	S2210	E1170	N4	7	35S	10W	http://www.waterrights.utah.gov/cgi-bin/docview.exe?Folder=WIN018746
J3	aac	S1300	W755	NE	14	35S	11W	UGS paper files
J4	abb	S470	E310	N4	9	35S	11W	http://www.waterrights.utah.gov/cgi-bin/docview.exe?Folder=WIN018226
J5	ccc	N150	E568	SW	9	35S	11W	UGS paper files
J6	cab	S400	E1845	W4	24	35S	12W	http://www.waterrights.utah.gov/cgi-bin/docview.exe?Folder=WIN018032
J7	dcb	N1100	E500	S4	19	35S	11W	UGS paper files
J8	aca	S1825	E1650	NE	26	35S	11W	http://www.waterrights.utah.gov/cgi-bin/docview.exe?Folder=WIN019668
J9	bdb	N750	E1900	W4	35	35S	11W	http://www.waterrights.utah.gov/cgi-bin/docview.exe?Folder=WIN019209
J10	ccb	N956	E155	SW	31	35S	11W	UGS paper files
J11	acd	S2660	E670	N4	32	36S	11W	UGS paper files
J12	2ccd	N428	E854	SW	2	37S	12W	http://www.waterrights.utah.gov/cgi-bin/docview.exe?Folder=WIN023134

Location[2] spans the USGS, Point of Diversion, Sec, T, R columns.

Notes

1. Corresponds to number on figure 14.
2. Location is given in "Point of Diversion" convention - see figures B.1 and B.2, respectively.
   Sec = Section, T = Township, R = Range.
3. Most logs are available from Utah Division of Water Rights, online (http://www. waterrights.utah.gov), but as of 7/11/02 some have not been posted. These logs are available from the UGS upon request.